Alma Mater Studiorum – Università di Bologna

DOTTORATO DI RICERCA IN
SCIENZE E TECNOLOGIE AGRARIE, AMBIENTALI E ALIMENTARI

Ciclo XXXV

Settore Concorsuale: 07/B2

Settore Scientifico Disciplinare: AGR/03

RED FLESH FRUIT IN EUROPEAN PEAR (*Pyrus communis*): Genetic Sources, QTLs, Candidate Genes and Tools for Breeding

Presentata da: Lorenzo Bergonzoni

Coordinatore Dottorato
Prof. Massimiliano Petracci

Supervisor:
Prof. Stefano Tartarini

Co-supervisors:
Prof. Luca Dondini
Prof. Richard V. Espley
Dr. Sara Montanari

Esame finale anno 2023

Table of content

List of abbreviations

ABCC: ATP-Binding Cassette

AF: Abate Fétel

ANS: Anthocyanidin Synthase

B: Pera Briaca

BBX: B-Box Transcription Factor

bHLH: Basic Helix-Loop-Helix

BZIP: Basic Leucine Zipper Domain

C: Carmen

CHI: Chalcone Isomerase

CHS: Chalcone Synthase

COP: Constitutive Photomorphogenic

CP: Cocomerina Precoce

CS: Cocomerina Selvatica Lacasa

CT: Cocomerina Tardiva

CTAB: Hexadecyltrimethylammonium Bromide

CUC: Cup-Shaped Cotyledon

DC: Decana Del Comizio

DEG: Differentially Expressed Genes

DFR: Dihydroflavonol 4-Reductase

ECPGR: European Cooperative Program for Plant Genetic Resources

ER: Emilia Romagna

ERF: Ethylene Responding Factor

F3′5′H: Flavonoid 3′,5′-Hydroxylase

F3′H: Flavonoid 3′-Hydroxylase

F3H: Flavanone3-Hydroxylase

FD: Fruit Diameter

FF: False Fruit or Fruit Flesh

FFi: Flesh Firmness

FL: Fruit Length

FPKM: Fragments Per Kilobase of Exon Per Million Mapped Fragments

FW: Fruit Weight

H2: Broad-Sense Heritability

HExp And HObs: Expected and Observed Heterozygosity

HPLC: High Performance Liquid Chromatography

HY: LONG HYPOCOTYL Gene

IA: Incrocio S.Alessio

IM: Interval Mapping

JA: Jasmonate

JAZ: Jasmonate Related Genes

KEGG: Kyoto Encyclopaedia of Genes and Genomes

KW: Kruskal-Wallis

LDOX: Leucocyanidin Oxygenase

LG: Linkage Group

LOD: Logarithm of Odds

MBW: MYB-Bhlh-WD40 Complex

MYB: Myeloblastosis-Related Proteins

NAC: NAM, ATAF1/2, and CUC2

NAM: No Apical Meristem

PAL: Phenylalanine Ammonia Lyase

PC: Principal Component

PCA: Principal Component Analysis

PCR: Polymerase Chain Reaction

PIC: Polymorphism Information Content

PS: Pera Sanguigna

QTL: Quantitative Trait Loci

R/W: Red/White Index

SBP: Squamosa Binding Protein

SL: Seed Locule

SNP: Single Nucleotide Polymorphism

SPET: Single Primer Enrichment Technology

SPL: Squamosa Promoter Binding Protein-Like

SSC: Soluble Solid Content

SSR: Simple Sequence Repeat

TA: Titratable Acidity

TAL: Tyrosine Ammonia Lyase

TF: True Fruit or Fruit Core

TFS: Transcription Factor Genes

TPL: Plant Corepressor TOPLESS

TTG: Transparent Testa Glabra

UFGT: Flavonoid-3-O-Glycosyltransferase

UPGMA: Unweighted Pair-Group Method

US: Under-Skin Region

W: William Bon Chretien

WAFB: Weeks After Full Bloom

WDR: Tryptophan-Aspartic Acid Repeat

WRKY: WRKYGQK

Abstract

Red flesh fruit is a character which interest is increasing in several commercial species, such as apple and peach. Some old landraces with this trait are known in pear and several breeding programs have already been started in order to obtain new élite varieties. In pear, the red colour is the result of the presence and accumulation of anthocyanin. This group of secondary metabolites are strong antioxidant molecules fundamental in human health. High anthocyanin content in the fruit flesh could increase the diet uptake of those compounds. The proposal of this work was to increase the understanding in this area and develop new tools to boost the ongoing pear breeding programs.

Following a review of the research on the biosynthesis and accumulation of anthocyanin in pears (Chapter 1) the general aim of the project is reported in Chapter 2.

Chapter 3 reports the results of a molecular analysis of 33 red-fleshed pear accessions, collected in different areas of the Emilia-Romagna region and genotyped with 18 simple sequence repeat (SSR) markers with the aim of improving germplasm conservation strategies for old, red-fleshed pears and for supporting ongoing breeding programs. The molecular profiles revealed both cases of synonymy and homonymy and only 6 unique genotypes were identified. The *S*-allele genotypes were also established in order to highlight the genetic relationships among these landraces. Four of the unique genotypes have been clustered based on pomological data.

Then, in the Chapter 4, the focus of the work was directed to shade light on the putative genomic regions involved in the appearance of this unusual character in pear fruit. For this purpose, a crossing population (‘Carmen’ x ‘Cocomerina Precoce’) segregating for the trait was phenotyped for 2 consecutive years and used for quantitative trait loci (QTL) analysis. The outcome was the identification of a strong QTL in a small genomic region related to the red flesh fruit trait approximately at 27 Mb from the start of LG5. Two candidate genes were

detected in this genomic region: ‘PcMYB114’ and ‘PcABC transporter C2’. Furthermore, the SSR marker, SSR114, designed inside the candidate gene MYB114, was found able to detect the red flesh phenotype segregation in all the red-fleshed pear accessions and segregating progenies tested.

The subsequent step, Chapter 5, of the identification of putative genes involved in red pear fruit flesh was to examine the trend of anthocyanin synthesis and accumulation during the fruit development, from fruit set to ripening time. In order to validate the candidate genes role in this process, three different trials were planned: qPCR and HPLC methods were carried out to correlate the genes expression with the anthocyanin accumulation in ‘Cocomerina Precoce’ and six progenies with different phenotypes of red flesh; and total transcriptome sequencing was used to compare the differential genes expression between red and white-fleshed fruit.

Finally, Chapter 6 reviews and analyses all the earlier study findings while providing new potential future perspectives.

1. General Introduction

Fruits and vegetables are known as sources of healthy compounds, such us polyphenols, flavonoids and anthocyanin. These latter compounds are responsible of the red and purple colour in most of the plant tissues. These molecules are naturally synthesised in different plant tissues and their role is mainly related to attract pollinating insects and seed dispersers, and to protect plants against irradiation damages and pathogens (Zhao *et al.*, 2010; Zhang *et al.*, 2014). Consumers frequently attribute superior organoleptic features to food items with red colour, which raises the value of goods with more intense red colouring.

Interest in genetic control and breeding for higher anthocyanin content in fruits is increasing. In several fruit species, red flesh fruit are known, from kiwifruit, to pitaya (dragon fruit) through different Rosaceae species, such as, cherry, plum, apricot, peach, apple and pear.

1.1. Genetic bases of red flesh fruit in apple

An interest in developing commercial red-fleshed apples has grown in recent years. In the past few years, the poor taste of the wild red-flesh varieties (*e.g.*, *Malus pumila* 'Niedzwetzkyana') has been improved through crossbreeding programs with good-flavoured white-fleshed apples to give a commercially viable red-fleshed eating variety (Deacon, 2016).

One of the first steps of this process was the discovery of a wild red-fleshed apple (*Malus pumila* 'Niedzwetzkyana') in the centre of origins of apple (Tian Shan Mountain forests of Inner and Central Asia) by the Russian botanist Niedzwetzky. Then, Niels Hansen and Albert Etter, two English apple breeders from early 900s, developed two main red-fleshed apples genotypes. Those apples were slightly closer in taste to commercially grown but with an unusual flavour and flesh texture unusual of strawberry, raspberry, or red currant.

Concerning the genetic basis of red-fleshed genotypes, functional alleles of MdMYBA/1/10 has been confirmed to generate red coloration only in fruit skin (Espley *et al.*, 2007; Takos *et al.*, 2006). However, two types of red flesh controls were found. The R6 allele (MdMYB10R6), which has a tandem minisatellite repeat in the promoter region, leads to red skin, red flesh/core, and red leaves through autoregulation (Espley *et al.*, 2009; Würdig *et al.*, 2014). The apples with R6 allele are classified as type 1 (Chagné *et al.*, 2013). In type 2 red-fleshed apples, the coloration of skin is still controlled by MdMYBA/1/10; whereas, fruit flesh colour is regulated by another gene: MdMYB110a (Chagné *et al.*, 2013). MdMYB10R6 of type 1 apples is located on linkage group 9 (Espley *et al.*, 2009). In contrast, MdMYB110a which controls the development of red coloration only in the type 2 fruit flesh mapped on linkage group 17 (Chagné *et al.*, 2013; Umemura *et al.*, 2013). Moreover, the red-fleshed trait of type 2 apples was found to be linked to the S3-RNase allele (Sekido *et al.*, 2010). Recently, in addition to skin colour, several kinds of red-fleshed apples, which are defined as type 2 apples (Chagné *et al.*, 2013), have been released in many countries (Bars-Cortina *et al.*, 2017; Silvestri *et al.*, 2016), *i.e.*, 'Baya Marisa' (Germany), 'Rosette' (England), 'Redlove' (Switzerland), and 'Weirouge' (Germany).

1.2. Genetic bases of red-fleshed fruit in peach

Numerous investigations on the genetics of the blood-flesh characteristic in peaches have been conducted. In seven F2 populations resulting from a 'Harrow Blood' x 'Rutgers Red Leaf 2n' cross, Werner *et al.*, (1998) discovered a segregation ratio of 1:3 blood flesh to white flesh and postulated that the blood-flesh characteristic (*bf*) is controlled by a single recessive gene. Gillen and Bliss (2005) mapped the '*bf*' locus on the top of LG 4. '*Bf*' trait is characterised by anthocyanin accumulation in the mesocarp after the onset of pit hardening and the leaves show a red midrib colour on the abaxial side (Chaparro *et al.*, 1995). Shen *et al.*, (2013) discovered

a new blood-flesh character in Chinese peach variety ‘Wu Yue Xian’. In this cultivar a single dominant locus on LG5 is putatively responsible for blood-flesh. This other phenotype is characterized by anthocyanin accumulation only in mesocarp during the late stages of fruit development (Shen *et al.,* 2013). Blood-flesh in Chinese cultivars is identical to that described in ‘Indian Cling’ (Werner *et al.,* 1998). As peach is native to China (Scorza and Okie, 1991), the blood-flesh trait in Chinese and India peach cultivars may share the same genetic basis, being introduced from China along the Silk Road. Additionally, utilizing an advanced backcross population resulting from a cross between *Prunus davidiana* and cv. 'Summergrand', two quantitative trait loci (QTLs) for the blood-flesh trait were discovered on LG1 and LG3 (Quilot *et al.,* 2004).

According to these findings, the red-flesh phenotype in peaches is a complicated feature that is presumably regulated by several genes (Zhou *et al.,* 2015). As things stand, peach, seems to have at least three distinct genetic regulation for the red flesh phenotypes.

1.3. Red-fleshed fruit in European pear

The red-flesh trait in European pear has known for centuries, nevertheless, the origin of this character is uncertain: red-fleshed pears were first mentioned at the end of XVII century in a manuscript of the Tuscan Academic Pier Antonio Micheli, which cited the ‘Pera Sanguignola’ (literally “bloody pear”). In the following centuries, red-fleshed pears were also reported in France, Belgium and Germany (Leroy, 1867-79; Downing, 1869; Mas, 1872-83; Hedrick, 1921). Those heirloom cultivars exhibited many pomological differences in tree habit, ripening time and/or fruit shape, possibly suggesting multiple genotypes. Moving to our days, red-fleshed pear varieties are reported in several genetic diversity studies in many countries. For instance, in France it is still reported the variety ‘Sanguinole’ (Lespinasse *et al.,* 2010),

‘Rottkottig Frau Ostergotland’ in Sweden, literally red flesh, and ‘Blodpäron’ (Sehic *et al.,* 2012), in Estonia two accessions are conserved at the Garden Research Centre in Polli (EST): ‘Pirnipuu 'Saaremaa Punane’ and ‘Suvisort’, while in Romania ‘Cu miezul roşu` is known (Braniste and Budan 2007). In Bosnia and Herzegovina are still cultivated a group of red-fleshed pear cultivars named ‘Lubenicarka’, the name in Serbian meaning watermelon (Mićić *et al.,* 2012). In Germany, ‘Girnghuber’, ‘Ingolstadt’ and ‘Vampira Pöschke’ are some of the red-fleshed pear reported. In Italy several red accessions are known: ‘Pera Sanguigna’, ‘Briaco’, ‘Briaca’, ‘Ingurien’, ‘Vinata’, ‘Cocomera’ and more. Particularly, in Emilia-Romagna the most known variety among the red-fleshed pears is ‘Pera Cocomerina’, whose cultivation area is located close to a small village named Verghereto (Forlì-Cesena, Italy). Two landraces with different ripening time are included in this group: ‘Cocomerina Precoce’ and ‘Cocomerina Tardiva’.

1.4. Anthocyanin structures

Notable secondary metabolites that are a part of flavonoids are anthocyanin. Generally speaking, the most prevalent anthocyanin has a flavylium cation (2-phenylbenzopyrylium or 2-phenylchromenylium) with 3,5,7-trihydroxylations. More than 650 distinct anthocyanin structures have been discovered in nature to date. Anthocyanin are formed by a carbon skeleton structure that consists of three aromatic rings (C6(A)-C3(C)-C6(B)). The six anthocyanin are created by various functional groups connected in positions 3′ and 5′ (Figure 1.1). The source of over 90% of these structures are only 35 monomeric anthocyanidins (Andersen and Jordheim, 2010). These monomeric anthocyanidins include cyanidin, delphinidin, pelargonidin, malvidin, peonidin, and petunidin. Cyanidin is the most frequent and it could be glycosylated, acylated, methylated, and containing various functional groups to form several different molecules (Shi and Xie, 2014). It is interesting to note that the profile of anthocyanin's

composition can shift in response to various stresses, albeit the biological causes of this phenomenon are still mostly unknown (Kovinich *et al.*, 2014, 2015).

Different colours of anthocyanin are produced as a result of methylation and hydroxylation changes carried out at various places on the ring. (Liu *et al.*, 2021; Table 1.1).

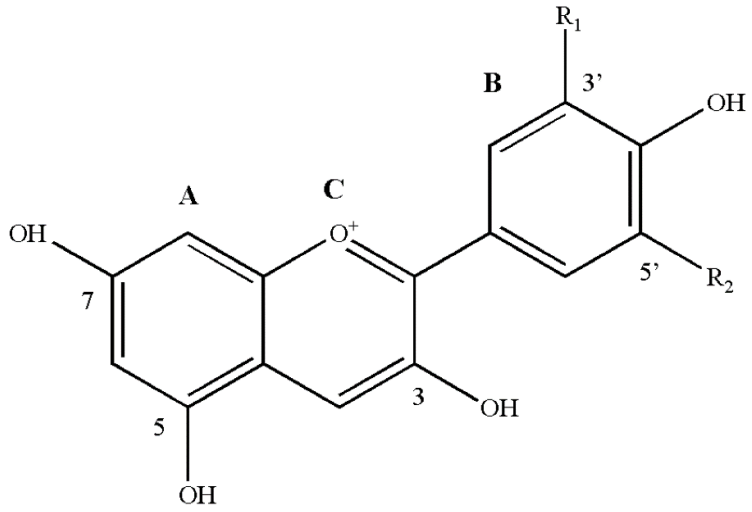

Figure 1.1. Basic chemical structures of anthocyanidin. A, C6; B, C6; C, C3, anthocyanin consisting of α-phenylbenzopyran cations are mainly composed of C6-C3-C6 carbon skeleton structures. R1 and R2, structural groups at various positions (3′ and 5′) on the B ring determine the different anthocyanin (Figure from Liu *et al.*, 2021).

In the molecular form of anthocyanin, pH is crucial. The molecular shape, and therefore colour, can vary when the pH of an aqueous solution is changed (Osawa, 1982). pH has also an effect on the anthocyanin degradation: anthocyanin degrades more quickly at higher pH levels under the same external conditions (Reyes *et al.*, 2007). Moreover, the stability of the chemical structure of anthocyanin is also influenced by the presence of metal ions, oxidative decay, vitamin C, carbohydrates, temperature, and light (Irani *et al.*, 2005; Liu *et al.*, 2019).

Table 1.1. Structural group (R) substitutions in the most common anthocyanin (Table from Liu *et al.*, 2021).

Name (Abbreviations)	Substitution		Colour
	R_1	R_2	
Pelargonidin (Pg)	H	H	Red
Cyanidin (Cy)	OH	H	Magenta
Delphinidin (Dp)	OH	OH	Purple
Peonidin (Pn)	OCH_3	H	Magenta
Petudinin (Pt)	OCH_3	OH	Purple
Malvidin (Mv)	OCH_3	OCH_3	Purple

1.5. Biosynthetic Pathway of Anthocyanin

Anthocyanin are one of the most important flavonoid pigments. They are synthesized through the phenylpropanoid pathway starting from phenylalanine or tyrosine, two aromatic aminoacid constructed by the shikimate pathway. The first step of this pathway is played by phenylalanine ammonia lyase (PAL), or by tyrosine ammonia lyase (TAL) with tyrosine as a substrate, to produce trans-cinnamic acid inside cytoplasm, at the endoplasmic reticulum membrane level (Rasmussen and Dixon, 1999: Park *et al.*, 2015). Going down to the pathway, the trans-cinnamic acid is converted into *p*-coumaric acid (4-coumaric acid or trans-*p*-hydroxycinnamic acid, pHCA) by cinnamate 4-hydroxylase. Alternatively, in some plant species, tyrosine can be converted to p-coumaric acid or even be used as a minor substrate by PAL (Manela *et al.*, 2015; Yoo *et al.*, 2013). The *p*-coumaric acid is usually the most limiting intermediate in this pathway (Nishiyama *et al.*, 2010), is conjugated with coenzyme A to produce *p*-coumaroyl-

CoA by 4-coumarate-CoA ligase. The flavonoid pathway advances with the condensation of p-coumaroyl-CoA with three molecules of malonyl-CoA to produce chalcone by chalcone synthase (CHS; Ferreyra *et al.*, 2012). Chalcone is converted by chalcone isomerase (CHI) to the flavanone naringenin, a central flavonoid intermediate. Thereon, flavanone3-hydroxylase (F3H) converts naringenin into the flavononol dihydrokaempferol, which can be used by flavonoid 3′-hydroxylase (F3′H) to produce dihydroquercetin, or alternatively by flavonoid 3′,5′-hydroxylase (F3′5′H) to form dihydromyricetin. Next, a set of enzymes with broad substrate specificity accepts flavononols to move the pathway forward. Dihydroflavonol 4-reductase (DFR) converts dihydrokaempferol (or the direct products of F3′H or F3′5′H enzymes) into leucoanthocyanidins, which are then converted into coloured anthocyanidins (*e.g.*, cyanidin, pelargonidin, delphinidin) by anthocyanidin synthase (ANS, same as leucocyanidin oxygenase: LDOX). These anthocyanidins can be further modified by transferases, such as methyltransferases (OMT) and acetylases (Sasaki *et al.*, 2014), and further processed by 3-O-glycosyltransferases (3GT, same as UDP-glucose: flavonoid-3-O-glycosyltransferase: UFGT) to produce anthocyanidin-3-O-glucosides, which are chemically stable, water-soluble pigments.

Finally, anthocyanin associate with glutathione S-transferase (GST) for efficient sequestration into the vacuole (Mueller *et al.*, 2000) with the assistance of ABC and MATE transporters localized at the tonoplast (Zhao and Dixon, 2009). Anthocyanin can also be enclosed in membrane-bound bodies (anthocyanin-rich vesicles, often called anthocyanoplasts), which are prevacuolar compartments (Kallam *et al.*, 2017). Furthermore, in some species, the accumulation at high levels of aromatically-acylated anthocyanins in the vacuole leads to the formation of aggregates called anthocyanin vacuolar inclusions (Markham *et al.*, 2000).

The synthesis of anthocyanin in plants is controlled by regulatory genes, typically transcription factor genes (TFs). At present, the identified genes involved in the regulation of the

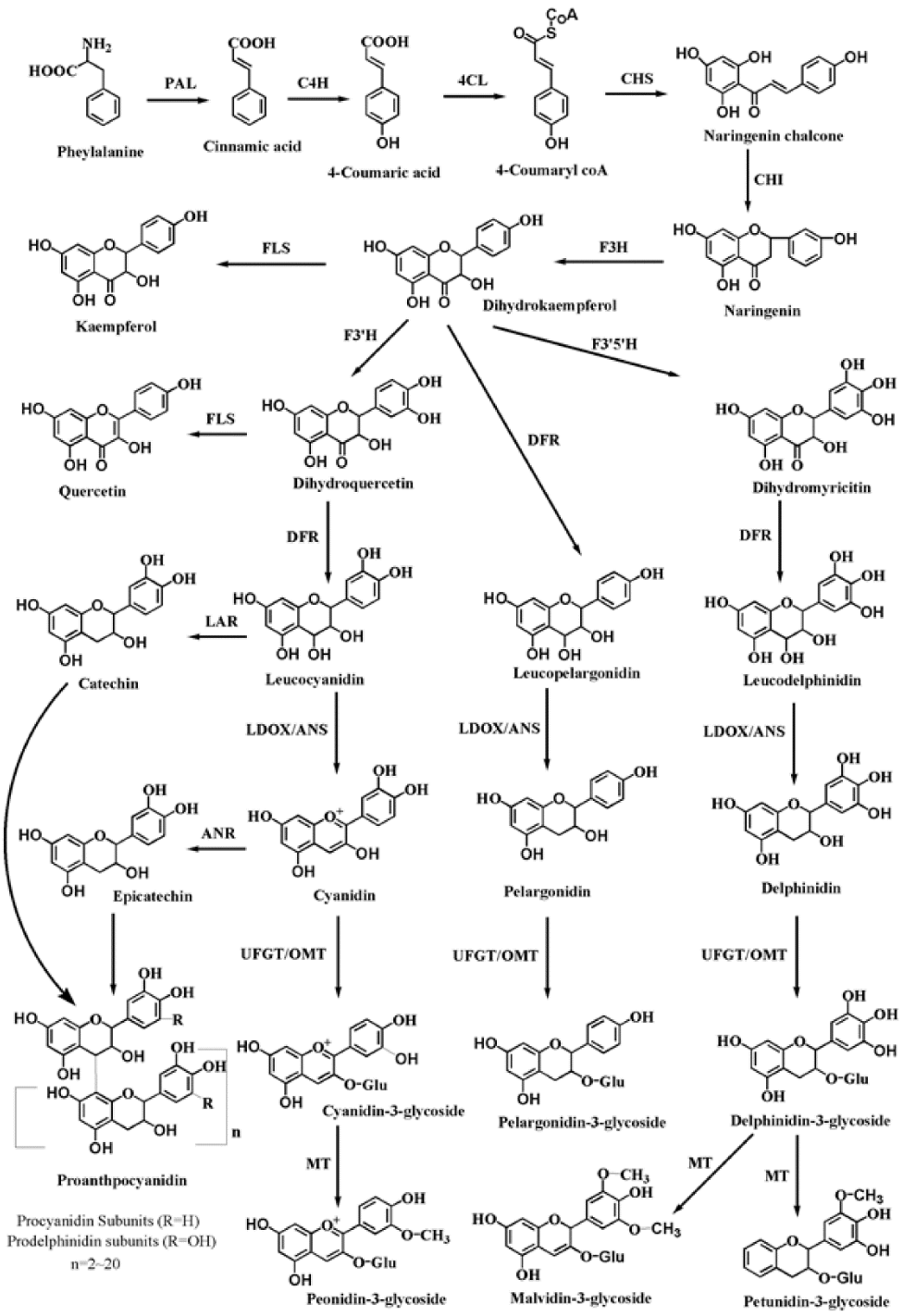

Figure 1.2. The biosynthetic pathway of anthocyanins/proanthocyanidins. PAL, phenylalanine ammonia lyase; C4H, cinnamate 4-hydroxylase; 4CL, 4-coumarate CoA ligase; CHS, chalcone synthase; CHI, chalcone isomerase; F3H, flavanone 3-hydroxylase; F3′H, flavonoid 3′ hydroxylase; F3′5′H, flavonoid 3′5′hydroxylase; FLS, flavonol synthase; DFR, dihydroflavonol 4-reductase; LAR, leucoanthocyanidin reductase; ANR, anthocyanidin reductase; ANS, anthocyanidin synthase; LDOX, leucoanthocyanidin dioxygenase; UFGT, UDP-galactose flavonoid 3-O-galactosyltransferase; OMT, O-methyl transferase; MT, methyltransferase (Figure from Liu *et al.*, 2021).

anthocyanin biosynthetic pathway consist of the myeloblastosis family (MYB) TFs, the basic helix-loop-helix (bHLH) TFs and the tryptophan-aspartic acid repeat (WDR) TFs (Payne *et al.*, 2000; Ramsay *et al.*, 2005). Generally, the members of these three families of regulatory factors mainly depend on the MYB-bHLH-WD40 (MBW) complex to exert their effects (Hichri *et al.*, 2010; Goswami *et al.*, 2018).

1.6. The regulatory mechanism of anthocyanin biosynthesis

Numerous factors influence the process of biosynthesis of anthocyanin, making their regulatory system in plants extremely complex. Since the knowledge had so far, environmental variables, plant hormones, transcription factors, and epigenetic change are the primary contributors to this complexity (Liu *et al.*, 2021).

1.6.1. The MYB/bHLH/WD complex

In plants, the key TF genes that modulate anthocyanin production are the MYB TFs. To control the production of anthocyanin, MYBs proteins typically interact with WD-repeat proteins and bHLH factors (Yan *et al.*, 2020). The transcriptional regulation of target genes and the production, accumulation, and transport of anthocyanin may both be significantly influenced by internal variables includes plant hormones and external factors such as light, temperature, soil fertility, carbohidrates, and drought (Winkel-Shirley, 2002; Xie *et al.*, 2012). Anthocyanin metabolic pathways and related gene transcription in different plant species respond to changes under different conditions (Figure 1.3).

The MYB-bHLH-WDR (MBW) complex directly controls the expression of structural genes during anthocyanin biosynthesis (Ramsay *et al.*, 2005). This regulatory mechanism, which may directly affect the expression of related genes and result in tissue-specific anthocyanin

accumulation depends on R2R3-MYB transcription factors (Jin *et al.*, 2016; Liu *et al.*, 2015). By stabilising the MYB complex or increasing its transcription, the bHLH transcription factors are crucial for the function of R2R3-MYBs (Yan *et al.*, 2020; Zhang *et al.*, 2003). For instance, through interacting with bHLH3 and WD40, several MYB transcription factors, such as MdMYB1, MdMYB9, MdMYB10, and MdMYB114, can increase apple fruit coloration (Ban *et al.*, 2007; Jiang *et al.*, 2021).

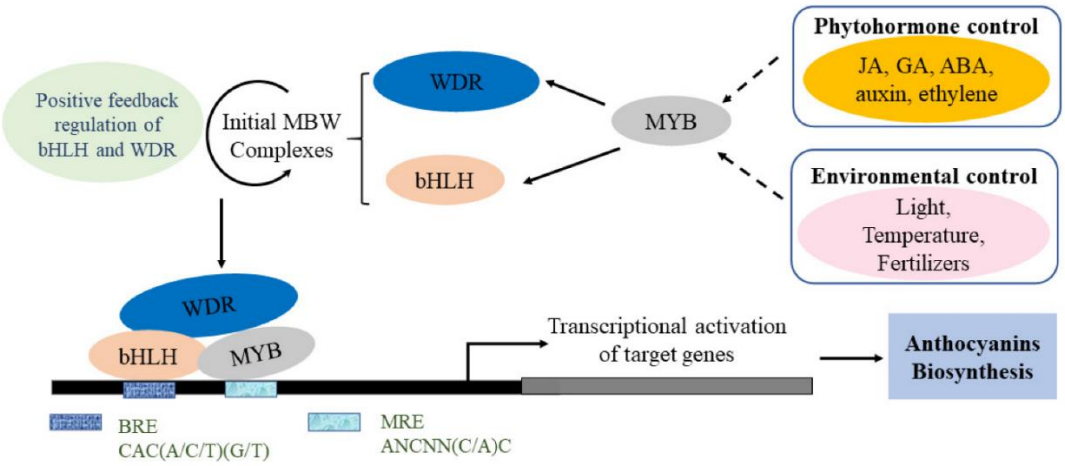

Figure 1.3. Simplified model of the regulatory mechanisms of anthocyanin biosynthesis. Developmental and environmental factors could induce MYB, which then activates WDR and bHLH to form the MBW complex. The MBW complex consists of MRE (MYB recognition elements) and BRE (bHLH recognition elements), which bind to the promoter of the target gene. The transcriptional activation of target genes promotes anthocyanin biosynthesis (Figure from Liu *et al.*, 2021).

According to multiple studies, anthocyanin accumulation, MdMYB1 transcript levels, and the expression of structural genes like MdDFR and MdUFGT are all positively correlated (Takos *et al.*, 2006; Hartmann *et al.*, 2005). The first WD40 protein to be discovered in an apple was MdTTG1, which, like AtTTG1 (Transparent Testa Glabra 1) in Arabidopsis, interacts with MdbHLH3 and MdMYB9 to regulate the expression of downstream structural genes. (Brueggemann *et al.*, 2010). Similar to this, PpMYB10 and PpMYB114 in Asian pears can aid

red pears develop their colour by building a complex with PpbHLH3 (Yao *et al.,* 2018). However, different TFs from the same family can have different functions in the regulation of anthocyanin biosynthesis. The production of anthocyanins is adversely regulated by certain MYB TFs, including Arabidopsis MYBL2, apple MYB16, peach MYB17-20, and strawberry MYB1 (Aharoni *et al.,* 2001; Feng *et al.,* 2010; Xu *et al.,* 2017). A competitive interaction between bHLH subunits and MYBL2 blocks the formation of the MBW complex. The transcription of early biosynthetic genes is increased, and anthocyanin accumulation rises if MYBL2 expression decreases (Liu *et al.,* 2021).

1.6.2. WRKY transcription factor genes

The WRKY TFs belong to one large gene family that regulates a series of physiological processes, including development, senescence and resistance to adverse environments (Peng *et al.,* 2012). WRKY TFs were identified by one or two conserved WRKY domain(s) usually followed by a zinc-finger motif. The WRKY TF contains a specific nucleic acid sequence (C/T)TGAC(T/C) named the W-box, which regulates the defence response to various stresses by self-regulation, and it could recognize and bind to the W-box or other promoters of the WRKY TFs to generate biological effects by achieving crosstalk of different WRKY25. Compared with the MYB TFs, WRKY is an emerging player in the plant signalling regulation network. The interaction between the upstream regulator of the WRKY TF and the downstream target gene constitutes a complex regulatory network (Zentgraf *et al.,* 2010; Chen *et al.,* 2012).

Recently, several reports have shown that WRKY proteins have an important role in the regulation of anthocyanin biosynthesis. For instance, GbWRKY1 in *Gossypium barbadense* was confirmed to have a positive correlation with anthocyanin accumulation when expressed in *Arabidopsis thaliana* (Xu *et al.,* 2012). In a previous study, AtWRKY75 responded to low

phosphate stress by decreasing anthocyanin accumulation in *A. thaliana* seedlings (Devaiah *et al.,* 2007). Moreover, the AtWRKY41 mutation resulted in increased anthocyanin content in *A. thaliana* rosette leaves (Duan *et al.,* 2018). AtWRKY6 promotes PR1 promoter activity, which is related to senescence and pathogen defence, and the plant responds to abiotic and biotic stresses by decreasing anthocyanin accumlation. It was recently discovered that the WRKY TF PhPH3 in petunias has a downstream role of the MBW complex and corresponds with variations in the colour of the petals (Verweij *et al.,* 2016). Furthermore, Amato *et al.,* (2017) demonstrated that VvWRKY26 gene in *Vitis vinifera* causes flavonoid accumulation. MdWRKY40 is a crucial regulator of wounding-induced anthocyanin production in apples (An *et al.,* 2019). According to Yang *et al.,* (2015), the red-skinned pear's anthocyanin biosynthesis was connected to the WRKY family. A temporary expression system was used to confirm the impact of anthocyanin accumulations following the co-transformation of PyWRKY31 or PyWRKY26 with its partners PyMYB10, PyMYB114, and PybHLH3 in tobacco leaves and strawberry receptacles (Li *et al.,* 2020).

1.6.3. BBox/BZIP transcription factor genes

Zinc finger transcription factors (TFs) constitute one of the most important and largest gene families in plants (approximately 15% of the total), which can be divided into multiple subfamilies based on their structures and functions (Ciftci-Yilmaz *et al.,* 2008). B-box (BBX) genes constitute a subfamily of zinc-finger TF family, and they exist in all eukaryotic genomes (Khanna *et al.,* 2009; Gangappa *et al.,* 2014). BBX proteins usually possess one or two B-box domain(s) required for transcriptional regulation and protein-protein interaction in the N-terminal region (Khanna *et al.,* 2009; Gangappa *et al.,* 2014; Talar *et al.,* 2021). In red pears, PpBBX16, has found to be a positive regulator of light-induced anthocyanin accumulation (Tao *et al.,* 2018). The PpBBX16-PpHY5 complex stimulates the promoter activity of PpMYB10

and subsequently strongly enhances light-induced anthocyanin accumulation, and the overexpression of PpBBX16 has also been found to promote anthocyanin accumulation in pear fruits skin (Liu *et al.,* 2013). As a positive regulator, PpBBX18 directly interacts with PpHY5, and the heterodimer PpBBX18-PpHY5 regulates anthocyanin accumulation by inducing PpMYB10 transcription (Tao *et al.,* 2020); conversely, as a negative regulator, PpBBX21 can physically interact with PpBBX18 and PpHY5, repressing anthocyanin biosynthesis by hindering the formation of the PpHY5-PpBBX18 complex (Tao *et al.,* 2018; Bai *et al.,* 2019).

1.6.4. NAC transcription factors

One of the biggest TF families consists of the plant-specific NAC (NAM, ATAF1/2, and CUC2) proteins, which are distinguished by a conserved NAC domain in the N-terminal region (Ooka *et al.,* 2003, Olsen *et al.,* 2005). Even though it has been amply proven that this family is involved in the regulation of many biological mechanisms, from plants growth to response to stresses, only a few members of the NAC family have been discovered as regulators of anthocyanin biosynthesis (Morishita *et al.,* 2009, Zhou *et al.,* 2015, Mahmood *et al.,* 2016). Under high-light stress, it was shown that ANAC078 in Arabidopsis increased anthocyanin production, however JUB1/ANAC042 and ANAC032 suppressed anthocyanin biosynthesis (Morishita *et al.,* 2009, Mahmood *et al.,* 2016). A NAC was found to be highly overexpressed in blood-fleshed peaches as compared to non-red-fleshed peaches and PpeNAC1 helped in anthocyanin accumulation in tobacco by interacting with PpeMYB10 (Zhou *et al.,* 2015). In the red-fleshed apple cultivar ‘Redlove’, overexpression of MdNAC42 in apple calli resulted in the up-regulation of flavonoid pathway genes, including MdCHS, MdCHI, MdF3H, MdDFR, MdANS and MdUFGT, thereby increasing the accumulation of anthocyanins (Zhang *et al.,* 2020). In pear a total of 185 PpNAC genes were found, of which 148 were mapped on the 17 chromosomes, while 37 were located on unanchored scaffolds. Among them, PpNACs

61, 70 (2A), 172, 176 and 23 (4E) were associated with fruit pigmentations in blue light (Ahmad *et al.,* 2018).

1.6.5. Light, Temperature and other Regulatory Factors

Light is one of the most important factors that affects plant growth. Additionally, it significantly affects the synthesis of anthocyanin. Numerous kinds of transduction signals including photoreactions and associated gene expression are activated by photostimulation in the photoreceptors (Zhang *et al.,* 2018). Some key components of the light signal, including constitutive photomorphogenic 1 (COP1), suppressor of PyHA (SPA), and elongated hypocotyl 5 (HY5), are implicated in this process. Generally speaking, HY5 may target but not activate the promoters of genes involved in anthocyanin production (Hoecker *et al.,* 2017; An *et al.,* 2019). Furthermore, several BBX proteins have been shown to interact with HY5 and promote the synthesis of anthocyanins (Wei *et al.,* 2016; Job *et al.,* 2018).

Studies have revealed that the DNA methylation antagonist 5-azacytidine has the ability of inducing red colour in apple and peach fruits. Demethylation and methylation of DNA additionally have significant roles in the regulation of anthocyanin accumulation (Telias *et al.,* 2011; Zhu *et al.,* 2015). For instance, a particular DNA methylation of the RsMYB1 promoter in red-fleshed radish suppresses anthocyanin production (Wang *et al.,* 2020). Furthermore, microRNAs are essential for the manufacture of anthocyanins. For instance, miR156 controls anthocyanin biosynthesis in poplar and Arabidopsis by targeting SQUAMOSA PROMOTER BINDING PROTEIN-LIKE (SPL) (Gou *et al.,* 2011; He *et al.,* 2019; Wang *et al.,* 2020), and mdm-miR828 blocks accumulation of anthocyanin in response to elevated temperature in *Malus* (Zhang *et al.,* 2020).

References

- Aharoni, A., De Vos, C. R., Wein, M., Sun, Z., Greco, R., Kroon, A., ... & O'Connell, A. P. (2001). The strawberry FaMYB1 transcription factor suppresses anthocyanin and flavonol accumulation in transgenic tobacco. The Plant Journal, 28(3), 319-332.
- Amato, A., Cavallini, E., Zenoni, S., Finezzo, L., Begheldo, M., Ruperti, B., & Tornielli, G. B. (2017). A grapevine TTG2-like WRKY transcription factor is involved in regulating vacuolar transport and flavonoid biosynthesis. Frontiers in Plant Science, 7, 1979.
- An, J. P., Qu, F. J., Yao, J. F., Wang, X. N., You, C. X., Wang, X. F., & Hao, Y. J. (2017). The bZIP transcription factor MdHY5 regulates anthocyanin accumulation and nitrate assimilation in apple. Horticulture research, 4.
- An, J. P., Zhang, X. W., You, C. X., Bi, S. Q., Wang, X. F., & Hao, Y. J. (2019). Md WRKY 40 promotes wounding-induced anthocyanin biosynthesis in association with Md MYB 1 and undergoes Md BT 2-mediated degradation. New Phytologist, 224(1), 380-395.
- An, J. P., Wang, X. F., Espley, R. V., Lin-Wang, K., Bi, S. Q., You, C. X., & Hao, Y. J. (2020). An apple B-Box protein MdBBX37 modulates anthocyanin biosynthesis and hypocotyl elongation synergistically with MdMYBs and MdHY5. Plant and Cell Physiology, 61(1), 130-143.
- Bai, S., Tao, R., Yin, L., Ni, J., Yang, Q., Yan, X., ... & Teng, Y. (2019). Two B-box proteins, PpBBX18 and PpBBX21, antagonistically regulate anthocyanin biosynthesis via competitive association with Pyrus pyrifolia ELONGATED HYPOCOTYL 5 in the peel of pear fruit. The Plant Journal, 100(6), 1208-1223.
- Baldini E. (1995) – Giorgio Gallesio. I giornali dei viaggi. Trascrizione, note e commento di Enrico Baldini. Firenze, Nuova stamperia Parenti.
- Baldini E. (2004) – Cinque secoli di pomologia italiana. Tipolito Tamari snc, Bologna.
- Ban, Y., Honda, C., Hatsuyama, Y., Igarashi, M., Bessho, H., & Moriguchi, T. (2007). Isolation and functional analysis of a MYB transcription factor gene that is a key regulator for the development of red coloration in apple skin. Plant and cell physiology, 48(7), 958-970.

- Chen, L., Song, Y., Li, S., Zhang, L., Zou, C., & Yu, D. (2012). The role of WRKY transcription factors in plant abiotic stresses. Biochimica et Biophysica Acta (BBA)-Gene Regulatory Mechanisms, 1819(2), 120-128.
- Ciftci-Yilmaz S, Mittler R. The zinc finger network of plants. Cell Mol Life Sci. 2008;65(7–8):1150–60.
- Deacon, N. The Diversity of Red Fleshed Apples, Vol. 2017. http://www.suttonelms.org.uk/apple104.html.
- Devaiah, BN, Arthikeyan, AS, Raghothama, KG. WRKY75 transcription factor is a modulator of phosphate acquisition and root development in Arabidopsis. Plant Physiol. (2007) 143, 1789–1801 1851818 10.1104/pp.106.093971.
- Duan, S *et al.*, Functional characterization of a heterologously expressed Brassica napus WRKY41-1 transcription factor in regulating anthocyanin biosynthesis in Arabidopsis thaliana. Plant Sci. (2018) 268, 47–53 10.1016/j.plantsci.2017.12.010 29362083.
- Dussi M.C., Sugar D., Wrolstad R.E., 1995. Characterizing and quantifying anthocyanins in red pears and the effect of light quality on fruit color. Journal of the American Society for Horticultural Science, 120: 785–789.
- Feng, S., Wang, Y., Yang, S., Xu, Y., & Chen, X. (2010). Anthocyanin biosynthesis in pears is regulated by a R2R3-MYB transcription factor PyMYB10. Planta, 232(1), 245-255.
- Fischer T.C., Gosch C., Pfeiffer J., Halbwirth H., Halle C., Stich K., Forkmann G., 2007. Flavonoid genes of pear (Pyrus communis). Trees-Structure and Function, 21: 521–529
- Francis F.J., 1970. Anthocyanins in pears. HortScience, 5: 42
- Gangappa SN, Botto JF. The BBX family of plant transcription factors. Trends Plant Sci. 2014;19(7):460–70.
- Gillen, A.M. and Bliss, F.A. (2005) Identification and mapping of markers linked to the Mi gene for root-knot nematode resistance in peach. J. Am. Soc. Hortic. Sci. 130, 24–33.
- Goswami, G., Nath, U. K., Park, J. I., Hossain, M. R., Biswas, M. K., Kim, H. T., ... & Nou, I. S. (2018). Transcriptional regulation of anthocyanin biosynthesis in a high-anthocyanin resynthesized Brassica napus cultivar. Journal of Biological Research-Thessaloniki, 25(1), 1-15.

- Gou, J. Y., Felippes, F. F., Liu, C. J., Weigel, D., & Wang, J. W. (2011). Negative regulation of anthocyanin biosynthesis in Arabidopsis by a miR156-targeted SPL transcription factor. The Plant Cell, 23(4), 1512-1522.
- Hartmann, U., Sagasser, M., Mehrtens, F., Stracke, R., & Weisshaar, B. (2005). Differential combinatorial interactions of cis-acting elements recognized by R2R3-MYB, BZIP, and BHLH factors control light-responsive and tissue-specific activation of phenylpropanoid biosynthesis genes. Plant molecular biology, 57(2), 155-171.
- He, J. and Giusti, M.M. (2010) Anthocyanins: natural colorants with health-promoting properties. Ann. Rev. Food Sci. Technol. 1(1), 163–187.
- He, L., Tang, R., Shi, X., Wang, W., Cao, Q., Liu, X., ... & Jia, X. (2019). Uncovering anthocyanin biosynthesis related microRNAs and their target genes by small RNA and degradome sequencing in tuberous roots of sweetpotato. BMC plant biology, 19(1), 1-19.
- Hichri, I., Heppel, S. C., Pillet, J., Léon, C., Czemmel, S., Delrot, S., ... & Bogs, J. (2010). The basic helix-loop-helix transcription factor MYC1 is involved in the regulation of the flavonoid biosynthesis pathway in grapevine. Molecular plant, 3(3), 509-523.
- Hoecker, U. (2017). The activities of the E3 ubiquitin ligase COP1/SPA, a key repressor in light signaling. Current opinion in plant biology, 37, 63-69.
- Hu, J., Fang, H., Wang, J., Yue, X., Su, M., Mao, Z., ... & Chen, X. (2020). Ultraviolet B-induced MdWRKY72 expression promotes anthocyanin synthesis in apple. Plant Science, 292, 110377.
- Huang J, Zhao X, Weng X, Wang L, Xie W. The rice B-box zinc finger gene family: genomic identification, characterization, expression profiling and diurnal analysis. PLoS One. 2012;7(10): e48242.
- Irani, N. G., & Grotewold, E. (2005). Light-induced morphological alteration in anthocyanin-accumulating vacuoles of maize cells. BMC Plant Biology, 5(1), 1-15.
- Jiang, S., Sun, Q., Zhang, T., Liu, W., Wang, N., & Chen, X. (2021). MdMYB114 regulates anthocyanin biosynthesis and functions downstream of MdbZIP4-like in apple fruit. Journal of Plant Physiology, 257, 153353.
- Jin, W., Wang, H., Li, M., Wang, J., Yang, Y., Zhang, X., ... & Zhang, K. (2016). The R 2 R 3 MYB transcription factor P av MYB 10.1 involves in anthocyanin

biosynthesis and determines fruit skin colour in sweet cherry (P runus avium L.). Plant Biotechnology Journal, 14(11), 2120-2133.

- Job, N., Yadukrishnan, P., Bursch, K., Datta, S., & Johansson, H. (2018). Two B-box proteins regulate photomorphogenesis by oppositely modulating HY5 through their diverse C-terminal domains. Plant Physiology, 176(4), 2963-2976.
- Khanna R, Kronmiller B, Maszle DR, Coupland G, Holm M, Mizuno T, *et al.*, The Arabidopsis B-box zinc finger family. Plant Cell. 2009;21(11):3416–20.
- Li, X., Zhang, J. Y., Gao, W. Y., Wang, Y., Wang, H. Y., Cao, J. G., & Huang, L. Q. (2012). Chemical composition and anti-inflammatory and antioxidant activities of eight pear cultivars. Journal of agricultural and food chemistry, 60(35), 8738-8744.
- Li, S., Wang, W., Gao, J., Yin, K., Wang, R., Wang, C., ... & Qiu, J. L. (2016). MYB75 phosphorylation by MPK4 is required for light-induced anthocyanin accumulation in Arabidopsis. The Plant Cell, 28(11), 2866-2883.
- Lin L.Z., Harnly J.M., 2008. Phenolic compounds and chromatographic profiles of pear skins (Pyrus spp.). Journal of Agricultural and Food Chemistry, 56: 9094–9101.
- Liu, Z., Shi, M. Z., & Xie, D. Y. (2014). Regulation of anthocyanin biosynthesis in Arabidopsis thaliana red pap1-D cells metabolically programmed by auxins. Planta, 239(4), 765-781.
- Liu, W., Wang, Y., Yu, L., Jiang, H., Guo, Z., Xu, H., ... & Wang, N. (2019). MdWRKY11 participates in anthocyanin accumulation in red-fleshed apples by affecting MYB transcription factors and the photoresponse factor MdHY5. Journal of agricultural and food chemistry, 67(32), 8783-8793.
- Liu, J., Osbourn, A., & Ma, P. (2015). MYB transcription factors as regulators of phenylpropanoid metabolism in plants. Molecular plant, 8(5), 689-708.
- Liu, H., Liu, Z., Wu, Y., Zheng, L., & Zhang, G. (2021). Regulatory mechanisms of anthocyanin biosynthesis in apple and pear. International Journal of Molecular Sciences, 22(16), 8441.
- Mahmood K, Xu Z, El-Kereamy A, Casaretto JA, Rothstein SJ (2016) The Arabidopsis transcription factor ANAC032 represses anthocyanin biosynthesis in response to high sucrose and oxidative and abiotic stresses. Front Plant Sci 7:1548.
- Mićić, N., Đurić, G., & Salkić, B. (2012). Pomological characterisation of pear varieties of "Lubenicarka" group. AGRO-KNOWLEDGE JOURNAL, 13(1), 15-30.

- Morishita T, Kojima Y, Maruta T, Nishizawa-Yokoi A, Yabuta Y, Shigeoka S (2009) Arabidopsis NAC transcription factor, ANAC078, regulates flavonoid biosynthesis under highlight. Plant Cell Physiol 50:2210–2222.
- Ngo T., Zhao Y.Y., 2009. Stabilization of anthocyanins on thermally processed red D'Anjou pears through complexation and polymerization. LWT-Food Science and Technology, 42: 1144–1152
- Olsen AN, Ernst HA, Leggio LL, Skriver K (2005) NAC transcription factors: structurally distinct, functionally diverse. Trends Plant Sci 10:79–87.
- Ooka H, Satoh K, Doi K (2003) Comprehensive analysis of NAC family genes in Oryza sativa and Arabidopsis thaliana. DNA Res 10:239–247.
- Osawa, Y. (1982). Copigmentation of anthocyanins. Anthocyanins as food colors, 41-68.
- Payne, C. T., Zhang, F., & Lloyd, A. M. (2000). GL3 encodes a bHLH protein that regulates trichome development in Arabidopsis through interaction with GL1 and TTG1. Genetics, 156(3), 1349-1362.
- Peng, X., Hu, Y., Tang, X., Zhou, P., Deng, X., Wang, H., & Guo, Z. (2012). Constitutive expression of rice WRKY30 gene increases the endogenous jasmonic acid accumulation, PR gene expression and resistance to fungal pathogens in rice. Planta, 236(5), 1485-1498.
- Pierantoni, L., Dondini, L., De Franceschi, P., Musacchi, S., Winkel, B. S., & Sansavini, S. (2010). Mapping of an anthocyanin-regulating MYB transcription factor and its expression in red and green pear, Pyrus communis. Plant Physiology and Biochemistry, 48(12), 1020-1026.
- Quilot, B., Wu, B.H., Kervella, J., Génard, M., Foulongne, M. and Moreau, K. (2004) QTL analysis of quality traits in an advanced backcross between Prunus persica cultivars and the wild relative species P. davidiana. Theor. Appl. Genet. 109, 884–897.
- Ramsay, N. A., & Glover, B. J. (2005). MYB–bHLH–WD40 protein complex and the evolution of cellular diversity. Trends in plant science, 10(2), 63-70.
- Reyes, L. F., & Cisneros-Zevallos, L. (2007). Degradation kinetics and colour of anthocyanins in aqueous extracts of purple-and red-flesh potatoes (Solanum tuberosum L.). Food Chemistry, 100(3), 885-894.

- Robatzek, S., & Somssich, I. E. (2002). Targets of AtWRKY6 regulation during plant senescence and pathogen defense. Genes & development, 16(9), 1139-1149.
- Sehic, J., Garkava-Gustavsson, L., Fernández-Fernández, F., & Nybom, H. (2012). Genetic diversity in a collection of European pear (Pyrus communis) cultivars determined with SSR markers chosen by ECPGR. Scientia horticulturae, 145, 39-45.
- Shan, B., Bao, G., Shi, T. *et al.*, Genome-wide identification of BBX gene family and their expression patterns under salt stress in soybean. BMC Genomics 23, 820 (2022).
- Shen, Z., Confolent, C., Lambert, P., Poëssel, J., Quilot-Turion, B., Yu, M., Ma, R. and Pascal, T. (2013) Characterization and genetic mapping of a new blood-flesh trait controlled by the single dominant locus DBF in peach. Tree Genet. Genomes, 9, 1435–1446.
- Shin, D. H., Choi, M., Kim, K., Bang, G., Cho, M., Choi, S. B., ... & Park, Y. I. (2013). HY5 regulates anthocyanin biosynthesis by inducing the transcriptional activation of the MYB75/PAP1 transcription factor in Arabidopsis. FEBS letters, 587(10), 1543-1547.
- Shuangyi Zhang, Yixi Chen, Lingling Zhao, Chenqi Li, Jingyun Yu, Tongtong Li, Weiyao Yang, Shengnan Zhang, Hongyan Su, Lei Wang, A novel NAC transcription factor, MdNAC42, regulates anthocyanin accumulation in red-fleshed apple by interacting with MdMYB10, Tree Physiology, Volume 40, Issue 3, March 2020, Pages 413–423, https://doi.org/10.1093/treephys/tpaa004
- Takos, A. M., Jaffé, F. W., Jacob, S. R., Bogs, J., Robinson, S. P., & Walker, A. R. (2006). Light-induced expression of a MYB gene regulates anthocyanin biosynthesis in red apples. Plant physiology, 142(3), 1216-1232.
- Talar U, Kielbowicz-Matuk A. Beyond Arabidopsis: BBX regulators in crop plants. Int J Mol Sci. 2021;22(6):2906.
- Tao, R., Bai, S., Ni, J., Yang, Q., Zhao, Y., & Teng, Y. (2018). The blue light signal transduction pathway is involved in anthocyanin accumulation in 'Red Zaosu'pear. Planta, 248(1), 37-48.
- Tao, R., Yu, W., Gao, Y., Ni, J., Yin, L., Zhang, X., ... & Teng, Y. (2020). Light-induced basic/helix-loop-helix64 enhances anthocyanin biosynthesis and undergoes CONSTITUTIVELY PHOTOMORPHOGENIC1-mediated degradation in pear. Plant physiology, 184(4), 1684-1701.

- Telias, A., Lin-Wang, K., Stevenson, D. E., Cooney, J. M., Hellens, R. P., Allan, A. C., ... & Bradeen, J. M. (2011). Apple skin patterning is associated with differential expression of MYB10. BMC Plant Biology, 11(1), 1-15.
- Verweij, W., Spelt, C. E., Bliek, M., de Vries, M., Wit, N., Faraco, M., ... & Quattrocchio, F. M. (2016). Functionally similar WRKY proteins regulate vacuolar acidification in petunia and hair development in Arabidopsis. The Plant Cell, 28(3), 786-803.
- Wang, Y., Liu, W., Wang, X., Yang, R., Wu, Z., Wang, H., ... & Fu, C. (2020). MiR156 regulates anthocyanin biosynthesis through SPL targets and other microRNAs in poplar. Horticulture research, 7.
- Wang, Q., Wang, Y., Sun, H., Sun, L., & Zhang, L. (2020). Transposon-induced methylation of the RsMYB1 promoter disturbs anthocyanin accumulation in red-fleshed radish. Journal of experimental botany, 71(9), 2537-2550.
- Wei, C. Q., Chien, C. W., Ai, L. F., Zhao, J., Zhang, Z., Li, K. H., ... & Wang, Z. Y. (2016). The Arabidopsis B-box protein BZS1/BBX20 interacts with HY5 and mediates strigolactone regulation of photomorphogenesis. Journal of Genetics and Genomics, 43(9), 555-563.
- Werner, D.J., Creller, M.A. and Chaparro, J.X. (1998) Inheritance of the blood-flesh trait in peach. HortScience, 33, 1243–1246.
- Winkel-Shirley, B. (2002). Biosynthesis of flavonoids and effects of stress. Current opinion in plant biology, 5(3), 218-223.
- Xu, H., Wang, N., Liu, J., Qu, C., Wang, Y., Jiang, S., ... & Chen, X. (2017). The molecular mechanism underlying anthocyanin metabolism in apple using the MdMYB16 and MdbHLH33 genes. Plant Molecular Biology, 94(1), 149-165.
- Yan, S., Chen, N., Huang, Z., Li, D., Zhi, J., Yu, B., ... & Qiu, Z. (2020). Anthocyanin Fruit encodes an R2R3-MYB transcription factor, SlAN2-like, activating the transcription of SlMYBATV to fine-tune anthocyanin content in tomato fruit. New Phytologist, 225(5), 2048-2063.
- Yang, Y., Yao, G., Yue, W., Zhang, S., & Wu, J. (2015). Transcriptome profiling reveals differential gene expression in proanthocyanidin biosynthesis associated with red/green skin color mutant of pear (Pyrus communis L.). Frontiers in Plant Science, 6, 795.

- Zentgraf, U, Laun, T, Miao, Y. The complex regulation of WRKY53, during leaf senescence of Arabidopsis thaliana. Eur. J. Cell Biol. (2010) 89, 133–137
- Zhang, F., Gonzalez, A., Zhao, M., Payne, C. T., & Lloyd, A. (2003). A network of redundant bHLH proteins functions in all TTG1-dependent pathways of Arabidopsis.
- Zhang, X. D., Allan, A. C., Chen, X. Q., Fan, L., Chen, L. M., Shu, Q., ... & Li, K. Z. (2012). Coloration, anthocyanin profile and metal element content of Yunnan Red Pear (Pyrus pyrifolia). Horticultural Science, 39(4), 164-171.
- Zhang, Y., Butelli, E., & Martin, C. (2014). Engineering anthocyanin biosynthesis in plants. Current opinion in plant biology, 19, 81-90.
- Zhang, Y., Xu, S., Cheng, Y., Peng, Z., & Han, J. (2018). Transcriptome profiling of anthocyanin-related genes reveals effects of light intensity on anthocyanin biosynthesis in red leaf lettuce. PeerJ, 6, e4607.
- Zhang, B., Yang, H. J., Yang, Y. Z., Zhu, Z. Z., Li, Y. N., Qu, D., & Zhao, Z. Y. (2020). mdm-miR828 participates in the feedback loop to regulate anthocyanin accumulation in apple peel. Frontiers in plant science, 11, 608109.
- Zhao, J., & Dixon, R. A. (2010). The ‘ins’ and ‘outs’ of flavonoid transport. Trends in plant science, 15(2), 72-80.
- Zhou H, Lin-Wang K, Wang H, Gu C, Dare AP, Espley RV, He H, Allan AC, Han Y (2015) Molecular genetics of blood-fleshed peach reveals activation of anthocyanin biosynthesis by NAC transcription factors. Plant J 82:105–121.
- Zhu, Z., Wang, H., Wang, Y., Guan, S., Wang, F., Tang, J., ... & Lu, Y. (2015). Characterization of the cis elements in the proximal promoter regions of the anthocyanin pathway genes reveals a common regulatory logic that governs pathway regulation. Journal of experimental botany, 66(13), 3775-3789.

2. Thesis Overview and General Aim

Red-fleshed fruit is a character which interest is increasing in several commercial species, such as apple and peach. Some old landraces with this trait are known in pear and several breeding programs have already been started in order to obtain new élite varieties. In pear, the red colour is the result of the presence of anthocyanin. This group of secondary metabolites are strong antioxidant molecules fundamental in human health. High anthocyanin content in the fruit flesh could increase the diet uptake of those compounds. The knowledge about this fascinating trait in pear was, until now, limited. As things stand, the proposal of this work was to increase the understanding in this area and develop new tools to boost the ongoing pear breeding programs.

The first part of this thesis arises from the need to investigate the genetic relationships among the different red-fleshed pear landraces collected in Emilia-Romagna region. To achieve this, different approaches were used; a genetic-based method (fingerprinting analysis) to estimate the genetic distances among the selected genotypes and a pomological method to evaluate differences of the fruit characters.

Then, the focus of the work was directed to shade light on the putative genomic regions involved in the appearance of this unusual character in pear fruit. For this purpose, a crossing population (‘Cocomerina Precoce’ x ‘Carmen’) segregating for the trait was phenotyped for two consecutive years and used for quantitative trait loci (QTL) analysis. By the identification of QTLs related to the anthocyanin accumulation, molecular markers able to help the selection for red flesh fruit in pear breeding, were developed and validated in different progenies having different source of red.

The subsequent step of the identification of putative genes involved in red pear fruit flesh was to examine the trend of anthocyanin synthesis and accumulation during the fruit development stages, from fruit set to ripening time. In order to validate the candidate genes role in this

process, three different trials were planned: qPCR and HPLC methods were carried out to correlate the genes expression with the anthocyanin accumulation in ‘Cocomerina Precoce’ and six progeny offsprings with different phenotypes of red flesh; and total transcriptome sequencing was used to compare the differential genes expression between red and white-fleshed fruit.

3. Characterization of Red-Fleshed Pear Accessions from Emilia-Romagna Region

(From Bergonzoni *et al.*, 2023. Scientia Horticulturae, Volume 312, 111857. https://doi.org/10.1016/j.scienta.2023.111857)

Abstract

Germplasm collections represent a reservoir of traits and genes that might be used in breeding programs to cope with the evolving market demand. Some old pear accessions still cultivated in the Apennine Mountains in Italy possess a red flesh fruit. This paper reports the molecular analysis of 33 red-fleshed pear accessions, collected in different areas of the Emilia-Romagna region and genotyped with 18 simple sequence repeat (SSR) markers with the aim of improving germplasm conservation strategies for old, red-fleshed pears and for supporting ongoing breeding programs. The molecular profiles revealed both cases of synonymy and homonymy and only 6 unique genotypes were identified. S-genotypes were also established in order to highlight the genetic relationships among these landraces. Four of the unique genotypes have been clustered based on pomological data.

3.1. Introduction

Pear cultivation has had a great importance in Italy since Roman times, as evidenced by the description of more than 40 varieties of pears by Pliny the Elder (Hendrick, 1921). In particular, in Emilia-Romagna (ER) pears have been cultivated for a very long time and the environmental variability of this region promoted the development of a rich local germplasm. The ancient landraces must be preserved not only because of their cultural value but also for their high genetic variability, mostly not yet exploited by breeders. Although often lacking in quality in respect to the modern varieties, ancient pear landraces could be used for introgressing valuable traits such as longer shelf-life, precocity of ripening, resilience to environmental or biotic stresses and to introduce peculiar fruit traits, including the red flesh (Sansavini, 2020). The most known variety among the red-fleshed pears in Emilia-Romagna is 'Pera Cocomerina', whose cultivation area is located close to a small village named Verghereto (Forlì-Cesena, Italy). In Italy, 'Pera Cocomerina' is recognised as 'Slow Food' presidium (https://www.slowfood.com/) (https://www.fondazioneslowfood.com/it/presidi-slow-food/pera-cocomerina/) and every year the 'Pera Cocomerina Fair' takes place in the Verghereto village where this pear variety and its by-products (*i.e.* jam, liquors,..) are promoted (https://www.peracocomerina.it/beta/le-sagre/).

The origin of these accessions is uncertain: red-fleshed pears were first mentioned at the end of XVII century in a manuscript of the Tuscan Academic Pier Antonio Micheli which cited the 'Pera Sanguignola' (literally "bloody pear"). In the following centuries, red-fleshed pears were also reported in France, Belgium and Germany (Leroy, 1867-79; Downing, 1869; Mas, 1872-83; Hedrick, 1921). Those heirloom cultivars exhibited many pomological differences in tree habit, ripening time and/or fruit shape, possibly suggesting multiple genotypes. Red flesh is an interesting trait for pear breeding due to the well-known nutraceutical value of anthocyanin in

the diet. Their beneficial effects on human health are now widely reported and range from reducing the risk of cardiovascular diseases and preventing the onset of cancer (Seeram *et al.*, 2004; Stevenson and Hurst, 2007; Butelli *et al.,* 2008; Manach *et al.,* 2009; Espley *et al.,* 2014; Antognoni *et al.,* 2020). In particular, the beneficial property of 'Pera Cocomerina' have been already reported in literature by Bucchini *et al.,* (2016), who described the high level of antioxidant compounds contained in these fruits.

There is an increase in the number of varieties with red skin colour on the market for several fruit crops including apricot (Bassi and Foschi, 2019), peaches (Chavez *et al.,* 2019), pears (Brewer and Volz, 2019; Caracciolo *et al.,* 2018) and apples (Chen *et al.,* 2021). The red-flesh trait was introgressed into many apple cultivars such as 'Red Moon ®', 'Red Love®' and 'Kissabel Rouge®' (Guerra 2018). The anthocyanin content in the fruit flesh could result in an increased intake of antioxidants in people's diet (Allan *et al.,* 2019).

Genetic diversity in pear could be efficiently estimated by SSR analysis as demonstrated by the huge number of published papers describing the characterisation of local germplasm in Asia (Ahmed *et al.,* 2010; Erfani *et al.,* 2012; Akçay *et al.,* 2014; Song *et al.,* 2014; Liu *et al.,* 2015; Rana *et al.,* 2015), in Europe (Fernandez-Fernandez *et al.,* 2006; Martinelli *et al.,* 2008; Bassil *et al.,* 2009; Sisko *et al.,* 2009; Urbanovich *et al.,* 2010; Miranda *et al.,* 2010; Deliquegiovanni *et al.,* 2012; Gasi *et al.,* 2013; Queiroz *et al.,* 2014; Ferradini *et al.,* 2017; Reim *et al.,* 2017; Bennici *et al.,* 2018; Baccichet *et al.,* 2019; Queiroz *et al.,* 2019; Sau *et al.,* 2020; Bielsa *et al.,* 2021; Velázquez-Barrera *et al.,* 2022) and in Africa (Brini *et al.,* 2008).

The identification of S-allele genotypes and phenotypic characterization can complement SSR analysis and confirm the results obtained through molecular characterization (Martinelli *et al.,* 2008; Bennici *et al.,* 2018 and 2020). S-allele diversity has been widely studied through S-genotyping in Japanese (Takasaki *et al.,* 2004; Gu *et al.,* 2009; Saito *et al.,* 2011) and European

pear (Zuccherelli *et al.,* 2002; Sanzol 2009; Nikzad *et al.,* 2014; Bennici *et al.,* 2020) in order to improve the knowledge about self-incompatibility and giving tools for boosting breeding programs.

In the current study, red-fleshed pear landraces of Emilia-Romagna were examined for their genetic diversity to provide insight on the genetic basis of the trait and promote breeding initiatives for its introduction into new pear varieties.

3.2. Materials and Methods

3.2.1. Plant material

A total of 33 red-fleshed accessions have been collected and analysed in this study, including 20 samples from private orchards and gardens in Verghereto (FC, Italy), 6 samples from CREA's pear germplasm collection (Forlì, FC Italy), 6 samples from UNIBO's pear germplasm collection (Cadriano, BO, Italy) and one from private nursery (Parma, PR, Italy). Three white-fleshed commercial cultivars, 'Abate Fétel' ('Abbe Fétel'; AF), 'Decana del Comizio' ('Doyenne du Comice'; DC) and 'William Bon Chretien' (W; also known as 'Bartlett'), obtained from the UNIBO collection were also included in this study as reference (Table S1).

3.2.2. DNA extraction

Young leaves were collected in springtime and stored at -80°C. DNA was extracted by using a CTAB protocol (Mercado *et al.,* 1999). Genomic DNA was quantified by NanodropTM ND-

1000 Spectrophotometer (Thermo Scientific, Wilmington, DE, USA) and diluted to 50 ng/µL as a working solution.

3.3.3. SSR genotyping, cluster analysis and S-allele genotyping

A panel of 18 SSR markers was chosen among the most used in literature: 14 of them are included in a former list recommended by the ECPGR (European Cooperative Programme for Plant Genetic Resources) *Malus/Pyrus* working group (Evans *et al.*, 2009) and four SSR markers were selected to be located in other chromosomes not covered.

Forward primers were labelled with four different fluorescent dyes (6-FAM, PET, HEX or NED) in order to combine PCR products in a single electrophoretic run. The list of primer and their characteristics are reported in supplementary material Table S2.

The PCR reactions were performed with the Thermal Cycler 2700 GeneAmp PCR System (ABI Prism) in 1 µL of DNA solution and 9 µL of master mix prepared according to Sau *et al.*, (2020) but by using the AmpliTaq Gold (Thermo Scientific, Wilmington, USA) as DNA polymerase. The reaction cycling conditions were as follows: initial denaturation step of 10 min at 95°C, followed by 6 cycles using a touchdown amplification program with an annealing temperature reduced by 1°C per cycle from 60°C to 55°C; then 32 cycles, each consisting of 30 s denaturation at 95°C, 90 s annealing at 55°C and 60 s elongation at 72°C and the last cycle ends with a final 10 min extension at 72°C.

Nine pooling groups of 2 SSRs labelled with different fluorescent dyes (Table S2) and characterised by different fragment lengths were designed for SSR genotyping by ABI PRISM 3730 DNA analyser. PCR products were pooled in a ratio of 1:1. One µl of each PCR product was added to 8 µl of formamide containing 0.2 µl of GeneScan 500 LIZ size standard (Applied

Biosystem). Fragments were analysed and visually scored using Peak Scanner v.1.0 (Applied Biosystem).

The SSR data were organised as a square matrix to be analysed by NTsys 2.0 (Rohlf, 1992). The cluster analysis was carried out by using the DICE coefficient (Dice, 1945) and the relative dendrogram was calculated by using the Unweighted Pair-Group Method (UPGMA). The results were used to identify synonyms and homonyms and unique genotypes. The number of alleles per locus (k), the expected and observed heterozygosity (HExp and HObs) and the polymorphism information content (PIC) of unique genotypes were estimated using CERVUS Software v3.0.3 (Kalinowski *et al.,* 2007). The frequency of null alleles, was calculated by using the maximum likelihood (ML) estimator of Kalinowski (2007)

S-allele combinations on the unique genotypes has been determined as reported by Nikzad *et al.,* (2014). The PCR products obtained with the S-allele consensus primers (PycomC1F1 and PycomC5R1) were separated by 1% agarose gels. Based on the amplicon lengths, allele-specific primers were used to confirm the S-genotypes (Table S3; Nikzad *et al.,* 2014).

3.3.4. Fruit quality analysis

At the ripening time, fruit length (FL), fruit diameter (FD), fruit weight (FW), flesh firmness (FFi), soluble solid content (SSC), juice pH and titratable acidity (TA) have been determined both on the four unique genotypes and on the three commercial cultivars (AF, W, DC) used as a reference. FF was determined using a digital penetrometer (Güss Fruit Texture Analyzer equipped with an 8-mm tip, Strand, South Africa) taking two measurements per fruit. SSC was measured in single fruits using a digital refractometer (Atago Pocket Refractometer PAL-1, Tokyo, Japan). TA was measured by titration of the juice obtained from a pool of 10 fruits with a NaOH 0.5 M solution (Crison Titromatic 1S, Barcelona, Spain). The flesh red colour intensity

was visually evaluated by using a 0 to 5 scale (0 corresponding to the absence of colour and 5 to its highest intensity). This evaluation was performed at four different positions within the fruit sections: seed locule (SL), fruit core (FC), fruit flesh (FF) and under-skin region (US). All analysis has been performed at ripening time on samples of 10 fruits from three plants per accession from the UNIBO's pear germplasm collection (Cadriano, BO, Italy). 'Cocomerina Selvatica LaCasa' and 'Incrocio Sant'Alessio' were excluded from this analysis because these accessions were single trees grown in other locations and the different pedoclimatic conditions could impact the amount of anthocyanin in the fruit flesh.

A cluster analysis was carried out by analysing the phenotypic data with the dissimilarity index of Canberra available on the software package NTSYSpc 2.0 (Rohlf, 1988).

3.3. Results

3.3.1. Genetic and cluster analysis

The 18 selected SSR markers amplified 133 alleles with an average of 7.389 alleles per locus. The number of alleles ranged from 4 in CH04e03 to 11 in CH03g07. The frequencies of the allele in each locus were reported in supplementary material (Table S4). The expected heterozygosity (HExp) ranged from 0.471 (CH04e03) to 0.915 (CH01d09 and CH04c07) with an average value of 0.795. The observed heterozygosity (HObs) ranged from 0.333 (CH01a02 and GD147) to 1.000 (CH01f07 and CH01d08) with an average of 0.729. The Polymorphism Information Content (PIC) value indicated that the most informative loci were CH04c07 and CH01d09, both with the value of 0.850; the lowest value was observed in CH04e03, with 0.409 (Table 3.1). The frequency of null alleles, as calculated by Cervus using the maximum likelihood (ML) estimator of Kalinowski (2007), is negligible (data not shown). This

observation is supported by the fact that almost all the analysed samples were in heterozygosis. for most of the loci while just a few were in putative homozygosis.

Table 3.1. The number of alleles (k), the observed (HObs) and expected (HExp) heterozygosity, the polymorphic information content (PIC) were reported for each SSR locus evaluated in the 9 analysed unique genotypes of *P. communis*.

Locus	K	HObs	HExp	PIC
CH01D09	10	0.889	0.915	0.850
CH05C06	7	0.889	0.771	0.696
CH01F07	8	1.000	0.889	0.820
CH02B10	8	0.778	0.869	0.798
CH01Vf	8	0.556	0.876	0.806
CH02C09	7	0.556	0.745	0.679
EMPC11	7	0.778	0.739	0.670
CH03D12	7	0.778	0.824	0.747
EMPC117	7	0.889	0.824	0.753
CH04E03	4	0.556	0.471	0.409
GD147	5	0.333	0.549	0.485
GD96	6	0.444	0.739	0.669
CH01D08	6	1.000	0.797	0.718
CH03G07	11	0.778	0.882	0.819
CH04C07	10	0.778	0.915	0.850
CH01A09	7	0.889	0.791	0.712
CH01H10	6	0.333	0.797	0.718
CH01H02	9	0.889	0.908	0.842
Average	7,39	0,729	0,795	0,725

Cluster analysis elucidated genetic relationships among varieties and four groups of synonyms were identified (Figure 3.1).

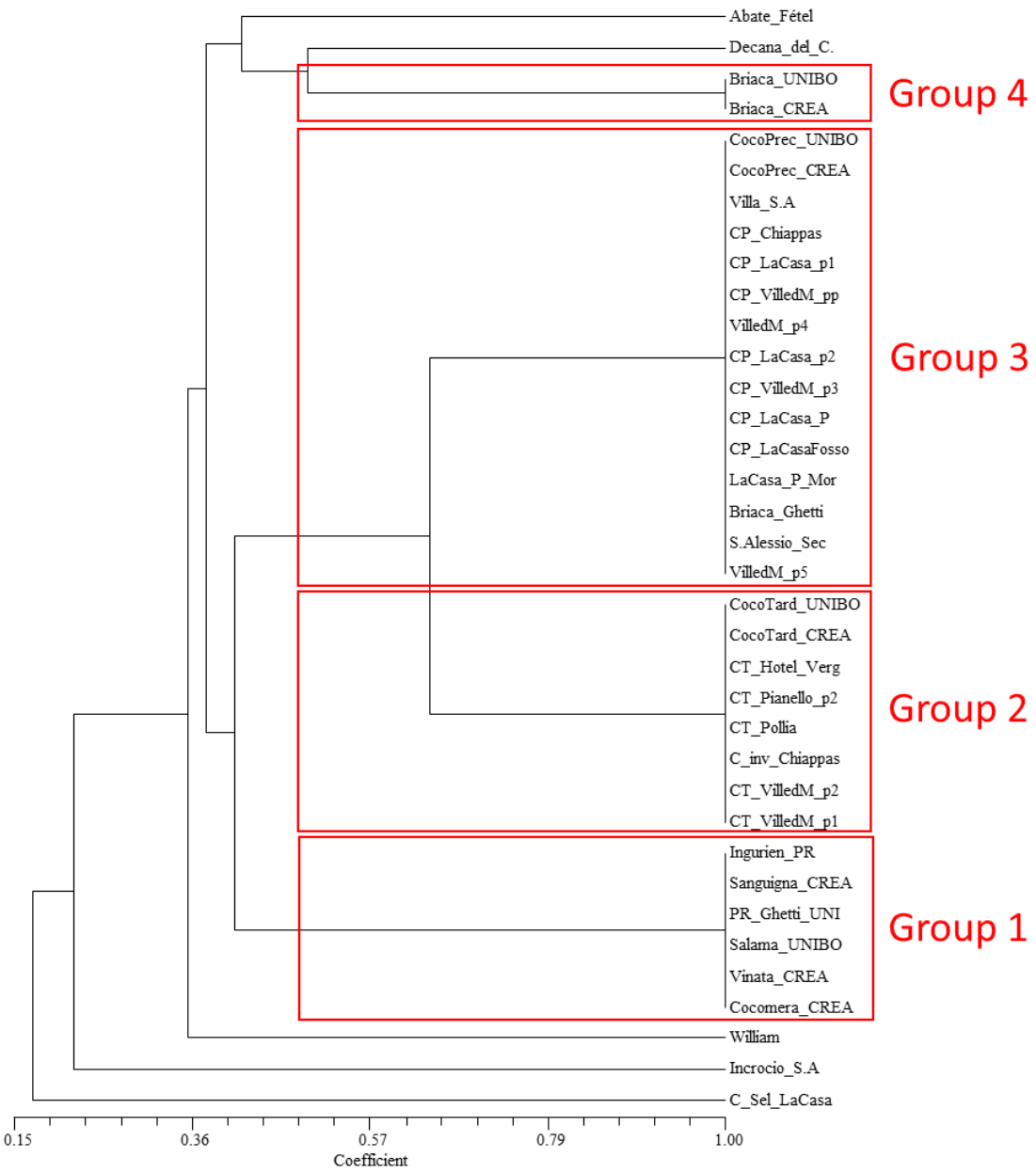

Figure 3.1. Dendrogram carried out by NTSYS using the Dice similarity index among the 33 pear landraces analysed. Three commercial cultivars were included as reference.

Group 1 includes 6 accessions with 6 different names: 'Pera Sanguigna', 'Pera Cocomera', 'Pera Vinata' from the CREA germplasm collection, 'Salama' and 'Pera Polpa Rossa' from UNIBO germplasm collection and 'Ingurien' from a private nursery in Parma. 'Pera Sanguigna' (PS) was selected as the reference for this group.

Group 2 clusters together all trees attributable to the landrace ‘Cocomerina Tardiva’ (CT; known also with the name ‘Cocomerina Invernale’). Most of the samples were collected in the Verghereto area. ‘Cocomerina Tardiva’ samples from UNIBO and CREA were used as reference.

Group 3 includes the samples of ‘Cocomerina Precoce’ (CP; with references from both UNIBO and CREA germplasm collections). All the samples denominated with this name from the Verghereto area are included in this cluster. An accession of ‘Briaca’ maintained in the UNIBO collection (‘Briaca Ghetti’) was unexpectedly included in this group.

The last group is composed of two ‘Briaca’ (B) accessions present in the UNIBO and CREA collections (group 4). Despite their common name, the three analysed ‘Briaca’ accessions showed two different molecular profiles.

The other two red-fleshed accessions, ‘Cocomerina Selvatica La Casa’ (CS) and ‘Incrocio S. Alessio’ (IA) resulted as unique genotypes and very diverse in respect to all the other genotypes.

3.3.2. Unique genotype S-allele determination

All the unique genotypes identified with the cluster analysis were analysed at first by using the consensus primer approach and based on the estimated fragment lengths; subsequently, a panel of allele-specific primers were used for confirming all *S*-allele attributions (Table S3).

Results evidenced the presence of 6 different S alleles in the 6 analysed accessions (*S101, S104, S105, S108, S120* and *S125*) with the allele *S104* that is the most frequent one being present in three accessions (CP, CT and IA). The allele *S120* was detected in CT and CS and *S125* in CP and PS. The remaining alleles *S101, S105* and *S108* were present only once in the analysed

samples. For the samples PS only one allele was clearly identified (*S125*) and more research will be needed for identifying the second one (Table 3.2).

Table 3.2. S-Allele combinations of each unique genotype determined by using consensus and allele-specific primers. The fragment size indicates the band size identified by using consensus primers.

Genotype	fragment size (bp)	S-alleles
Cocomerina Tardiva	750/800	*S104/S120*
Cocomerina Precoce	750/1700	*S104/S125*
Briaca	650/1300	*S105/S101*
Pera Sanguigna	1700	*S125*
Cocomerina Sel LaCasa	800/1300	*S120/S101*
Incrocio S. Alessio	680/750	*S108/S104*

3.3.3. Fruit quality analyses

Four of the 6 unique genotypes and the 3 reference cultivars were also analysed for their fruit quality features and for the intensity and distribution of the red colour in the fruits (Table 3.3). The red-fleshed genotypes IA and CS were not analysed because they are single trees located in a not comparable environment.

Based on the variance analysis among cultivars, statistical differences of significant level were observed in most of the considered parameters such as fruit diameter, fruit length, fruit weight, fruit firmness and sugar. In fact, only pH did not show significant differences among samples. As expected, all the fruit size-related traits were higher in reference cultivars than in the red-fleshed genotypes.

Table 3.3. Fruit quality data determined at the ripening time: fruit weight (FW), flesh firmness (FFi), Soluble Solid Content (SSC), seed locules red intensity (SL), fruit core red intensity (FC), fruit flesh red intensity (FF), under fruit skin red intensity (US), titratable acidity (TA), pH of the juice, fruit length (FL), fruit diameter (FD), fruit length and fruit diameter ratio (FL/FD).

Genotype	FW	FFi	SSC	SL	FC	FF	US	TA	pH	FL (mm)	FD (mm)	FL/FD
Briaca	43.5cd	4.76bc	17.9b	2.3b	1.0b	1.0b	0.0b	5.1ab	4.2a	38.9de	41.2cd	0.94d
Pera Sanguigna	44.7c	5.46b	18.9a	2.7ab	1.3b	1.0b	0.0b	4.5b	4.3a	44.5d	43.3c	1.02d
Cocomerina Precoce	45.9c	4.67Bc	18.4a	2.2b	1.0b	1.0b	0.0b	5.2a	4.4a	43.3d	45.5c	0.95d
Cocomerina Tardiva	37.1d	8.12a	19.7a	3.2a	2.8a	2.6a	3.0a	4.6ab	4.2a	35.2e	35.3d	0.99d
Abate Fétel	151.3a	4.25c	15.7c	0.0c	0.0c	0.0c	0.0b	4.8ab	4.2a	133.9a	62.5b	2.14a
Decana del Comizio	154.2a	5.01bc	18.2ab	0.0c	0.0c	0.0c	0.0b	5.1ab	4.1a	100.6c	68.4a	1.47c
William	139.8b	4.49bc	16.4bc	0.0c	0.0c	0.0c	0.0b	4.9ab	4.2a	120.1b	63.3b	1.89b

* Data followed by different letters are significantly different (ANOVA followed by Tukey test. $p < 0.05$).

CT reached the highest firmness values 8.12 kg/cm^2, when compared to the other cultivar. When it comes to sugar content in the fruit (SSC), AF cultivar reached the lowest value (15.7), while CT cultivar had the highest ones (19.7). About the flesh colour trait, the reddest one was CT within the highest values for each parameter. No significant differences could be identified among the other three accessions.

Regarding different intensity and position of red colour CP and B looks quite similar, with the highest concentration of anthocyanin in the fruit core and some reddish spots all over the flesh. PS has a characteristic strong red colour ring around the fruit core. The flesh has very strong pigmentation in CT, as well as the fruit core. Also, in these fruits the red was not uniformly spread but it appeared in patches (Figure 3.2).

Figure 3.2. Different intensity and position of red colour in fruits of red-fleshed accessions fruits. 'Cocomerina Precoce' (top left); 'Cocomerina Tardiva' (top right); 'Briaca' (bottom left) and 'Pera Sanguigna' (bottom right). Fruit equatorial section (left) and lateral shape (right) are represented.

A new cluster analysis was carried out by using a dissimilarity index (Canberra) with these analytical data (Figure 3.3 B). In both graphs CP, CT and PS were clustered together. Reference varieties are grouped along with each other in both the analyses. Nevertheless, they showed a more marked similarity in the fruit quality related graph.

In contrast to the genetic data-related dendrogram, 'Briaca' was included in the red fleshed cluster within the phenotype analysis.

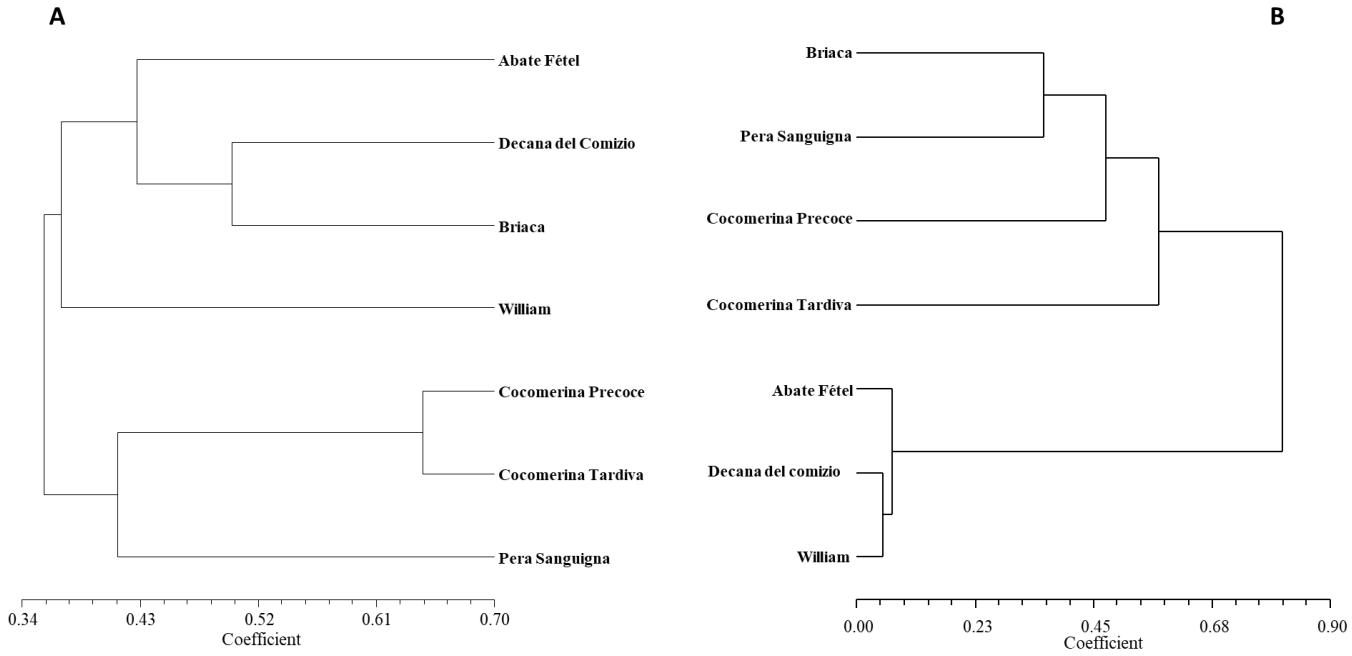

Figure 3.3. Dendrograms calculated based on genotypic (A; SSR with the DICE similarity index) and phenotypic data (B; with Canberra dissimilarity index) among 4 red-fleshed pear landraces and the 3 commercial cultivars used as a reference.

3.4. Discussion

In this study the molecular characterization of a panel of 33 accessions collected in a very narrow area of the Emilia-Romagna Apennines and from two germplasm collections resulted in the identification of six unique genotypes. Four of these genotypes were also characterised for their fruit quality features and for the red colour distribution and intensity in order to estimate how much the genetic diversity determined by SSRs reflects the phenotypic variability. The importance of characterising pear germplasm collections with molecular markers, particularly by SSRs, was widely reported in literature as a tool for assessing pear genetic diversity (Fernandez-Fernandez *et al.,* 2006; Evans *et al.,* 2009; Sehic *et al.,* 2012; Dequigiovanni *et al.,* 2012; Urrestarazu *et al.,* 2015).

The panel of 18 specific SSR markers allowed to identify four clusters of unique genotypes. Regarding the effectiveness of each marker, as already reported in literature, CH01D09 and CH01F07a were found to have a high discrimination power. Moreover, CH04E03 had shown low levels of PIC as previously reported (Gasi *et al.,* 2013; Baccichet *et al.,* 2019; Queiroz *et al.,* 2019; Sau *et al.,* 2020; Bielsa *et al.,* 2021).

CP and CT genotypes were confirmed as well-known varietiesand only a misnomer was found. At the opposite, PS had shown several different accession names all related to the same genotype.

The large genetic distance observed for CS and IA might have originated by hybridisation with other *Pyrus* species, such as *Pyrus pyraster*, that are widespread in the upper Apennine Mountains as already reported by Bennici et al 2018. The genetic diversity analysis of *Pyrus* collection performed by Montanari *et al.,* (2019) provides further hint that red fleshed may be connected to the wild species, particularly with *Pyrus pyraster* since three red-fleshed

genotypes (‘Sanguignole’, ‘Rottkottig’ and ‘Summer Blood Birne’) were included in the admixture group between *Pyrus communis* and *Pyrus pyraster*. Further investigations should be conducted to determine whether the red-fleshed trait is present in the local wild pear populations and to figure out in which direction the gene flow occurred.

The identification of synonyms and homonyms highlighted the importance of determining the true-to-types plants to be used as reference for the correct conservation of these genotypes and for preserving them against a possible genetic erosion. The availability of well-genotyped plants, as references, is also important for supporting the correct nursery propagation of ‘Cocomerina Precoce’ and ‘Cocomerina Tardiva’ for which there is an interest among pear growers of the Verghereto district. It should be remembered that all the names given to red-fleshed landraces referred to their peculiar trait, which could be the reason why there were so many cases of homonyms and synonyms. For example, ‘Briaca’ is the most used term in Tuscany for red-fleshed pears and, probably, in the past, with the names ‘Briaca’ or ‘Briaco’ were also used for trees that were clearly ascribable to the accessions ‘Cocomerina Tardiva’ and ‘Cocomerina Precoce’ as reported in previous works (Camangi *et al.,* 2006; Martinelli *et al.,* 2008; Ferradini *et al.,* 2017; Pastore *et al.,* 2020).

The use of the consensus (Sanzol and Robbins, 2008) and allele-specific primers (Sanzol, 2009; Nikzad *et al.,* 2014) demonstrated to be a very efficient method for the determination of the *S* allele combinations of pear modern varieties and old landraces (Sanzol, 2009; Nikzad *et al.,* 2014; Shi 2018; Bagheri *et al.*,2020; Bennici *et al.,* 2020; Gasi *et al.,* 2020). Nevertheless, a ‘Pera Sanguigna’ S-allele has not been identified. The S-genotypes obtained from the analysis allowed to establish that all the accessions are inter-fertile. The presence of an allele in common in most of the red-fleshed varieties present in a very narrow environment also support the possible presence of genetic relationships among these genotypes.

For a better estimation of this aspect the results of the genetic diversity determined by SSRs have been compared with those obtained by using a dissimilarity index for analysing the variability present in analytical data.

The two dendrograms obtained using these two approaches evidenced a clear separation between the red-fleshed landraces and the references ‘Abate Fétel’, ‘William’ and ‘Decana’. Considering the red-fleshed landraces, both approaches possibly indicated a relationship between ‘Cocomerina Tardiva’ and ‘Cocomerina Precoce’, as expected considering that they originated in the same area. The evidence that these two varieties share at least one common allele for each examined locus, including *S*-locus *S104* allele, suggest that they may be very closely related: indeed, this segregation pattern could be compatible with a direct kinship such as mother-daughter. On the other hand, their kinship with ‘Pera Sanguigna’ seems to be less strong, but still consistent due to the sharing of several alleles all over the characterised loci, among which the most significant was the partaken S-locus S125 allele within CP. Interestingly, this allele resulted to be infrequent within the varieties of the Italian germplasm (Bennici *et al.*, 2020).

3.5. Conclusions

The identification of unique references for the main four red-fleshed accessions will pave the way to their propagation since the emerging interest in these old landraces. In particular, a 'Cocomerina' pear consortium was established to promote the cultivation of these accessions in the upper Savio valley (FC, Italy). The organisation harvests the fruit each year and either sells the pears unprocessed or transformed into jams and liquors. The 'Slow Food Presidium' has counted all the surviving trees, assisted farmers with harvesting, and it has the purpose to establish an educational and experimental orchard where the plants may be propagated.

The knowledge of the S-allele combinations in the six unique red-fleshed genotypes is very important to properly design the new orchards since the increasing interest and demand of this type of fruit. The right choice of cultivar combination, with compatible *S*-genotype, could significantly improve the fruit set and therefore the field productivity.

Concerning this fascinating trait in pear, it should be advisable to analyse more samples collected in different areas, for example, testing other European red-fleshed landraces could further shed light about the origin of the trait. Nevertheless, finding more genotypes that possess this trait may be the key to develop a molecular marker that might be very helpful for the ongoing pear breeding programs.

3.6. References

- AA.VV Sansavini S. & Ancarani V. *Antiche pere dell'Emilia-Romagna.* Bologna, Istituto per i Beni Artistici Culturali e Naturali della Regione Emilia-Romagna, 2020
- Ahmed M, Akbar M, Muhammad A, Khan Q, Pearce S (2015) Evaluation of genetic diversity in Pyrus germplasm native to Azad Jammu and Kashmir (Northern Pakistan) revealed by microsatellite markers. Afr J Biotechnol 9(49):8323–8333
- Akçay ME, Burak M, Kazan K, Yuksel C, Mutaf F, Bakir M *et al.*, (2014) Genetic analysis of Anatolian pear germplasm by simple sequence repeats. Ann Appl Biol 164:441–452
- Allan, A. C., Schwinn, K. E., & Espley, R. V. (2019). Anthocyanin accumulation is controlled by layers of repression. Recent Adv. Polyphen. Res, 6, 71-87.
- Antognoni, F., Potente, G., Mandrioli, R., Angeloni, C., Freschi, M., Malaguti, M., ... & Tartarini, S. (2020). Fruit quality characterization of new sweet cherry cultivars as a good source of bioactive phenolic compounds with antioxidant and neuroprotective potential. Antioxidants, 9(8), 677.
- Baccichet, I., Foria, S., Messina, R., Peccol, E., Losa, A., Fabro, M., ... & Testolin, R. (2020). Genetic and ploidy diversity of pear (Pyrus spp.) germplasm of Friuli Venezia Giulia, Italy. Genetic Resources and Crop Evolution, 67(1), 83-96.
- Bagheri, M., & Ershadi, A. (2020). Self-incompatibility alleles in Iranian pear cultivars. Biocatalysis and Agricultural Biotechnology, 27, 101672.
- Bao L, Chen K, Zhang D, Cao YF, Yamamoto T, Teng YW (2007) Genetic diversity and similarity of pear (Pyrus L.) cultivars native to East Asia revealed by SSR (simple sequence repeat) markers. Genet Resour Crop Evol 54:959–971
- Bassil NV, Postman J (2009) Identification of European and Asian pears using EST-SSRs from Pyrus. Genet Resour Crop Evol 57:357–370
- Bennici S, Las Casas G, Distefano G, Di Guardo M, Continella A, Ferlito F et al (2018) Elucidating the contribution of wild related species on autochthonous pear germplasm: a case study from Mount Etna. PLoS ONE 13(6): e0198512.
- Bennici, S., Di Guardo, M., Distefano, G., Las Casas, G., Ferlito, F., De Franceschi, P., ... & La Malfa, S. (2020). Deciphering S-RNase Allele Patterns in Cultivated and Wild Accessions of Italian Pear Germplasm. Forests, 11(11), 1228.

- Bielsa, F. J., Irisarri, P., Errea, P., & Pina, A. (2021). Genetic Diversity and Structure of Local Pear Cultivars from Mountainous Areas from Aragon (Northeastern Spain). Agronomy, 11(9), 1778.
- Brewer, L., & Volz, R. (2019). Genetics and breeding of pear. In The pear genome (pp. 63-101). Springer, Cham.
- Brini W, Mars M, Hormaza JI (2008) Genetic diversity in local Tunisian pears (Pyrus communis L.) studied with SSR markers. Sci Hortic 115:337–341
- Bucchini, A., Scoccianti, V., Ricci, D., & Giamperi, L. (2016). Cocomerina pear: an old and rare fruit with red pulp. Analysis of phenolic content and antioxidant/anti-inflammatory capacity. CyTA-Journal of Food, 14(4), 518-522.
- Camangi F, Stefani A, Sebastiani L, Martinelli F, Segantini L, Serravelli M, Nappini E, Busconi M, Fogher C (2006) Vecchie cultivar di pero (Pyrus communis L.) censite nel casentino (AR): caratterizzazione morfologica, biometrica e molecolare (SSR). Italus Hortus 13(2):194–197
- Caracciolo, G., Sirri, S., & Baruzzi, G. (2021). Update on CREA Centro di Ricerca Olivicoltura, Frutticoltura e Agrumicoltura pear breeding program. Acta Hortc. 1303, 29-36.
- Chagne´ D, Crowhurst RN, Pindo M, Thrimawithana A, Deng C, Ireland H et al (2014) The draft genome sequence of European pear (Pyrus communis L. 'Bartlett'). PLoS ONE 9(4): e92644.
- Chavez, D. J., Itle, R. A., Mancero-Castillo, D., Chaparro, J. X., & Beckman, T. G. (2019). Advances and challenges in peach breeding. Achieving sustainable cultivation of temperate zone tree fruits and berries, 3-24.
- Chen, Z., Yu, L., Liu, W., Zhang, J., Wang, N., & Chen, X. (2021). Research progress of fruit color development in apple (Malus domestica Borkh.). Plant Physiology and Biochemistry, 162, 267-279.
- Dequigiovanni G, Rech F, Gatti Gomes FG, Somensi Cerotti I, Faoro I, Dias de Oliveira PR, Quecini V, Ritschel P (2012) Identification of a Simple Sequence Repeat molecularmarker set for large-scale analyses of pear germplasm. Crop Breed Appl Biotechnol 12:118–125
- Downing A.J. (1869) – The fruits and fruit-trees of America, or, The culture, propagation, and management, in the garden and orchard, of fruit -trees generally: with descriptions of all the finest varieties of fruit, native and foreign, cultivated in this

country. 2nd Edition rev. and corrections, with large additions by Charles Downing. J. Wiley, New York.

- Doyle JJ, Doyle JL (1990) Isolation of plant DNA from fresh tissue. Focus 12:13–15
- Erfani J, Ebadi A, Abdollahi H, Fatahi R (2012) Genetic diversity of some pear cultivars and genotypes using Simple Sequence Repeat (SSR) markers. Plant Mol Biol Rep 30:1065–1072
- Evans KM, Fernàndez-Fernàndez F, Govan C (2009) Harmonising fingerprinting protocols to allow comparisons between germplasm collections—Pyrus. Acta Hortic 814:103–106
- Fernàndez-Fernàndez F (2009) Fingerprinting the National apple & pear collections. Final report GC0140 fingerprinting the National apple & pear collections. WEB site Accessed 30 April 2019
- Ferradini N, Lancioni H, Torricelli R, Russi L, Ragione ID et al (2017) Characterization and phylogenetic analysis of ancient Italian landraces of pear. Front Plant Sci 8:751
- Ferreira dos Santos AR, Ramos-Cabrer AM, Dı´az-Herna´ndez MB, Pereira-Lorenzo Santos S (2011) Genetic variability and diversification process in local pear cultivars from northwestern Spain using microsatellites. Tree Genet Genomes 7:1041–1056
- Fideghelli C (coord) (2017) Atlante dei fruttiferi autoctoni italiani [Atlas of autoctonous Italian fruit crops], vol I. Belt Multimedia. ISBN 978-88-99595-35-7
- Gaius Plinius Secundus (Pliny the Elder) (1984) Storia naturale. III Botanica (Natural History. III Botany). Giulio Einaudi Editore, Torino, pp 996
- Gallesio G (1817-–839) Pomona italiana ossia trattato degli alberi fruttiferi [Italian Pomona namely treatise of fruit crops]. Capurro, Pisa
- Gasi F, Kurtovic M, Kalamujic B, Pojskic N, Grahic J, Kaiser C et al (2013) Assessment of European pear (Pyrus communis L.) genetic resources in Bosnia and Herzegovina using microsatellite markers. Sci Hortic 157:74–83
- Gasi, F., Frøynes, O., Kalamujić Stroil, B., Lasić, L., Pojskić, N., Fotirić Akšić, M., & Meland, M. (2020). S-Genotyping and Seed Paternity Testing of the Pear Cultivar 'Celina'. Agronomy, 10(9), 1372.
- Guerra, W. (2018). Mele a polpa rossa, pronti al decollo! Rivista di frutticoltura e di ortofloricoltura, 82(10), 20-25.
- Hedrick UP (1921) The pears of New York. JB Lyon Company, Albany, p 636
- Leroy A (1867–1869) Dictionnaire de Pomologie. Tome 1 & 2 Poires. Paris

- Liu Q, Song Y, Liu L et al (2015) Genetic diversity and population structure of pear (Pyrus spp.) collections revealed by a set of core genome-wide SSR markers. Tree Genet Genomes 11:128.
- Kalinowski, S. T., Taper, M. L., & Marshall, T. C. (2007). Revising how the computer program CERVUS accommodates genotyping error increases success in paternity assignment. Molecular ecology, 16(5), 1099-1106
- Martinelli F, Busconi M, Camangi F, Fogher C, Stefani A, Sebastiani L (2008) Ancient Pomoideae (Malus domestica Borkh. and Pyrus communis L.) cultivars in ‘‘Appenino Toscano’’ (Tuscany, Italy): molecular (SSR) and morphological characterization. Caryologia 61(3):320–331
- Mas A. (1872-1883) - Pomologie générale. Librairie de G. Masson, Parigi. Volume 7.
- Mercado, J. A., El Mansouri, I., Jiménez-Bermúdez, S., Pliego-Alfaro, F., & Quesada, M. A. (1999). A convenient protocol for extraction and purification of DNA from Fragaria. In Vitro Cellular & Developmental Biology-Plant, 35(2), 152-153.
- Miranda C, Urrestarazu J, Santesteban LG, Royo JB, Urbina V (2010) Genetic diversity and structure in a collection of ancient Spanish pear cultivars assessed by microsatellite markers. J Am Soc Hortic Sci 135(5):428–437
- Molon G (1901) Pomologia [Pomology]. Hoepli, Milano, p 717
- Montanari, S., Bianco, L., Allen, B. J., Martínez-García, P. J., Bassil, N. V., Postman, J., ... & Neale, D. B. (2019). Development of a highly efficient Axiom™ 70 K SNP array for Pyrus and evaluation for high-density mapping and germplasm characterization. BMC genomics, 20(1), 1-18.
- Morettini A, Baldini E, Scaramuzzi F, Mittempergher L (1967) Monografia delle principali cultivar di pero. CNR, Firenze
- Nikzad Gharehaghaji, A., Arzani, K., Abdollahi, H., Shojaeiyan, A., Dondini, L., & De Franceschi, P. (2014). Genomic characterization of self-incompatibility ribonucleases in the Central Asian pear germplasm and introgression of new alleles from other species of the genus Pyrus. Tree Genetics & Genomes, 10(2), 411-428.
- Nikzad Gharehaghaji, A., Arzani, K., Abdollahi, H., Shojaeiyan, A., Dondini, L., & De Franceschi, P. (2015). Identification and S-genotyping of Novel S-alleles in Wild Species of Pyrus Genus. Isfahan University of Technology-Journal of Crop Production and Processing, 5(17), 239-252.

- Pastore C., Ancarani V., Venturi S., Dondini L. (2020). Diversità genetica delle pere dell'Emilia-Romagna. Capitolo 4. Antiche Pere dell'Emilia-Romagna. IBC, Bologna, Italia.
- Puska´s M, Ho¨fer M, Sestras RE, Peil A, Sestras AF, Hanke MV, Flachowsky E (2015) Molecular and flow cytometricevaluation of pear (Pyrus L.) genetic resources of the German and Romanian national fruit collections. Genet Res Crop Evol 63(6):1023–1033
- Queiroz A, Assunc¸a˜o A, Ramadas I, Viegas W, Veloso MM (2015) Molecular characterization of Portuguese pear landraces (Pyrus communis L.) using SSR markers. Sci Hortic 183:72–76
- Queiroz, Á., Bagoin Guimarães, J., Sánchez, C., Simões, F., Maia de Sousa, R., Viegas, W., & Veloso, M. M. (2019). Genetic diversity and structure of the Portuguese pear (Pyrus communis L.) germplasm. Sustainability, 11(19), 5340.
- Rana JC, Chahota RK, Sharma V, Rana M, Verma N, Verma B et al (2015) Genetic diversity and structure of Pyrus accessions of Indian Himalayan region based on morphological and SSR markers. Tree Genet Genomes 11:821. https://doi.org/10.1007/s11295-014-0821-2
- Reim S, Lochschmidt F, Proft A, Wolf H, Wolf H (2017) Species delimitation, genetic diversity and structure of the European indigenous wild pear (Pyrus pyraster) in Saxony, Germany. Gen Resour Crop Evol 64:1075–1085 123 Genet Resour Crop Evol (2020) 67:83–96 95
- Rohlf F (1988) NTSYS-pc—Numerical taxonomy and multivariate analysis system. 2.1. Applied Biostatistics Inc, New York, p 43.
- Sanzol, J., & Robbins, T. P. (2008). Combined analysis of S-alleles in European pear by pollinations and PCR-based S-genotyping; correlation between S-phenotypes and S-RNase genotypes. Journal of the American Society for Horticultural Science, 133(2), 213-224.
- Sanzol, J. (2009). Genomic characterization of self-incompatibility ribonucleases (S-RNases) in European pear cultivars and development of PCR detection for 20 alleles. Tree genetics & genomes, 5(3), 393-405.
- Sehic J, Garkava-Gustavsson L, Ferna´ndez-Ferna´ndez F, Nybom H (2012) Genetic diversity in a collection of European pear (Pyrus communis) cultivars determined with SSR markers chosen by ECPGR. Sci Hortic 145:39–45

- Sisko M, Javornik B, Siftar A, Ivancic A (2009) Genetic relationships among Slovenian pears assessed by molecular markers. J Am Soc Hortic Sci 134(1):97–108
- Song Y, Fan L, Chen H, Zhang M, Ma Q, Zhang S, Wu J (2014) Identifying genetic diversity and a preliminary core collection of Pyrus pyrifolia cultivars by a genome-wide set of SSR markers. Sci Hortic 167:5–16
- Suprun II, Tokmakov SV, Bandurkob IA, Ilnitskaya ET (2016) SSR polymorphism of modern cultivars and autochthonous forms of the pear tree from north Caucasus. Russ J Genet 52(11):1149–1156
- Urbanovich OY, Kazlouvskaya ZA, Yakimovich OA, Kartel NA (2011) Polymorphism of SSR alleles in pear cultivars grown in Belarus. Russ J Genet 47:305–313
- Urrestarazu J, Royo JB, Santesteban LG, Miranda C (2015) Evaluating the influence of the microsatellite marker set on the genetic structure inferred in Pyrus communis L. PLoS ONE.
- Velázquez-Barrera, M.E., Ramos-Cabrer, A.M., Pereira-Lorenzo, S. and Ríos-Mesa, D.J., 2022. Genetic Pool of the Cultivated Pear Tree (Pyrus spp.) in the Canary Islands (Spain), Studied Using SSR Molecular Markers. Agronomy, 12(7), p.1711.

3.7. Supplementary materials

Table S1. List of the 33 collected accessions and their location

Accession name	Short name	Collecting area
Abate Fétel (Abbè Fétel)	Abate	Collection UNIBO, Cadriano, BO
Decana del Comizio (Doyenne du Comice)	Decana	Collection UNIBO, Cadriano, BO
William Bon Chretien (Bartlett)	William	Collection UNIBO, Cadriano, BO
Briaca UNIBO	Briaca_UNIBO	Collection UNIBO, Cadriano, BO
Cocomerina Precoce UNIBO	CocoPrec_UNIBO	Collection UNIBO, Cadriano, BO
Cocomerina Tardiva UNIBO	CocoTard_UNIBO	Collection UNIBO, Cadriano, BO
Ingurien PR	Ingurien_PR	Castelpiombino, PR
Incrocio Sant'Alessio	Incrocio_S.A	Sant'Alessio, Verghereto, FC
Cocomerina Tardiva CREA	CocoTard_CREA	Collection CREA, Forlì, FC
Cocomerina Precoce CREA	CocoPrec_CREA	Collection CREA, Forlì, FC
Briaca CREA	Briaca_CREA	Collection CREA, Forlì, FC
Pera Sanguigna CREA	Sanguigna_CREA	Collection CREA, Forlì, FC
Cocomerina Selvatica LaCasa	C_Sel_LaCasa	Pianello, Verghereto, FC
Villa Sant'Alessio	Villa_S.A	Sant'Alessio, Verghereto, FC
Cocomerina Precoce LaCasa 2	CP_LaCasa_p2	Pianello, Verghereto, FC
Sant'Alessio pianta Secolare	S.Alessio_Sec	Sant'Alessio, Verghereto, FC
Briaca Ghetti	Briaca_Ghetti	Collection UNIBO, Cadriano, BO
Pera Vinata CREA	Vinata_CREA	Collection CREA, Forlì, FC
Pera Cocomera CREA	Cocomera_CREA	Collection CREA, Forlì, FC
Cocomerina Tardiva Hotel Verghereto	CT_Hotel_Verg	Verghereto, FC
Cocomerina Precoce LaCasa Fosso	CP_LaCasaFosso	Pianello, Verghereto, FC
Cocomerina Precoce LaCasa 3	CP_LaCasa_P	Pianello, Verghereto, FC
Cocomerina Tardiva Pianello 1	CT_Pianello_p2	Pianello, Verghereto, FC
Cocomerina Tardiva Pollia	CT_Pollia	Pianello, Verghereto, FC
Cocomerina invernale Chiappasonno	C_inv_Chiappas	Sant'Alessio, Verghereto, FC
Cocomerina Tardiva Ville di Montecoronaro 1	CT_VilledM_p1	Ville di Montecoronaro, Verghereto, FC
Cocomerina Tardiva Ville di Montecoronaro 2	CT_VilledM_p2	Ville di Montecoronaro, Verghereto, FC
Cocomerina Precoce Ville di Montecoronaro 3	CP_VilledM_p3	Ville di Montecoronaro, Verghereto, FC
Cocomerina Precoce Ville di Montecoronaro 4	VilledM_p4	Ville di Montecoronaro, Verghereto, FC
Cocomerina Precoce Ville di Montecoronaro 5	VilledM_p5	Ville di Montecoronaro, Verghereto, FC
Cocomerina Precoce Ville di Montecoronaro 6	CP_VilledM_pp	Ville di Montecoronaro, Verghereto, FC
LaCasa pianta morente	LaCasa_P_Mor	Pianello, Verghereto, FC
Cocomerina Precoce LaCasa 1	CP_LaCasa_p1	Pianello, Verghereto, FC
Cocomerina Precoce Chiappasonno	CP_Chiappas	Sant'Alessio, Verghereto, FC
Pera polpa rossa Ghetti UNIBO	PR_Ghetti_UNI	Collection UNIBO, Cadriano, BO
Salama UNIBO	Salama_UNIBO	Collection UNIBO, Cadriano, BO

Table S2 Characteristics of the 18 SSR marker primers used in this study

SSR marker	Forward	Reverse	Range	Label	Source species	Linkage group	Reference	Pooling group
CH_Vf1	ATCACCACCAGCAGCAAAG	CATACAAATCAAAGCACAACCC	120-170	HEX	*Malus X domestica*	1	Vinatzer *et al.*, 2004	1
CH01d08	CTCCGCCGCTATAACACTTC	TACTCTGGAGGGTATGTCAAAG	238–321	6-FAM	*Malus X domestica*	15	Liebhard et al 2002	2
CH01d09	GCCATCTGAACAGAATGTGC	CCCTTCATTCACATTTCCAG	134–172	6-FAM	*Malus X domestica*	12	Liebhard et al 2002	3
CH01f07a	CCCTACACAGTTTCTCAACCC	CGTTTTTGGAGCGTAGGAAC	174–206	6-FAM	*Malus X domestica*	10	Liebhard et al 2002	4
CH02b10	CAAGGAAATCATCAAAGATTCAAG	CAAGTGGCTTCGGATAGTTG	121–159	HEX	*Malus X domestica*	2	Gianfranceschi et al 1998	4
CH03d12	GCCCAGAAGCAATAAGTAAACC	ATTGCTCCATGCATAAAGGG	108–154	HEX	*Malus X domestica*	6	Liebhard et al 2002	5
CH03g07	AATAAGCATTCAAAGCAATCCG	TTTTTCCAAATCGAGTTTCGTT	119–181	PET	*Malus X domestica*	3	Liebhard et al 2002	2
CH04c07	GGCCTTCCATGTCTCAGAAG	CCTCATGCCCTCCACTAACA	98–135	HEX	*Malus X domestica*	14	Liebhard et al 2002	6
CH04e03	TTGAAGATGTTTGGCTGTGC	TGCATGTCTGTCTCCTCCAT	179–222	HEX	*Malus X domestica*	5	Liebhard et al 2002	7
CH05c06	ATTGGAACTCTCCGTATTGTGC	ATCAACAGTAGTGGTAGCCGGT	104–126	HEX	*Malus X domestica*	16	Liebhard et al 2002	3
EMPc11	GCGATTAAAGATCAATAAACCCATA	AAGCAGCTGGTTGGTGAAAT	123-171	6-FAM	*Pyrus communis*	11	Fernández-Fernández et al 2006	5
EMPc117	GTTCTATCTACCAAGCCACGCT	CGTTTGTGTGTTTTACGTGTTG	82-142	6-FAM	*Pyrus communis*	7	Fernández-Fernández et al 2006	7
GD147	TCCCGCCATTTCTCTGC	AAACCGCTGCTGCTGAAC	124-156	PET	*Malus X domestica*	13	Hokanson et al 1998	8
GD96	CGGCGGAAAGCAATCACCT	GCCAGCCCTCTATGGTTCCAGA	152-197	HEX	*Malus X domestica*	17	Hokanson et al 1998	8
CH01h10	TGCAAAGATAGGTAGATATATGCCA	AGGAGGGATTGTTTGTGCAC	94–114	HEX	*Malus X domestica*	8	Gianfranceschi et al 1998	9
CH01h02	AGAGCTTCGAGCTTCGTTTG	ATCTTTTGGTGCTCCCACAC	236–256	NED	*Malus X domestica*	9 & 17	Gianfranceschi et al 1998	9
CH01a09	GATGTGGTTCCAGAAGCTAC	CACATGCATGAAAAGCATAT	198–384	6-FAM	*Malus X domestica*	14	Liebhard et al 2002	6
CH02C09	TTATGTACCAACTTTGCTAACCTC	AGAAGCAGCAGAGGAGGATG	233–257	NED	*Malus X domestica*	15	Liebhard et al 2002	1

Table S3. Pool of specific primer assessed in each genotype. `+` positive, `-` negative, `nt` non tested

	Consensus fragment size (bp)					
	Cocomerina Tardiva	**Cocomerina Precoce**	**Briaca**	**Pera Sanguigna**	**Cocomerina selvatica LaCasa**	**Incrocio S.Alessio**
Allele specific primers	750/800	750	650/1300	1700	800/1200	650/750
PcS101	nt	-	+	-	+	nt
PcS102	nt	-	-	-	-	nt
PcS103	nt	-	-	-	-	nt
PcS104	+	+	-	-	-	+
PcS105	-	-	+	-	-	-
PcS106	-	-	-	-	-	-
PcS107	-	-	-	-	-	-
PcS108	-	-	-	-	-	+
PcS109	-	-	-	-	-	-
PcS110	nt	-	-	-	-	nt
PcS111	-	-	-	-	-	-
PcS112	nt	-	-	-	-	nt
PcS113	nt	-	-	-	-	nt
PcS114	-	-	-	-	-	-
PcS115	-	-	-	-	-	-
PcS116	-	-	-	-	-	-
PcS117	nt	-	-	-	-	nt
PcS120	+	-	-	-	+	-
PcS121	-	-	-	-	-	-
PcS122	-	-	-	-	-	-
PcS123	-	-	-	-	-	-
PcS124	-	-	-	-	-	-
PcS125	nt	+	-	+	-	nt
S-genotype	S104/S120	S104/S125	S101/S105	S125/-	S101/S120	S104/S108

Table S4. Allele frequencies estimated by Cervus 3.0.7 for each Locus analysed.

CH01D9	126	128	132	134	138	147	149	151	153	155
	0,06	0,22	0,06	0,06	0,06	0,06	0,17	0,17	0,06	0,11
CH5C06	87	91	92	95	103	105	107			
	0,44	0,22	0,06	0,11	0,06	0,06	0,06			
CH1F7a	175	180	181	183	188	193	198	206		
	0,17	0,22	0,06	0,22	0,06	0,11	0,11	0,06		
CH2B10	120	122	124	126	128	132	134	136		
	0,11	0,06	0,06	0,22	0,06	0,17	0,28	0,06		
CHVf1	-1	124	128	132	134	139	148	150		
	0,11	0,11	0,22	0,11	0,06	0,06	0,28	0,06		
CH02C09	-1	226	238	240	242	244	248			
	0,11	0,06	0,11	0,11	0,06	0,50	0,06			
EMPC11	138	140	142	149	151	153	157			
	0,17	0,06	0,06	0,50	0,06	0,06	0,11			
CH3D12	108	112	120	123	125	132	157			
	0,28	0,33	0,06	0,06	0,11	0,11	0,06			
EMPC117	82	88	95	111	113	116	123			
	0,11	0,11	0,06	0,17	0,39	0,11	0,06			
CH4E03	178	182	196	203						
	0,72	0,06	0,17	0,06						
GD147	121	127	131	141	155					
	0,67	0,17	0,06	0,06	0,06					
GD96	141	150	157	159	163	173				
	0,11	0,50	0,06	0,11	0,11	0,11				
CH1D08	239	276	280	282	286	294				
	0,06	0,39	0,06	0,17	0,22	0,11				
CH03G7	220	224	226	230	234	242	245	246	256	261
	0,06	0,06	0,06	0,06	0,06	0,17	0,06	0,33	0,06	0,06
CH04C7	95	97	110	112	116	120	124	130	134	148
	0,06	0,06	0,11	0,06	0,06	0,06	0,17	0,06	0,17	0,22
CH01A9	168	170	172	174	176	182	184			
	0,39	0,11	0,28	0,06	0,06	0,06	0,06			
CH01H10	98	100	102	104	110	124				
	0,06	0,11	0,39	0,22	0,06	0,17				
CH01H2	222	226	228	230	234	236	238	240	252	
	0,06	0,17	0,06	0,17	0,11	0,11	0,06	0,22	0,06	

4. Development and Validation of Markers Linked to Red-Fleshed Fruit Trait in European Pear Crossing Populations

Abstract

Red-fleshed fruits are becoming more and more popular among consumers worldwide due to their high concentration of bioactive compounds, primarily anthocyanin. The red-fleshed fruit trait genetic regulation has been studied in several different fruit species such as apple, peach, plum, sweet cherry and so on. Very few studies have been performed on red-fleshed pear, even if this trait has been known for centuries. In this study, the identification by quantitative trait loci (QTL) analysis were carried out using a crossing population segregating for the trait ('Cocomerina Precoce' x 'Carmen'). The outcome was the identification of a small genomic region related to the red flesh fruit trait approximately at 27 Mb from the start of LG5. Two candidate genes were detected in this genomic region: 'PcMYB114' and 'PcABC transporter C2'. Furthermore, the SSR marker SSR114 was found able to detect the red flesh phenotype segregation in all the red-fleshed pear accessions and crossing populations tested.

4.1. Introduction

Red-fleshed fruits are becoming more and more popular among consumers worldwide due to the beneficial effects of anthocyanin in human health, from reducing the risk of cardiovascular diseases to preventing the onset of cancer (Hou *et al.,* 2004; Seeram *et al.,* 2004; Stevenson and Hurst 2007; Butelli *et al.,* 2008; Manach *et al.,* 2009; Espley *et al.,* 2014; Antognoni *et al.,* 2020). Increased dietary intake of these secondary metabolites might certainly be promoted by the consumption of red fleshed fruits (Allan *et al.,* 2019). This trait has been studied in several fruit species such as apple (Chagné *et al.,* 2013; Espley *et al.,* 2007; Lin-Wang et a. 2010), peach (Zhou *et al.,* 2015), plum (Fang *et al.,* 2016; Liu *et al.,* 2020), sweet cherry (Starkevič *et al.,* 2015; Sabir *et al.,* 2022) orange (Buttelli *et al.,* 2012; 2017), bilberry (Lafferty *et al.,* 2022; Plunkett *et al.,* 2018: Montanari *et al.,* 2022) and strawberry (Wang *et al.,* 2020).

Very few studies have been carried out until now on red-fleshed pear, even if this trait have been known for centuries: the Tuscan Academic Pier Antonio Micheli, described the fruits of 'Pera Sanguignola', literally "bloody pear", first mentioned at the end of 1600. In the following centuries, red-fleshed pears were also reported in France, Belgium and Germany (Leroy, 1867-79; Downing, 1869; Mas, 1872-83; Hedrick, 1921). Many red-fleshed landraces have been included in the last years in some genetic diversity studies in European pear (Braniste and Budan 2007; Lespinasse *et al.,* 2010; Baccichet *et al.,* 2019, Sau *et al.,* 2020, Sehic *et al.,* 2012, Ferradini *et al.,* 2017). Nevertheless, the origin of this trait is still unknown. Recently, some Italian red-fleshed pear landraces were analysed by SSR markers and 4 different genotypes with a short genetic distance were identified suggesting a possible common ancestor for that peculiar trait (see chapter 3). Red colour is a very relevant trait in fruit breeding; however, the attention has played particularly on peel colour. The rising number of red variants in all species of the Rosaceae family makes it easy to see this tendency, from apricots (Bassi and Foschi

2019) to peaches (Chavez *et al.*, 2019), to pears (Brewer and Volz 2019; Caracciolo *et al.*, 2018) and apples (Chen *et al.*, 2021). The red flesh trait has been already introgressed in other fruit tree species, such as apple, and several commercial cultivars have just been released, *i.e.*, 'Red Moon ®', 'Red Love®' and 'Kissabel Rouge®' (Guerra 2018).

Anthocyanins are one of the most important flavonoid pigments. They were synthesized through the phenylpropanoid pathway starting from phenylalanine or tyrosine, two aromatic aminoacid derived from the shikimate pathway. The transcription of the structural genes of anthocyanin pathway is regulated by the activity of several transcription factors (TFs). The most important TFs involved are MYBs, bHLHs e WD-repeat proteins. This three TFs form a complex (MBW complex) that have the potential to activate the transcription of anthocyanin pathway structural genes (Ramsay *et al.*, 2005).

Many studies were performed to understand the genetic regulation of anthocyanin production. Anthocyanin accumulation is primarily controlled at the transcriptional level in the Rosaceae, as it is in the majority of other plant species, and MYB transcription factors family genes are playing a critical role (Lin-Wang *et al.*, 2010). According to Pierantoni *et al.*, (2010), the European pear (*P. communis*) PcMYB10 transcription factor, is expressed at much higher levels in 'Max Red Bartlett' than in 'Bartlett' and is positively correlated with anthocyanin accumulation during fruit development. In line with the segregation observed in seven progenies using 'Max Red Bartlett', 'Cascade' or 'California' as red-skinned fruit parental line, red fruit colour in European pears was found to be a monogenic dominant trait (Dondini *et al.*, 2008). Additionally, the spontaneous red skin mutant of 'Bartlett' ('Max Red Bartlett') was mapped onto LG 4 (Dondini *et al.*, 2008) which correspond to the genomic region found by Ou *et al.*, (2020) including the PpBBX24 gene belonging to the B-box a subfamily of zinc-finger TF. In particular, 14 nucleotide deletion mutation in the coding region of the PpBBX24 gene was associated with the red skin of the "Zaosu Red" pear (Ou *et al.*, 2020). In a progeny

derived from the red-skinned pear hybrid variety "Bayuehong", three distinct QTLs were found for red fruit skin colour (Wu *et al.,* 2014). One of these QTLs is mapped on LG 4; nevertheless, the location appears to be different from the one discovered in 'Max Red Bartlett' (Dondini *et al.,* 2008). The other two QTLs have been located on LGs 13 and 16. Additionally, a recent re-examination of the data from the same population had led to the discovery of a novel QTL situated at the base of LG 5 and a new candidate gene has been identified: PyMYB114 (Yao *et al.,* 2017). The expression level of this gene was confirmed as positively correlated with red skin, and studies made by transient transformation has revealed that PyMYB114 is able to induce anthocyanin biosynthesis (Yao *et al.,* 2017). The same QTL was identified by Xue *et al.,* (2017) in *P. pyrifolia* with the identification of PyMYB114 as a candidate gene. Further investigations about this gene were made by Ni *et al.,* (2019) that reported that PpMYB114 could be able to increase the expression of PpUFGT in complex with PpbHLH3, as well as PcMYB10. Furthermore, in *P. communis* a QTL for fruit skin blush has been found in the same position at the bottom of LG 5, in a progeny of 'Flamingo' × 'Abbé Fétel' (Ntladi *et al.,* 2018). These results support the theory that anthocyanin production and accumulation could be controlled by similar genes in Asian and European pears. However, the red phenotype could be derived by several mutations in different genetic backgrounds and the diverse genomic regions linked to this trait suggest a complex genetic regulation, with several loci playing a role (De Franceschi and Dondini 2019).

In this chapter, the identification of quantitative trait loci (QTL) linked to the red fleshe trait is reported as well as the discover of putative candidate genes within the genomic regions involved in anthocyanin accumulation in fruit flesh. Then, a tightly linked marker was designed on a candidate gene and tested in other cross populations to demonstrate its efficiency in discern for red-fleshed seedlings.

4.2. Materials and methods

4.2.1. Plant material and DNA extraction

A total of 12 populations segregating for red-fleshed fruit obtained from controlled crosses were used in this study (Table 4.1). The `Cocomerina Precoce` (CP) x `Carmen` (C) population, hold by CREA (Consiglio per La Ricerca e La Sperimentazione in Agricoltura, Forlì-Cesena, Italy), consisting of 127 seedlings was used to perform the QTL analysis. All the other populations were used for the validation of the closest molecular marker linked to the trait.

Table 4.1. Number of seedlings, genealogy and locations of the segregating populations tested with the marker SSR114. In pink highlighted the sources of red-flesh fruit trait.

Population	n° Seedlings	Parent 1	Parent 2	Location	N° Seedlings tested
CP x C	127	**Cocomerina Precoce**	Carmen	CREA Forlì, FC, Italy	127
CT x AF	83	**Cocomerina Tardiva**	Abate Fetel	UNIBO Cadriano, BO, Italy	83
CP x AF	50	**Cocomerina Precoce**	Abate Fetel	UNIBO Cadriano, BO, Italy	50
CP x Cs	71	**Cocomerina Precoce**	Cascade	UNIBO Cadriano, BO, Italy	71
CT x Cf	66	**Cocomerina Tardiva**	Conference	UNIBO Cadriano, BO, Italy	66
CP x SRB	52	**Cocomerina Precoce**	Sensation Red Bartlett	UNIBO Cadriano, BO, Italy	52
CP x W	19	**Cocomerina Precoce**	William	UNIBO Cadriano, BO, Italy	19
P13.018	154	**R234 (Sanguinole*)**	**R 256 (Sanguinole*)**	PFR Motueka, Tasman, New Zealand	80
P13.019	35	**R234 (Sanguinole*)**	R546	PFR Motueka, Tasman, New Zealand	20
P13.020	67	**R234 (Sanguinole*)**	R375	PFR Motueka, Tasman, New Zealand	20
P13.021	60	**R234 (Sanguinole*)**	R276	PFR Motueka, Tasman, New Zealand	20
P16.005	154	**R143 (Samsoe*)**	R823	PFR Motueka, Tasman, New Zealand	20
Total	940				628

* In bold the red-fleshed parent; in brackets the ancestral donor of the red-fleshed trait

DNA was extracted from around 50 mg of young leaves powder using DNeasy Plant Mini extraction kit (Qiagen, Hilden, Germany). DNA quality and quantity were verified by NanodropTM ND-1000 Spectrophotometer (Thermo Scientific, Wilmington, DE, USA). All DNA solutions were diluted to 50 ng/µL as a working solution.

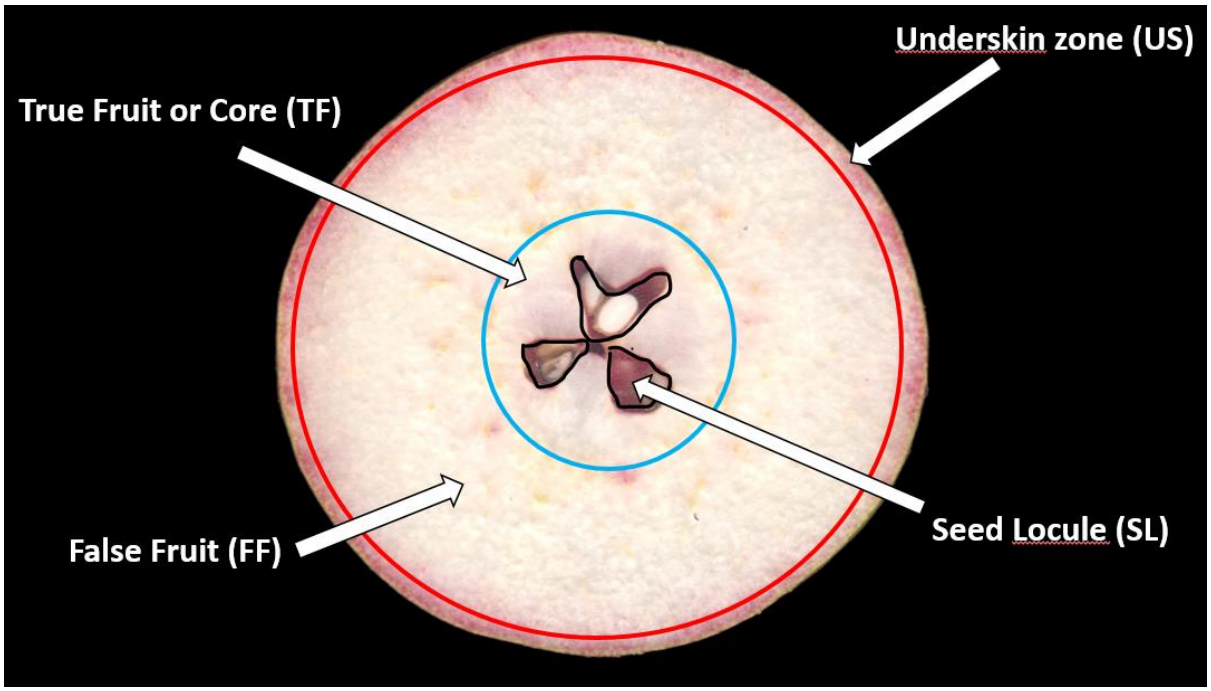

Figure 4.1. Schematic representation of the pear equatorial fruit section zones scored for colour phenotyping.

4.2.2. Fruit flesh colour phenotyping

In the CP x C progeny, the phenotyping was performed on about 5-10 mature fruits from each seedling and parental plant in 2 consecutive years (2020 and 2021). Red colour presence and intensity were visually scored and dissected in four different traits to take into account the distribution of the red colour within the different fruit tissues visible on equatorial section (Figure 1): False Fruit (pome, flesh or pseudocarp; FF), True Fruit (core or mesocarp; TF), Seed Locule (endocarp; SL) and Under-Skin (the first layer of flesh near the fruit skin; US). A 0 to 5 scale was assigned for FF and TF (0 means complete absence of red and 5 very intense

red colour). For SL and US a binary code (0/1) for presence/absence of red was used. In addition, an absolute red/white flesh score (R/W) was assigned to each seedling based on the previous values.

4.2.3. Statistical analysis

To confirm the bimodal distribution of the red-flesh trait, and the Mendelian segregation of the red-fleshed (R) or white-fleshed (W) seedlings, the χ^2 was calculated. For each year, Shapiro–Wilk test was also performed to test for normal data distribution. Moreover, the correlation between the means of the different trait were tested, using either the Pearson or the Spearman test according to the normal/not normal distribution of each trait. Red-flesh intensity parameter, TF and FF, data were analysed by ANalysis Of VAriance (ANOVA) followed by Tukey's test under R environment using ''agricolae'' R package (https://www.r-project.org). In addition, histograms related to the red intensity distribution and also a Principal Component Analysis (PCA) of yearly data of SL, TF, FF and US was performed by R as well.

4.2.4. Generation of SPET markers, map construction and QTL analysis

Sequencing and library preparation of parental DNAs was carried out by IGA Technology Services (IGATech Udine, Italy), using a NextSeq. 500 sequencing platform (Illumina, San Diego, CA, USA) in single-end mode (150 bp). The obtained reads were aligned to the reference sequence of *Pyrus communis* (Linsmith *et al.*, 2019) to obtain the genomic sequence of the parental cultivar `Cocomerina Precoce` (CP) and `Carmen` (C). By comparing the two parental genome sequencing and the reference sequence (Linsmith *et al.*, 2019) a 10k panel of intragenic SNPs was designed in order to fully covering the seventeen chromosomes of *Pyrus communis*, with the aim to build a high-density linkage map. This panel was used to design the

probes for the Single Primer Enrichment Technology analysis (SPET; NuGen. San Carlos CA, United States). Parents and progeny genotypes alleles were mined from this panel using the Allegro Targeted Genotyping V2 procedure (IGATech Udine, Italy).

SNPs markers showing more than 10% of missing data and not bi-allelic segregation were excluded from the analysis. Only markers segregating in either one of the two parents were employed for building CP and C linkage map; SNPs heterozygous in both parents were not used. Only the first SNP per probe was selected in order to reduce information redundancy during the mapping. Seedling with no fructification, more than 10% of missing data or with an outcross-type of segregation were excluded from the analysis, as well.

Molecular maps of CP and C were constructed using JoinMAp 4.1 software (Van Ooijen, 2006). A Grouping tree was made using a minimum LOD score of 8 and the map distances was calculated using regression mapping by Kosabi`s function. After the first mapping all the genotype probability identified by the software were excluded and the maps recalculated to obtain the final maps that were drawn using MapChart 2.3 (Voorrips, 2002).

QTL mapping was performed with the MapQTL 6.0 software (Van Ooijen 2004), using interval mapping (IM) (Lander and Botstein 1989). QTLs were also detected using the non-parametric Kruskal–Wallis (KW) test for traits with not-normal distribution in the progeny (Alonso-Blanco *et al.*, 2006). The significant logarithm of odds (LOD) threshold ($\rho = 0.05$) for each trait was determined after genome-wide permutation tests (Churchill and Doerge 1994) using 1000 permutations.

The traits considered for QTL mapping were: Seed Locules (SL), False Fruit (FF), True Fruit (TF), Under Skin (US) and, additionally, the output data obtained from the Principal Component Analysis (PC1, PC2, PC3 and PC4) as suggest by Gilbert & Le Roy (2003).

The broad-sense heritability (H^2) of genotypic means for all these traits was estimated using the formula:

$$H^2 = \sigma_g^2 \div (\sigma_g^2 + \sigma_e^2/n)$$

where 'n' is the mean number of replicates per genotype, 'σ_g^2' is the genetic variance (*i.e.*, inter-genotype variance), and 'σ_e^2' is the residual error variance (Calenge *et al.*, 2005; Durel *et al.*, 2009; Montanari *et al.*, 2015). The percentage of the phenotypic variation explained by all the significant ($\rho < 0.05$) QTLs (R^2 or coefficient of multiple determination) was estimated using the global formula:

$$R^2 = 1 - (SS_{res}/SS_{tot})$$

where SS_{res} is the residual sum of squares and SS_{ate} is the total sum of squares.

4.2.5. Candidate genes marker design and validation

Putative candidate genes for the red-flesh trait were searched at genome level by screening the predicted gene database of the *Pyrus communis* 'Bartlett' Double Haploid v.2.0 genome (Linsmith *et al.*, 2019) available on the GDR website (https://www.rosaceae.org).

After major candidate genes identification two additional markers were designed to define the QTL region. Putative heterozygous molecular markers were found at genome level examining the resequencing data of the CP parent. Two pair of primers were designed inside the candidate genes sequences in order to determine their segregation (Table 4.1).

The first marker, SSR114, was designed to detect a putative polymorphic microsatellite. Forward primer was labelled with 6-FAM. The PCR reactions were performed with the Thermal Cycler 2700 GeneAmp PCR System (ABI Prism) in 50 ng of DNA solution and 9 µL of master mix prepared according to Sau *et al.*, (2020). The reaction cycling conditions were

as follows: initial denaturation step of 5 min at 94°C, followed by 35 cycles each consisting of 30 s denaturation at 94°C, 45 s annealing at 60°C and 45 s elongation at 72°C and the last cycle ends with a final 7 min extension at 72°. The amplicon fragment length was genotyped by ABI PRISM 3730 DNA analyser. One µl of each PCR product was added to 9 µl of formamide containing 0.2 µl of GeneScan 500 LIZ size standard (Applied Biosystem, Waltham, Massachusetts, US). Fragments were analysed and visually scored using Peak Scanner v.1.0 (Applied Biosystem, Waltham, Massachusetts, US).

Table 4.1. Primers designed to enrich the QTL region.

Marker	Type	Sequence	Tm	Fragment size	Position in Mb from beginning of Chr5
SSR114	Forward	AGGTATTTTATTTTGTATGTATCAATGA	54	225 b	27.1
	Reverse	GTAGGTAAATTATTTCACACACACAT	56		
CAPS2	Forward	GGGCCCAATCACCAAAATCA	58	607 b	27.0
	Reverse	TGAACTCTAGTCTTGGCGGA	59		

The second marker, CAPS2, was designed to detect a putative polymorphic restriction site. The PCR reactions were performed with the Thermal Cycler 2700 GeneAmp PCR System (ABI Prism) in 50 ng of DNA solution and 9 µL of master mix prepared according to Sau *et al.,* (2020). The reaction cycling conditions were as follows: initial denaturation step of 5 min at 94°C, followed by 35 cycles each consisting of 30 s denaturation at 94°C, 45 s annealing at 61°C, 60 s elongation at 72°C and the last cycle ends with a final 10 min extension at 72°. PCR products were digested using the restriction enzyme Bsp143I (CTAG; Thermo Fisher Scientific, Waltham, Massachusetts, US). Digestion reactions were performed, as manufacture instructions, in a dry bath at 37°C for 2 h using 5 µL of PCR reaction, 5 µL of

digestion buffer and 1 µL of Bsp143I enzyme. Digested PCR products were analysed by electrophoresis in 1% agarose gel.

The SSR114 marker was selected to analyse other 11 red-fleshed fruit segregating populations obtained from different donors of the red flesh trait. A total of six populations located in Cadriano (BO, Italy) in UNIBO's experimental field and five in Motueka, (Tasman, New Zealand) in Plant and Food Research's field (Table 4.2). SSR114 PCR was carried out as reported previously for the crossing population CP x C. Phenotyping of the additional 11 populations were performed in 2020 and 2021. The phenotyping of these progeny was focused only on presence or absence of the red colour in the fruit flesh using a red/white binary index in order to validate the efficiency of this marker in selecting red-fleshed genotypes.

4.3. Results and Discussion

4.3.1. Flesh Colour Phenotyping

In the CP x C progeny, a total of 903 fruits from 107 seedlings and 789 fruits from 106 seedlings were evaluated for red colour distribution and intensity in the fruit flesh in 2020 and 2021, respectively.

A 1:1 Mendelian segregation ratio was found, confirmed by the χ^2 test, for all the analysed traits within the CP x C crossing population, *i.e.*, for the R/W index 55 red-fleshed seedlings and 66 white-fleshed were detected (Table 4.3). A 1:1 Segregation ration of the red-fleshed trait was already reported in literature by Lespinasse *et al.*, (2010) in a cross population obtained from `Red Comice` and `Sanguigne d`Italie` and by Braniste and Budan (2007) in a cross population `Napoca` X `Cu miezul roşu`. The monogenic inheritance of the trait has been already theorized by Brown back in 1966 (Brown 1966).

The distribution of the adjusted means for all the traits showed a not-normal distribution after the Shapiro-Wilks test (data not shown) according to their Mendelian segregations. The red colour intensity was varying among the seedlings ranging from very little red spots in just one of the fruit areas (SL, TF, FF or US) to an almost complete coverage with high intensity within the whole fruit section. By excluding the white genotypes, the FF and TF trait showed a normal distribution and this is supporting the hypothesis that, a main gene is able to switch on the red colour development in the fruit flesh but, other genes could be involved in the modulation of the colour intensity (Figure 4.2.).

Table 4.3. Two years cumulated data of the number of Red fleshed (R) and White fleshed (W) seedlings referred to the different scored trait. R/W = Red/White colour in the fruit flesh independently from the distribution; SL = inside the Seed Locules; TF = at True Fruit level; FF = at False Fruit level; US = Under the fruit Skin. *P* value ≥ 0.05 confirm the expected segregation of the trait.

	Flesh phenotype			
Trait	Red	White	Expected Segregation	X^2 *p* value
R/W	55	66	1:1	0.317
SL	54	67	1:1	0.237
TF	51	70	1:1	0.084
FF	54	67	1:1	0.237
US	50	71	1:1	0.056

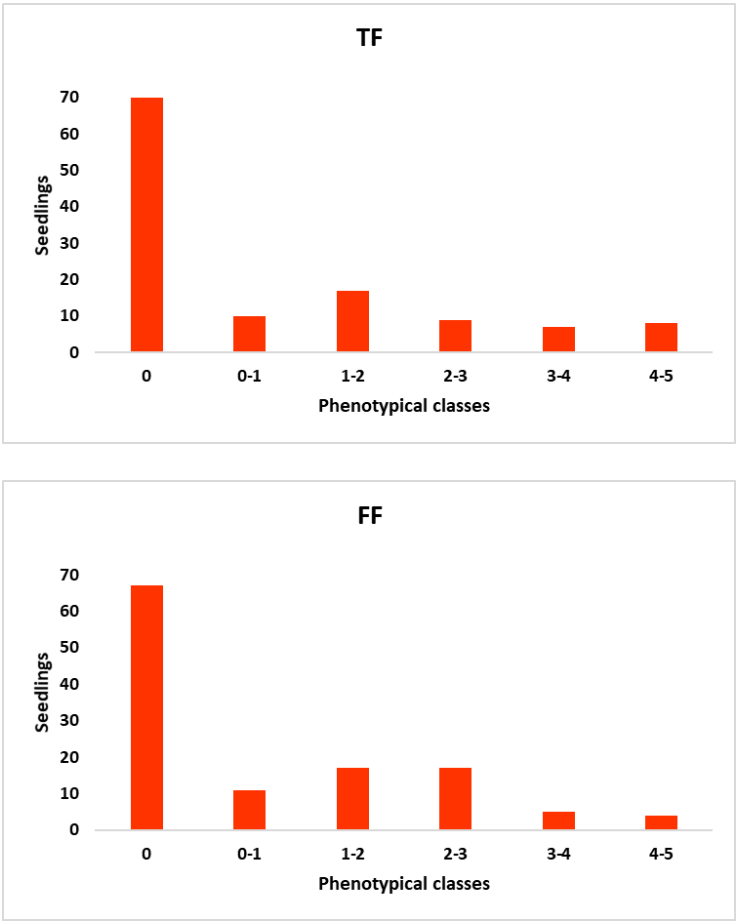

Figure 4.2. Red intensity distribution histograms related to the crossing population CP x C in True Fruit (up) and False Fruit (down). Average data of 2 years.

The average phenotypic data were very stable throughout the two years. In particular, the parental genotypes, CP and C showed not significant differences between the two years of analysis for all the traits. Regarding the crossing population CP x C, the averages of SL, US and TF showed not significant variation comparing 2020 and 2021, instead, the FF was significantly different, reaching a higher average value in 2020 in respect to 2021 (2.08 vs 1.78; Table 4.4). The different environmental conditions between the two years of observations, being 2021 warmer than 2020, could explain this variation. It was plausible that the anthocyanin accumulation was more affected by the light and external temperature at fruit flesh level rather than in the fruit core.

Table 4.4. Comparison of the average red intensity in the two years of phenotyping of the F1 seedlings and the CP parent.

Red colour distribution	Year	F1 (CP X C)	CP
SL	2020	1.00 a	1.00 a
	2021	1.00 a	1.00 a
TF	2020	1.92 a	1.63 a
	2021	1.97 a	1.67 a
FF	2020	2.08 a	1.00 a
	2021	1.78 b	1.00 a
US	2020	0.88 a	0.38 a
	2021	0.82 a	0.21 a

*the value reported are referred to the scale 0 to 5. Significance was tested by ANOVA and Tukey test.

Significant correlations were found between the scored traits in the two years of observation (Figure 4.3). In particular, the correlation for FF and TF showed a correlation index (r_s) of 0.91

and 0.88, respectively. Moreover, they were highly correlated with r_s = 0.88 in 2020 and r_s = 0.90 in 2021.

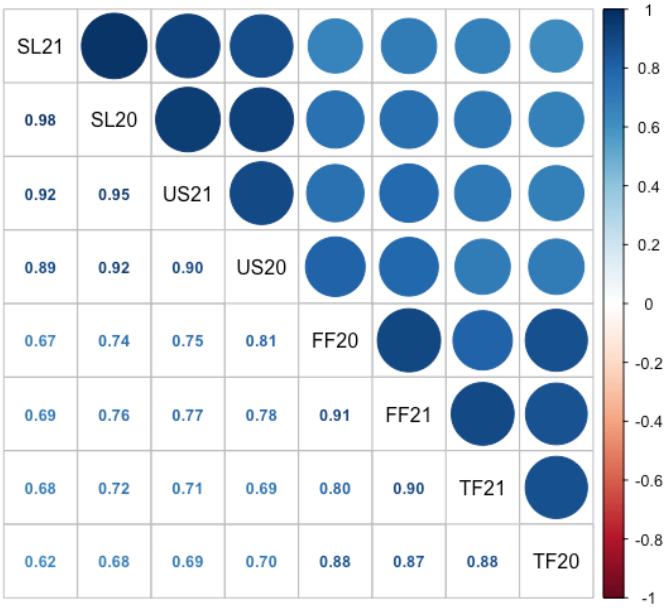

Figure 4.3. Correlation matrix representing the Spearman correlation value among the phenotyping data (SL, US, TF and FF) in 2020 and 2021.

In order to have an overview about the variability observed in the red-flesh phenotype within the population, a PCA was carried out for each year of observation. In both the analysis, the explained variability (Figure 4.4) by the first two Principal Component (PC) were very high: 95.30% in 2020 and 95.35% in 2021. In both years' analysis, white genotypes cluster all together in the same position on the left side of the graphs. On the other hand, the red-fleshed ones showed a distribution on the right side according to their phenotype. Generally, the gradient of red intensity moves left right, with the redder genotypes located to the bottom right part of the graph. Positions of seedlings throughout the two years were quite constant, suggesting a strong genetic control of the phenotypical variability of the trait. The total variability was explained by four PC in both years. The first PC (PC1) for red-fleshed fruit

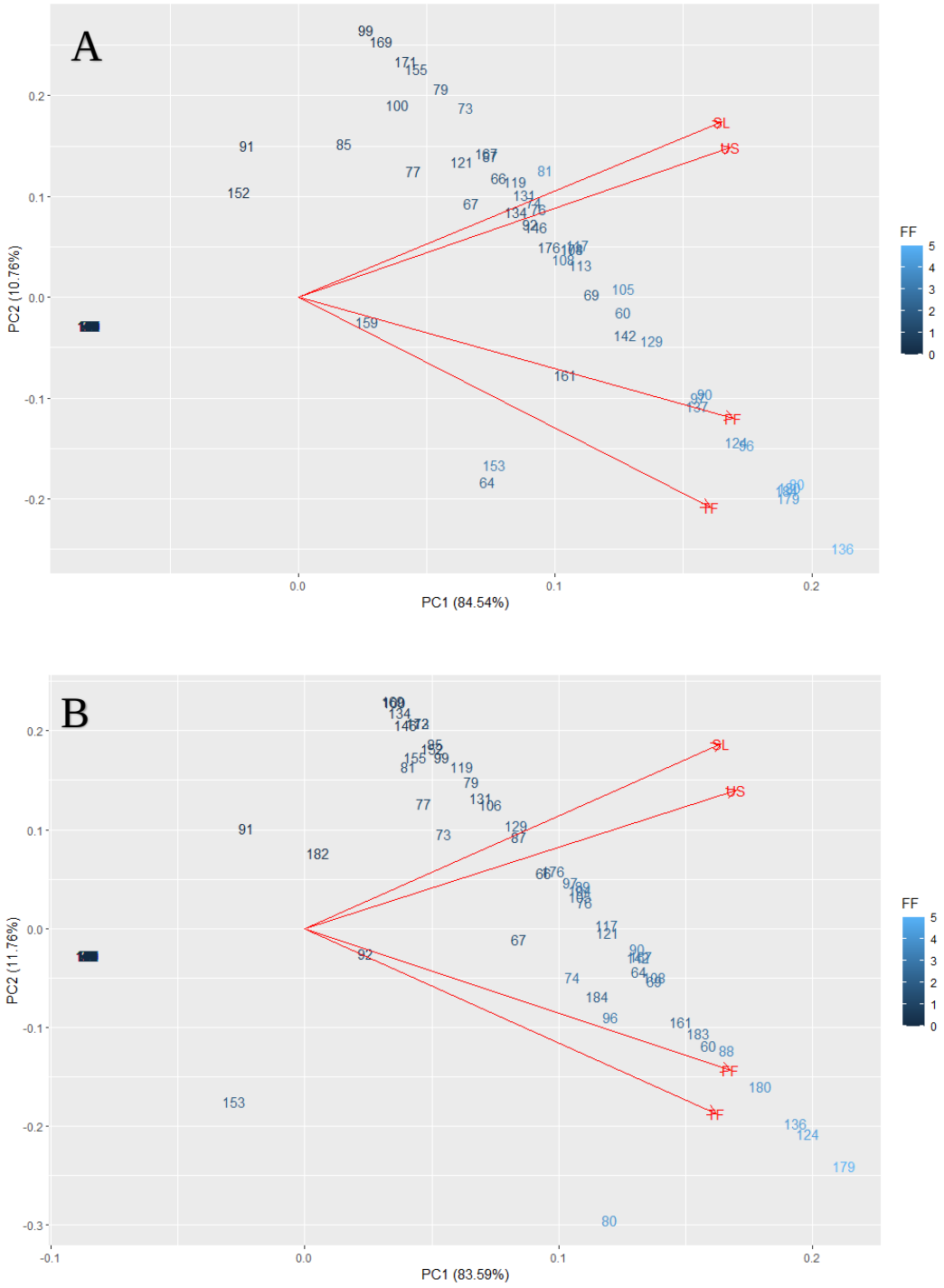

Figure 4.4. Plots of the Principal Component Analysis (PCA) conducted using the phenotypical data collected in 2020 (A) and 2021 (B). Numbers represent seedlings and lines the vectors of the 4 scored variables (SL, US, FF and TF).

accounted for 84.54% of the total variation in 2020 and 83.59% in 2021. The PC2 explained 10.76% of total variation with loadings for SL and US being positive-substantial and those for

TF and FF negative-substantial. The PC3 and PC4 explained only a very small part of the total variability in both years (Table 4.5).

Table 4.5. Results of the PCA analysis performed with phenotypic data in the two years of observations.

	2020				2021			
	PC1	**PC2**	**PC3**	**PC4**	**PC1**	**PC2**	**PC3**	**PC4**
Eighenvalue	1,839	0,656	0,343	0,265	1,829	0,686	0,357	0,242
Proportion of variance	0,8454	0,1076	0,0295	0,0175	0,8359	0,1176	0,0318	0,0147
Cumulative variance	0,8454	0,953	0,982	1	0,8359	0,9535	0,9853	1

4.3.2. High-Density Linkage Map Construction

A total of 39,451 SNPs were detected in the `Cocomerina precoce` x `Carmen` progeny by SPET analysis. Among them, 5,976 showed a segregation “lm x ll” in ‘Cocomerina Precoce’ and 4,257 a segregation “nn x np” in ‘Carmen’. Other 3,615 SNPs with segregation “hk x hk” were identified but these markers were not used for maps construction because of their low informativeness for mapping. After filtering a SNP probe and removing the SNPs with unexpected segregation ratio or more than 10% of missing data, a total of 1,697 and 1,377 SNPs, segregating “lm x ll” and “nn x np”, were used to build the parental genetic linkage maps of ‘Carmen’ and ‘Cocomerina Precoce’. Markers were grouped in 17 linkage groups (LGs), using a LOD threshold of 8. All the markers developed on a specific chromosome mapped on the corresponding LG. CP map covers a total genetic distance of 1,211 cM, with an average length of 71.2 cM per LG. The number of loci per LG was ranging from 48 (LG16) to 172 (LG15) with an average of 99.8 locus per LG. Marker density was also very high with an average genetic distance between two flanking markers of 0.76 cM, with the highest value in LG16 and the lowest in LG9 (1.35 and 0.51 cM per marker). Chromosome coverage was in general very high (more than 94%) except for LG16 (65.9%; Table 4.6). The lower value

observed in LG16 of CP was because of the lack of heterozygous markers in the top part of the chromosome.

Table 4.6. Number of SNP markers, genetic distance, marker density and Chromosome coverage of CP Genetic Linkage Map

LG	No. SNP markers	Genetic distance (cM)	Marker density (cM/locus)	Chromosome coverage
1	69	48.2	0.70	97.3%
2	123	67.3	0.55	97.8%
3	80	104.1	1.30	99.2%
4	79	55.6	0.70	96.4%
5	139	76.7	0.55	96.6%
6	95	65.0	0.68	98.6%
7	112	66.4	0.59	98.9%
8	69	65.2	0.94	98.2%
9	121	62.0	0.51	97.3%
10	106	73.6	0.69	98.4%
11	84	103.4	1.23	96.2%
12	78	51.8	0.66	99.1%
13	97	69.0	0.71	97.8%
14	95	58.6	0.62	98.2%
15	172	110.0	0.64	95.9%
16	48	64.6	1.35	65.9%
17	130	69.7	0.54	94.1%
Average	99.8	71.2		
Total	1697	1211.2	0.76	95.4%

*The chromosome coverage was estimated as a percentage of the length between first and last markers compared to the total length of the chromosome in the pear reference genome.

The C linkage map had a total genetic distance of 1029.7 cM with an average of 60.6 cM per LG. The average of chromosomes coverage was similar to that of the CP map (95.4 %) swinging from 85.2% in LG4 to 98.7% in LG17. The marker density was very similar with an average of 0.75 cM per locus, ranging from 0.53 in LG17 to 1.06 in LG13 (Table 4.7).

Table 4.7. Number of SNP markers, genetic distance, marker density and Chromosome coverage of C Genetic Linkage Map

LG	No. SNP markers	Genetic distance (cM)	Marker density (cM/locus)	Chromosome coverage
1	58	59,2	1,02	98,3%
2	66	57,5	0,87	94,3%
3	63	61,6	0,98	97,6%
4	78	58,1	0,74	85,2%
5	110	64,8	0,59	98,3%
6	84	48,7	0,58	86,6%
7	90	56,0	0,62	96,0%
8	69	51,1	0,74	93,5%
9	61	53,7	0,88	95,0%
10	119	67,2	0,56	96,7%
11	77	58,9	0,76	94,9%
12	77	46,8	0,61	96,1%
13	71	75,2	1,06	98,3%
14	77	54,7	0,71	98,6%
15	117	99,2	0,85	98,5%
16	65	67,1	1,03	92,7%
17	95	49,9	0,53	98,7%
Average	81,0	60,6		
Total	1377	1029,7	0,75	95,4%

*The chromosome coverage was estimated as a percentage of the length between first and last markers compared to the total length of the chromosome in the pear reference genome.

Some of the LG0 scaffolds from the reference sequence (Linsmith *et al.*, 2019) were mapped to specific LGs: *e.g.*, `Super Scaffold 111` markers were assembled, according to its segregation in both, C and CP maps, to the top of LG9, as well as `Super Scaffold 420` markers that were clustered to the bottom of LG13. The complete list and position of scaffolds and contigs that could be mapped in this study was indicate in Table 4.8.

Table 4.8. Number of markers within unplaced scaffold that were mapped in C and CP linkage group maps.

	C map		CP map	
Scaffold name	**No. of SNP markers**	**Position**	**No. of SNP markers**	**Position**
SuperScaffold 420	4	bottom LG13	5	bottom LG13
tig00001755	1	middle LG2	1	middle LG2
tig00012652	1	middle LG2	1	middle LG2
tig00001310	-	-	1	middle LG2
SuperScaffold 290	-	-	1	top LG2
tig00012527	1	middle LG3	-	-
tig00000133	3	middle LG4	4	middle LG4
tig00000976	1	middle LG4	1	middle LG4
tig00000215	1	top LG5	1	top LG5
tig00001128	1	middle LG5	1	middle LG5
tig00001315	-	-	1	top LG7
tig00000348	1	middle LG8	-	-
SuperScaffold 111	13	top LG9	18	top LG9
tig00000808	-	-	1	middle LG9
tig00000629	1	middle LG12	1	middle LG12
tig00012494	2	bottom LG13	1	bottom LG13
tig00000395	1	middle/bottom LG15	2	middle/bottom LG15
tig00000110	-	-	1	middle/top LG15
Superscaffold 581	1	bottom LG16	-	-
tig00012419	1	middle LG17	3	middle LG17

4.3.3. Quantitative Trait Loci detection

Significant QTLs for all measured traits were identified only in the CP map both by Interval Mapping (IM) and Kruskal-Wallis (KW) methods, with the significance of genome-wide LOD thresholds ranging between 2.7 and 3.2 after permutation test (Table 4.9). The detected QTLs were the same when the data of the two years were considered separately or the average data were used. Interestingly, a major QTL was found in the same region, in both years and for 5 different traits: SL, TF, FF, US and PC1. The peak of this QTL is located approximately at 27Mb from the beginning of chromosome 5 (Figure 4.5); markers with the highest LOD were SNP_Chr5_26846468 and SNP_Chr5_27064350 with values ranging between 15.5 and 72.2 in the year 2020 for the traits TF and SL, respectively. Xue *et al.,* (2017) mapped the red/green (R/G) locus in a similar position to the bottom of LG5, using a red and green-skinned pear population derived from a cross between red-skinned Asian pear cultivars. Furthermore, in *P. communis* a QTL for fruit skin blush was found in the same position, the bottom of LG 5, in a progeny of 'Flamingo' × 'Abbé Fétel' by Ntladi *et al.,* (2018). Other 2 minor QTLs for red flesh intensity were identified using PC2 and PC3 on LG5 and LG4 respectively. The QTL identified on LG5 by the second principal component was located in a region at about 20-22 Mb from the beginning of Chr 5, with the highest LOD in 2020 (LOD=5.4) and the lowest in 2021 (LOD=3.6). The PC3 variable permitted to identify a third QTL with a significant LOD for the year 2020 and for the analysis carried out with the average data (LOD equal to 3.2 and 3.7, respectively). This QTL was present in 2021 too; however, the maximum LOD was below the threshold calculated by permutation test. All these minor QTLs were not reported before, however a QTL in LG4, in a different position, was mapped by Dondini *et al.,* (2008) and Wu *et al.,* (2014) in European and Asian pear, respectively. No significant QTLs were detected for PC4 (Table 4.9). The phenotypical variation explained by QTLs (R^2) were generally very high for the phenotypical trait data, the lowest value was obtained in TF 2020 (R^2 =0.5), the highest

in SL 2020 (R^2 =0.96) as evidence of the high level of phenotypical variability explained by this major QTL. Similar value was obtained for PC1 in all the years of observation, R^2 from 0.85 to 0.86 (Table 4.9).

Table 4.9. QTLs mapped for all the traits observed in the years of analysis.

	Interval Mapping					Kruskal-Wallis		
	LG	Peak's closest marker	LOD	LOD threshold	R^2	LG	Peak's closest marker	K-W
2020								
SL	5	Chr5_27163802	72,16	3,2	0,96	5	Chr5_27064350	97,29
TF	5	Chr5_27163802	15,05	3,1	0,50	5	Chr5_27064350	65,97
FF	5	Chr5_27163802	20,51	3	0,61	5	Chr5_27163802	82,5
US	5	Chr5_27163802	44,22	3,2	0,87	5	Chr5_27064350	88,99
PC1	5	Chr5_27163802	43,04	3,1	0,85	5	Chr5_27064350	90,36
PC2	5	Chr5_21380960	5,44	3	0,21	5	Chr5_22726793	25,6
PC3	4	Chr4_17457444	3,24	2,7	0,13	4	Chr4_16185729	12,92
PC4	No QTLs detected			2,7		No QTLs detected		
2021								
SL	5	Chr5_27163802	50,91	3,1	0,92	5	Chr5_27163802	91,61
TF	5	Chr5_27163802	16,09	3,1	0,52	5	Chr5_27163802	79,29
FF	5	Chr5_27163802	19,65	3	0,59	5	Chr5_27163802	81,98
US	5	Chr5_27163802	41,07	3,2	0,86	5	Chr5_27163802	84,71
PC1	5	Chr5_27163802	22,8	3,2	0,85	5	Chr5_27064350	67,07
PC2	5	Chr5_20999224	3,61	2,9	0,13	5	Chr5_22136132	11,05
PC3	No QTLs detected			2,8		4	Chr4_14971775	12,57
PC4	No QTLs detected			2,7		4	Chr4_16185729	12
Average								
SL	5	Chr5_27163802	70,19	3,2	0,95	5	Chr5_27064350	107,23
TF	5	Chr5_27163802	19,53	3,1	0,53	5	Chr5_27064350	92,3
FF	5	Chr5_27163802	26,52	3,1	0,64	5	Chr5_27064350	97,9
US	5	Chr5_27163802	49,2	3,2	0,85	5	Chr5_27064350	101,02
PC1	5	Chr5_27163802	50,3	3,1	0,86	5	Chr5_27064350	100,77
PC2	5	Chr5_21380960	4,35	3,1	0,15	5	Chr5_22726793	23,95
PC3	4	Chr4_17457444	3,68	2,9	0,13	4	Chr4_14971775	24,34
PC4	No QTLs detected			2,6		No QTLs detected		

*The marker's name corresponds to its physical position in the reference genome.

Figure 4.5. Result chart of the QTLs detected by IM analysis for the data FF (a), PC2 (b) and PC3 (c) data. The dotted line represents the significance LOD threshold of the QTLs.

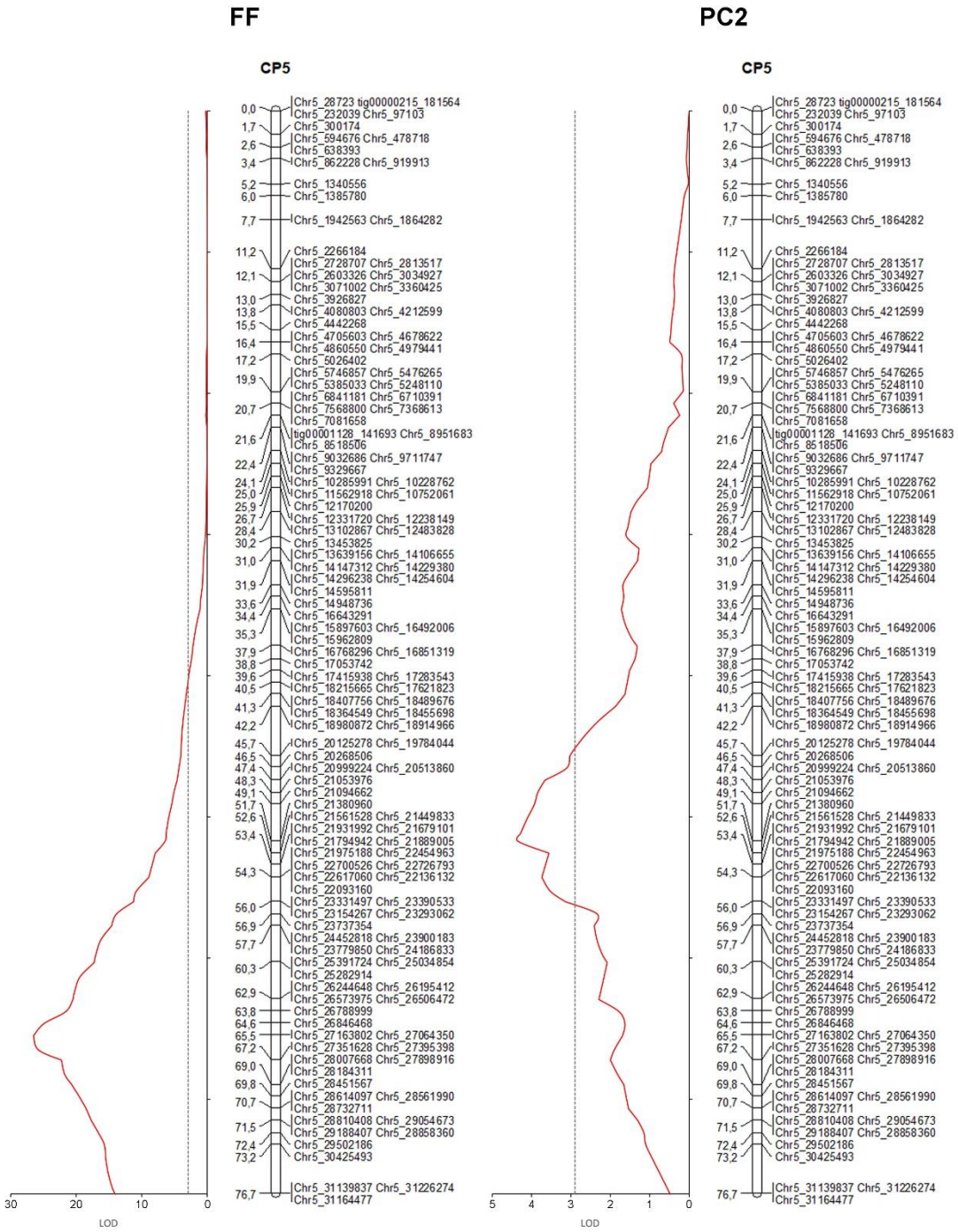

PC3

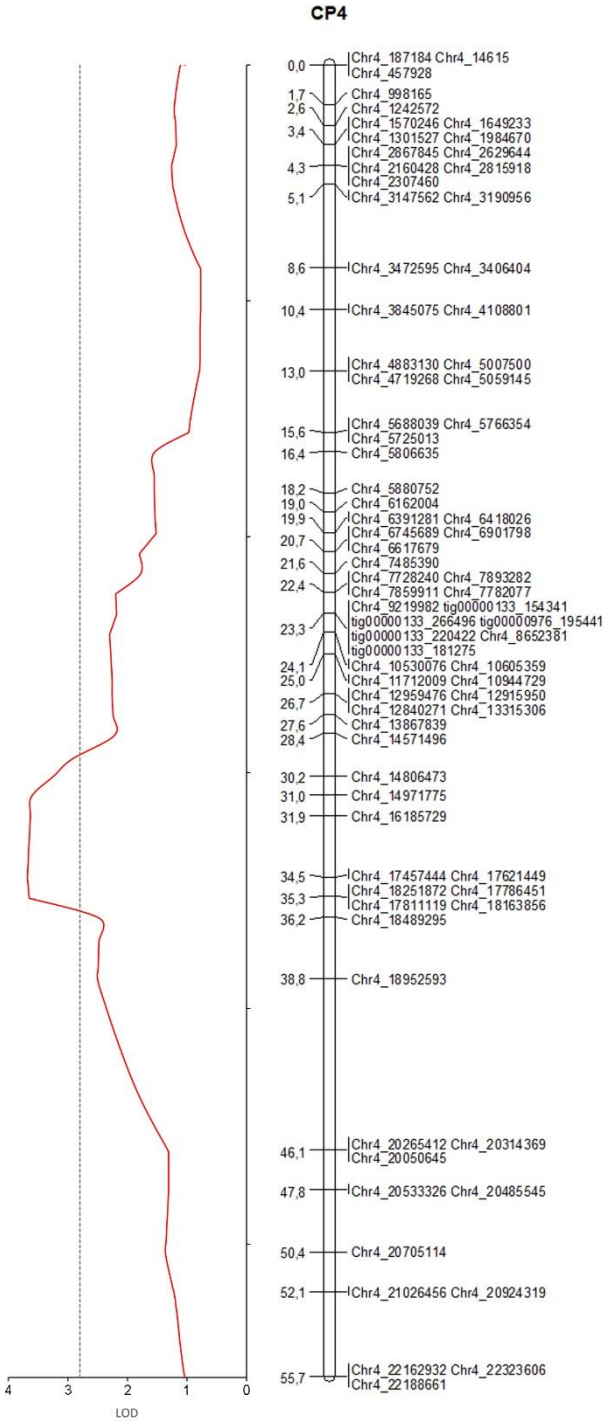
CP4
0,0 Chr4_187184 Chr4_14615 Chr4_457928
1,7 Chr4_998165
2,6 Chr4_1242572
3,4 Chr4_1570246 Chr4_1649233 Chr4_1301527 Chr4_1984670 Chr4_2867845 Chr4_2629644
4,3 Chr4_2160428 Chr4_2815918 Chr4_2307460
5,1 Chr4_3147562 Chr4_3190956
8,6 Chr4_3472595 Chr4_3406404
10,4 Chr4_3845075 Chr4_4108801
13,0 Chr4_4883130 Chr4_5007500 Chr4_4719268 Chr4_5059145
15,6 Chr4_5688039 Chr4_5766354 Chr4_5725013
16,4 Chr4_5806635
18,2 Chr4_5880752
19,0 Chr4_6162004
19,9 Chr4_6391281 Chr4_6418026
20,7 Chr4_6745689 Chr4_6901798 Chr4_6617679
21,6 Chr4_7485390
22,4 Chr4_7728240 Chr4_7893282 Chr4_7859911 Chr4_7782077
23,3 Chr4_9219982 tig00000133_154341 tig00000133_266496 tig00000976_195441 tig00000133_220422 Chr4_8652381 tig00000133_181275
24,1 Chr4_10530076 Chr4_10605359
25,0 Chr4_11712009 Chr4_10944729
26,7 Chr4_12959476 Chr4_12915950 Chr4_12840271 Chr4_13315306
27,6 Chr4_13867839
28,4 Chr4_14571496
30,2 Chr4_14806473
31,0 Chr4_14971775
31,9 Chr4_16185729
34,5 Chr4_17457444 Chr4_17621449
35,3 Chr4_18251872 Chr4_17786451 Chr4_17811119 Chr4_18163856
36,2 Chr4_18489295
38,8 Chr4_18952593
46,1 Chr4_20265412 Chr4_20314369 Chr4_20050645
47,8 Chr4_20533326 Chr4_20485545
50,4 Chr4_20705114
52,1 Chr4_21026456 Chr4_20924319
55,7 Chr4_22162932 Chr4_22323606 Chr4_22188661
4 3 2 1 0
LOD

No QTLs were discovered in ‘Carmen’ (C).

The estimated broad-sense heritability (H^2) was generally extremely high for each trait in both years (Table 4.10), with the highest value observed for SL (1 in 2020 and 0.996 in 2021). The lowest level of estimated heritability was obtained for TF in 2021 however, with a high value: 0.98.

Table 4.**10**. Broad-sense heritability (H^2) estimation and phenotypic variation explained by the significant QTLs (R^2) for red-fleshed fruit traits in CP x C segregating population.

	2020		2021		Average	
Trait	**H^2**	**R^2**	**H^2**	**R^2**	**H^2**	**R^2**
SL	1,000	0,962	0,996	0,924	0,998	0,948
TF	0,995	0,498	0,980	0,517	0,990	0,531
FF	0,990	0,608	0,981	0,585	0,989	0,639
US	0,991	0,865	0,980	0,856	0,990	0,853

However, the R^2 explained by the QTLs were always lower than the H^2, which indicates that we were not able to detect all the loci linked to red-fleshed trait. The reasons were imputable to the type and size of the mapping population that we used. Being an intraspecific F1 population, all individuals were supposedly highly heterozygous; hence, the progeny was highly variable with possible complex genetic architecture of the studied traits involving gene interactions, which are more difficult to map. Moreover, our population consisted of 116 genotypes and with this size only the largest effect can be detected.

4.3.4. Candidate Genes Identification

A total of 30 putatively candidate genes involved in anthocyanin accumulation in the fruit flesh were found within the regions of three significant QTLs (Table 4.11). Specifically, for the major QTL, detected in LG5 of 'CP' around 27Mb from the beginning of the chromosome, 2 out of 77 annotated genes within the region between 26'623'085 b and 27'356'731 b were identified as putative candidate genes: `PcABC transporter C family member 2-like` (pycom05g25670) and `PcMYB114` (pycom05g25770). Moreover, 18 putative candidate genes were identified across the region of a second minor QTL on LG5; the genomic position of interest spanned from 20'290'000 b to 22'750'000 b from the top of chromosome 5. Most of the 18 candidate genes detected in this QTL were transcription factor genes (TFs) belonging the families of WRKY (one gene), MYB (one gene), NAC (one genes), ERF (one gene), WD (two genes) and bHLH (four genes). A total of seven 'ABC transporter genes' were also found in this region. Additionally, inside the area of the third minor QTL, detected in LG4, further 10 candidate genes for red flesh fruit were revealed. The physical location of this QTL was between 14'800'000 b and 18'400'000 b on the chromosome 4. As for the previous QTL the majority of candidate gene identified were TFs; two bHLH genes, two MYB genes and four WRKY genes. Also, two UDPGT (glucosyl-transferase gene) were also located in that region (Table 4.11).

Table 4.11. Summary of the candidate genes found in the genomic regions of the quantitative trait loci (QTLs) of fruit red-fleshed fruit detected by interval mapping (IM) and the Kruskal–Wallis (KW) test.

Gene ID	Chromosome	Gene Start	Gene End	Gene Length	Gene Family
major QTL LG5 CP					
pycom05g25670	Chr5	27000730	27010566	3393	ABC_tran
pycom05g25770	Chr5	27101018	27103432	714	Myb_DNA-binding
minor QTL LG4 CP					
pycom04g11930	Chr4	14915111	14916565	615	WRKY
pycom04g12270	Chr4	15237547	15241814	2136	bHLH
pycom04g12860	Chr4	15858714	15862608	1467	UDPGT
pycom04g12870	Chr4	15872925	15873296	372	UDPGT
pycom04g13920	Chr4	16791772	16793400	756	Myb_DNA-binding
pycom04g14360	Chr4	17261741	17264601	2166	bHLH
pycom04g14550	Chr4	17428297	17429855	876	Myb_DNA-binding
pycom04g14890	Chr4	17663438	17665420	1563	WRKY
pycom04g15480	Chr4	18358920	18360504	786	WRKY
pycom04g15490	Chr4	18368841	18370660	1056	WRKY
minor QTL LG5 CP					
pycom05g17030	Chr5	20292509	20295023	1542	WD repeat
pycom05g17160	Chr5	20395789	20397246	1047	WD repeat
pycom05g17170	Chr5	20402876	20407557	2967	ABC_tran
pycom05g17180	Chr5	20407666	20408704	723	ABC_tran
pycom05g17200	Chr5	20415308	20416447	423	ABC_tran
pycom05g17210	Chr5	20417334	20420353	1383	ABC_tran
pycom05g17230	Chr5	20451549	20452277	729	ABC_tran
pycom05g17240	Chr5	20452351	20458335	3807	ABC_tran
pycom05g17670	Chr5	20813164	20813421	258	-
pycom05g18180	Chr5	21172697	21174504	864	ABC_tran
pycom05g18260	Chr5	21240400	21244009	741	NAC
pycom05g18450	Chr5	21367193	21369061	804	Myb_DNA-binding
pycom05g18900	Chr5	21818289	21819706	726	bHLH
pycom05g18910	Chr5	21824937	21825278	342	bHLH
pycom05g18950	Chr5	21888207	21889715	1509	bHLH
pycom05g19060	Chr5	21974291	21975004	714	ERF
pycom05g19070	Chr5	21978228	21980136	1071	WRKY
pycom05g19830	Chr5	22701588	22703209	636	NAC

4.3.5. Marker validation

Three different alleles were found by the marker SSR114 testing the parental genotypes C and CP. The two parentals shared the 226 allele; however, the alleles 194 and 202 were specific for C and CP, respectively. According to the Mendelian segregation, four different allelic combinations were found in the progeny: 194-202, 194-226, 202-226 and 226 (Table 4.12). Comparing the allelic profiles and the phenotypes a perfect match between the allele 202 and the red flesh phenotypes was found.

Table 4.12. Allele combination and respective flesh phenotype of the progeny CP x C of the two additional markers designed inside the candidate genes.

N° of seedling tested	Allele combinations	Red flesh	White flesh
	SSR114		
22	194-**202**	22	0
35	**202**-226	35	0
36	194-226	0	36
25	226	0	25
	CAPS2		
61	AA	0	61
57	A**a**	57	0

Note: SSR114 parent's allelic profile: CP = 202-226, C = 194-226; CAPS2 parent's allelic profile: CP = Aa, C = AA.

Regarding the CAPS2 marker, only two allelic profiles were found in the progeny according to the parental segregation. Among the progeny, 61 'AA' genotypes were found and all of them had the white flesh phenotype, while the seedlings presenting the 'Aa' genotype showed the red flesh phenotype.

Both markers showed the same segregation as the best SNP marker 'Chr5_27064350' and the red/white flesh phenotype. Unfortunately, no recombination between the two candidate genes was found, making it impossible to establish which has the most important role in the anthocyanin accumulation within the fruit flesh. By testing the SSR114 molecular marker in the parental lines of 12 segregating populations (Table 4.2) and the red-fleshed genotypes obtained from the cluster analysis in chapter 3, 8 different alleles were identified (Table 4.13). The allele length ranged from 192 to 226 bp. The allele **202** was found only in red-fleshed genotypes, confirming the specificity of this allele to detect the flesh colour phenotype.

Table 4.13. Allelic profile of the SSR114 marker of the parental genotypes and their corresponding flesh colour phenotype.

Cultivar/Parent	**SSR114 allelic profile**	**Flesh phenotype**
Incrocio S.Alessio	192-**202**	Red
Cocomerina S. Lacasa	192-**202**	Red
Pera Sanguigna	198-**202**	Red
Cocomerina Tardiva	196-**202**	Red
Cocomerina Precoce	**202**-226	Red
Cascade	194-226	White
Sensation Red Bartlett	226	White
Abate Fétel	194-224	White
William	226	White
Carmen	194-226	White
Conference	226	White
R234 (Sanguinole)	**202**-216	Red
R256 (Sanguinole)	**202**-216	Red
R143 (Samsoe)	**202**-226	Red
R546	226	White
R375	194-226	White
R276	194-226	White
R823	216-226	White

Testing the progenies, no unexpected segregations were detected; in fact, only the alleles owned by the parents were found in the respective progeny. Furthermore, the presence of the 202 allele was verified in agreement to the red flesh phenotype (Table 4.14). These results suggest a possible common ancestor for the red flesh trait in the tested populations.

Table 4.14. Allele combination and respective flesh phenotype of the progenies evaluated with the SSR114 molecular marker.

Population	Total n° tested seedlings	SSR114 Allele combination	Red flesh	White flesh
CT x AF				
83 seedlings	22	194-196	0	22
	21	194-**202**	21	0
	21	**202**-224	21	0
	19	196-224	0	19
CP x AF				
50 seedlings	16	194-**202**	16	0
	6	194-226	0	6
	20	**202**-224	20	0
	8	224-226	0	8
CP x Cs				
71 seedlings	37	**202**-226	37	0
	34	226	0	34
CT x Cf				
66 seedlings	31	196-226	0	31
	35	**202**-226	35	0
CP x SRB				
52 seedlings	22	**202**-226	22	0
	30	226	0	30
CP x W				
19 seedlings	11	**202**-226	11	0
	8	226	0	8
P13.018				
80 seedlings	27	**202**	26	0
	36	**202**-216	31	0
	17	216	0	16
P13.019				
20 seedlings	12	**202**-226	12	0
	8	216-226	0	8
P13.020				
20 seedlings	6	194-**202**	6	0
	5	194-216	0	5
	4	**202**-226	4	0
	5	216-226	0	5
P13.021				
20 seedlings	4	194-**202**	4	0
	6	194-216	0	6
	4	**202**-226	4	0
	6	216-226	0	6
P16.005				
20 seedlings	5	216-**202**	5	0
	5	**202**-226	5	0
	5	216-226	0	5
	5	226	0	5

4.4. Conclusions

A better understanding of the genetic control of the accumulation of anthocyanin in the pear fruit flesh has been achieved with this work. A small genomic region related to the red flesh fruit trait was found by the QTL analysis performed on the CP x C pear cross population. Two candidate genes were detected within the QTL region at the bottom of LG5: 'PcMYB114' and 'PcABC transporter C2'. MYB114 has been already found able to promote the expression of the structural genes of the anthocyanin pathway in Asian pear (Yao *et al.*, 2017); supporting the hypothesis of its involvement in the appearance of this phenotype in European pear. Nevertheless, this QTL does not explain all the variability showed among the progenies examined. In particular, it seems that this genomic region could explain only the presence/absence of the anthocyanin accumulation and not the observed variability in its content level. The low number of offsprings in the mapping population, just a few more than 100, certainly affected the capability to identify additional QTLs for the trait as the anthocyanin accumulation level.

Four out of the tested markers had shown an identical segregation to red flesh trait. In particular, for SSR114 marker, the allele 202 was found to be associated to the red flesh phenotype in all the red-fleshed pear accessions and the 12 tested cross populations. The discovery of this molecular marker might be a fundamental tool for boosting the ongoing red-fleshed pear breeding programs.

To confirm the role of the identified candidate genes in the anthocyanin synthesis and accumulation further investigations are needed. For instance, studying their expression in the fruit flesh tissues might improve the understanding of the whole process.

4.5. References

- Allan, A. C., Schwinn, K. E., & Espley, R. V. (2019). Anthocyanin accumulation is controlled by layers of repression. Recent Adv. Polyphen. Res, 6, 71-87.
- Alonso-Blanco C, Koornneef M, van Ooijen J (2006) QTL analysis. In: Salinas J, Sanchez-Serrano JJ (eds) Arabidopsis protocols. Methods in molecular biology, vol 323, pp 79–99. Humana Press, Inc., Totowa, NJ
- Antognoni, F., Potente, G., Mandrioli, R., Angeloni, C., Freschi, M., Malaguti, M., ... & Tartarini, S. (2020). Fruit quality characterization of new sweet cherry cultivars as a good source of bioactive phenolic compounds with antioxidant and neuroprotective potential. Antioxidants, 9(8), 677.Alonso-Blanco C., Koornneef M., van Ooijen J. W. (2006). QTL analysis. Methods Mol. Bio. 323 79–99. 10.1385/1-59745-003-0:79
- Baccichet, I., Foria, S., Messina, R., Peccol, E., Losa, A., Fabro, M., ... & Testolin, R. (2020). Genetic and ploidy diversity of pear (Pyrus spp.) germplasm of Friuli Venezia Giulia, Italy. Genetic Resources and Crop Evolution, 67(1), 83-96.
- Bassi, D., & Foschi, S. (2019, July). Raising the standards in breeding apricots at MAS. PES, Italy. In XVII International Symposium on Apricot Breeding and Culture 1290 (pp. 27-30).
- Braniste, N., & Budan, S. (2007, September). Inheritance of red fruit skin and flesh color in Pyrus communis cultivars. In XII EUCARPIA Symposium on Fruit Breeding and Genetics 814 (pp. 241-244).
- Brewer, L., & Volz, R. (2019). Genetics and breeding of pear. In The pear genome (pp. 63-101). Springer, Cham.
- Brown, A. G. (1966). Genetical studies in pears V. Red mutants. Euphytica, 15(3), 425-429.
- Butelli, E., Titta, L., Giorgio, M., Mock, H. P., Matros, A., Peterek, S., ... & Martin, C. (2008). Enrichment of tomato fruit with health-promoting anthocyanins by expression of select transcription factors. Nature biotechnology, 26(11), 1301-1308.
- Butelli, E., Licciardello, C., Zhang, Y., Liu, J., Mackay, S., Bailey, P., ... & Martin, C. (2012). Retrotransposons control fruit-specific, cold-dependent accumulation of anthocyanins in blood oranges. The Plant Cell, 24(3), 1242-1255.

- Butelli, E., Garcia-Lor, A., Licciardello, C., Las Casas, G., Hill, L., Recupero, G. R., ... & Martin, C. (2017). Changes in anthocyanin production during domestication of Citrus. Plant Physiology, 173(4), 2225-2242.
- Calenge F, Drouet D, Denancé C et al (2005) Identification of a major QTL together with several minor additive or epistatic QTLs for resistance to fire blight in apple in two related progenies. Theor Appl Genet111:128–35. doi:10.1007/s00122-005-2002-z
- Caracciolo, G., Sirri, S., & Baruzzi, G. (2018, December). Update on CREA Centro di Ricerca Olivicoltura, Frutticoltura e Agrumicoltura pear breeding program. In XIII International Pear Symposium 1303 (pp. 29-36).
- Chagné, D., Lin-Wang, K., Espley, R. V., Volz, R. K., How, N. M., Rouse, S., ... & Allan, A. C. (2013). An ancient duplication of apple MYB transcription factors is responsible for novel red fruit-flesh phenotypes. Plant physiology, 161(1), 225-239.
- Chavez, D. J., Itle, R. A., Mancero-Castillo, D., Chaparro, J. X., & Beckman, T. G. (2019). Advances and challenges in peach breeding. Achieving sustainable cultivation of temperate zone tree fruits and berries, 3-24.
- Chen, Z., Yu, L., Liu, W., Zhang, J., Wang, N., & Chen, X. (2021). Research progress of fruit color development in apple (Malus domestica Borkh.). Plant Physiology and Biochemistry, 162, 267-279.
- Churchill, G. A., & Doerge, R. (1994). Empirical threshold values for quantitative trait mapping. Genetics, 138(3), 963-971.
- De Franceschi, P., & Dondini, L. (2019). Molecular mapping of major genes and QTLs in pear. The Pear Genome, 113-131.
- Dondini, L., Pierantoni, L., Ancarani, V., D'Angelo, M., Cho, K. H., Shin, I. S., ... & Sansavini, S. (2008). The inheritance of the red colour character in European pear (Pyrus communis) and its map position in the mutated cultivar 'Max Red Bartlett'. Plant Breeding, 127(5), 524-526.
- Downing A.J. (1869) – The fruits and fruit-trees of America, or, The culture, propagation, and management, in the garden and orchard, of fruit -trees generally: with descriptions of all the finest varieties of fruit, native and foreign, cultivated in this country. 2nd Edition rev. and corrections, with large additions by Charles Downing. J.Wiley, New York.

- Durel C-E, Denancé C, Brisset MN (2009) Two distinct major QTL for resistance to fire blight co-localize on linkage group 12 in apple genotypes 'Evereste' and Malus floribunda clone 821. Genome 52:139–147. doi:10.1139/G08-111
- Espley, R. V., Hellens, R. P., Putterill, J., Stevenson, D. E., Kutty-Amma, S., & Allan, A. C. (2007). Red colouration in apple fruit is due to the activity of the MYB transcription factor, MdMYB10. The Plant Journal, 49(3), 414-427.
- Espley, R. V., Butts, C. A., Laing, W. A., Martell, S., Smith, H., McGhie, T. K., ... & Hellens, R. P. (2014). Dietary flavonoids from modified apple reduce inflammation markers and modulate gut microbiota in mice. The Journal of nutrition, 144(2), 146-154.
- Fang, Z. Z., Zhou, D. R., Ye, X. F., Jiang, C. C., & Pan, S. L. (2016). Identification of candidate anthocyanin-related genes by transcriptomic analysis of 'Furongli'plum (Prunus salicina Lindl.) during fruit ripening using RNA-seq. Frontiers in Plant Science, 7, 1338.
- Ferradini N, Lancioni H, Torricelli R, Russi L, Ragione ID et al (2017) Characterization and phylogenetic analysis of ancient Italian landraces of pear. Front Plant Sci 8:751
- Gilbert, H., & Le Roy, P. (2003). Comparison of three multitrait methods for QTL detection. Genetics Selection Evolution, 35(3), 281-304.
- Guerra, W. (2018). Mele a polpa rossa, pronti al decollo! Rivista di frutticoltura e di ortofloricoltura, 82(10), 20-25.
- Haley CS, Knott SA (1992) A simple regression method for mapping quantitative trait loci in line crosses using flanking markers. Heredity (Edinb) 69:315–24
- Hedrick UP (1921) The pears of New York. JB Lyon Company, Albany, p 636
- Hou, D. X., Fujii, M., Terahara, N., & Yoshimoto, M. (2004). Molecular mechanisms behind the chemopreventive effects of anthocyanidins. Journal of Biomedicine and Biotechnology, 2004(5), 321.
- Lafferty, D. J., Espley, R. V., Deng, C. H., Günther, C. S., Plunkett, B., Turner, J. L., ... & Albert, N. W. (2022). Hierarchical regulation of MYBPA1 by anthocyanin-and proanthocyanidin-related MYB proteins is conserved in Vaccinium species. Journal of Experimental Botany, 73(5), 1344-1356.
- Lander ES, Botstein D (1989) Mapping mendelian factors underlying quantitative traits using RFLP linkage maps. Genetics 121:185–99
- Leroy A (1867–1869) Dictionnaire de Pomologie. Tome 1 & 2 Poires. Paris

- Lespinasse, Y., & Guérif, P. (2010, November). Inheritance of red leaf colour from pear red sports of'Doyenné du Comice','Bartlett'and'Beurré Hardy'. In XI International Pear Symposium 909 (pp. 97-102).
- Lin-Wang, K., Bolitho, K., Grafton, K., Kortstee, A., Karunairetnam, S., McGhie, T. K., ... & Allan, A. C. (2010). An R2R3 MYB transcription factor associated with regulation of the anthocyanin biosynthetic pathway in Rosaceae. BMC plant biology, 10(1), 1-17.
- Linsmith, G., Rombauts, S., Montanari, S., Deng, C. H., Celton, J. M., Guérif, P., ... & Bianco, L. (2019). Pseudo-chromosome–length genome assembly of a double haploid "Bartlett" pear (Pyrus communis L.). Gigascience, 8(12), giz138.
- Liu, J., Zhuang, Y., Hu, Y., Xue, S., Li, H., Chen, L., & Fei, P. (2020). Improving the color stability and antioxidation activity of blueberry anthocyanins by enzymatic acylation with p-coumaric acid and caffeic acid. Lwt, 130, 109673.
- Manach, C., Hubert, J., Llorach, R., & Scalbert, A. (2009). The complex links between dietary phytochemicals and human health deciphered by metabolomics. Molecular nutrition & food research, 53(10), 1303-1315.
- Mas A. (1872-1883) - Pomologie générale. Librairie de G. Masson, Parigi. Volume 7.
- Montanari, S., Guérif, P., Ravon, E. *et al.*, Genetic mapping of Cacopsylla pyri resistance in an interspecific pear (Pyrus spp.) population. Tree Genetics & Genomes 11, 74 (2015).
- Montanari, S., Thomson, S., Cordiner, S., Günther, C. S., Miller, P., Deng, C. H., ... & Espley, R. (2022). High-density linkage map construction in an autotetraploid blueberry population and detection of quantitative trait loci for anthocyanin content. Frontiers in Plant Science, 13.
- Ni, J., Bai, S., Zhao, Y., Qian, M., Tao, R., Yin, L., ... & Teng, Y. (2019). Ethylene response factors Pp4ERF24 and Pp12ERF96 regulate blue light-induced anthocyanin biosynthesis in 'Red Zaosu'pear fruits by interacting with MYB114. Plant molecular biology, 99, 67-78.
- Ntladi, S. M., Human, J. P., Bester, C., Vervalle, J., Roodt-Wilding, R., & Tobutt, K. R. (2018). Quantitative trait loci (QTL) mapping of blush skin and flowering time in a European pear (Pyrus communis) progeny of 'Flamingo'×'Abate Fetel'. Tree Genetics & Genomes, 14, 1-24.

- Ou, C., Zhang, X., Wang, F., Zhang, L., Zhang, Y., Fang, M., ... & Zhang, Z. (2020). A 14 nucleotide deletion mutation in the coding region of the PpBBX24 gene is associated with the red skin of "Zaosu Red" pear (Pyrus pyrifolia White Pear Group): a deletion in the PpBBX24 gene is associated with the red skin of pear. Horticulture research, 7.
- Pierantoni, L., Dondini, L., De Franceschi, P., Musacchi, S., Winkel, B. S., & Sansavini, S. (2010). Mapping of an anthocyanin-regulating MYB transcription factor and its expression in red and green pear, Pyrus communis. Plant Physiology and Biochemistry, 48(12), 1020-1026.
- Plunkett, B. J., Espley, R. V., Dare, A. P., Warren, B. A., Grierson, E. R., Cordiner, S., ... & Schwinn, K. E. (2018). MYBA from blueberry (Vaccinium section Cyanococcus) is a subgroup 6 type R2R3MYB transcription factor that activates anthocyanin production. Frontiers in Plant Science, 9, 1300.
- Ramsay, N. A., & Glover, B. J. (2005). MYB–bHLH–WD40 protein complex and the evolution of cellular diversity. Trends in plant science, 10(2), 63-70.
- Sabir, I. A., Manzoor, M. A., Shah, I. H., Liu, X., Jiu, S., Wang, J., ... & Zhang, C. (2022). Identification and comprehensive ggenome-wide analysis of glutathione S-transferase gene family in sweet cherry (Prunus avium) and their expression profiling reveals a likely role in anthocyanin accumulation. Frontiers in Plant Science, 13.
- Sau, S., Pastore, C., D'hallewin, G., Dondini, L., & Bacchetta, G. (2020). Characterisation of microsatellite loci in Sardinian pears (Pyrus communis L. and P. spinosa Forssk.). Scientia Horticulturae, 270, 109443.
- Seeram, N. P., Lee, R., & Heber, D. (2004). Bioavailability of ellagic acid in human plasma after consumption of ellagitannins from pomegranate (Punica granatum L.) juice. Clinica chimica acta, 348(1-2), 63-68.
- Sehic, J., Garkava-Gustavsson, L., Fernández-Fernández, F., & Nybom, H. (2012). Genetic diversity in a collection of European pear (Pyrus communis) cultivars determined with SSR markers chosen by ECPGR. Scientia horticulturae, 145, 39-45.
- Starkevič, P., Paukštytė, J., Kazanavičiūtė, V., Denkovskienė, E., Stanys, V., Bendokas, V., ... & Ražanskas, R. (2015). Expression and anthocyanin biosynthesis-modulating potential of sweet cherry (Prunus avium L.) MYB10 and bHLH genes. PLoS One, 10(5), e0126991.

- Stevenson, D. E., & Hurst, R. D. (2007). Polyphenolic phytochemicals–just antioxidants or much more?. Cellular and Molecular Life Sciences, 64(22), 2900-2916.
- Van Ooijen JW (2004) MapQTL 5, Software for the mapping of quantitative trait loci in experimental population. Kyazma BV, Wageningen
- Voorrips, R. (2002). MapChart: software for the graphical presentation of linkage maps and QTLs. Journal of heredity, 93(1), 77-78.
- Wang, Q., Wang, Y., Sun, H., Sun, L., & Zhang, L. (2020). Transposon-induced methylation of the RsMYB1 promoter disturbs anthocyanin accumulation in red-fleshed radish. Journal of experimental botany, 71(9), 2537-2550.
- Wu, J., Li, L. T., Li, M., Khan, M. A., Li, X. G., Chen, H., ... & Zhang, S. L. (2014). High-density genetic linkage map construction and identification of fruit-related QTLs in pear using SNP and SSR markers. Journal of experimental botany, 65(20), 5771-5781.
- Xue, C., Yao, J. L., Qin, M. F., Zhang, M. Y., Allan, A. C., Wang, D. F., & Wu, J. (2019). PbrmiR397a regulates lignification during stone cell development in pear fruit. Plant biotechnology journal, 17(1), 103-117.
- Yao, G., Ming, M., Allan, A. C., Gu, C., Li, L., Wu, X., ... & Wu, J. (2017). Map-based cloning of the pear gene MYB 114 identifies an interaction with other transcription factors to coordinately regulate fruit anthocyanin biosynthesis. The Plant Journal, 92(3), 437-451.
- Zhou H, Lin-Wang K, Wang H, Gu C, Dare AP, Espley RV, He H, Allan AC, Han Y (2015) Molecular genetics of blood-fleshed peach reveals activation of anthocyanin biosynthesis by NAC transcription factors. Plant J 82:105–121.

5. Red-Fleshed Fruit Development and Major Candidate Genes Expression

Abstract

Anthocyanin are the main secondary compounds that contribute to fruits coloration. Three independent trails have been carried out for clarifying the modification of the global gene expression due to the presence of the red flesh trait. Several classes of genes have been, as expected, modulated with the class of phenylpropanoid related genes that grouped the largest number of differentially expressed genes (DEG). The plant hormones seem playing crucial roles in anthocyanin biosynthesis regulatory systems in agreement with the abundant literature.

5.1. Introduction

Anthocyanin are important secondary metabolites, and their multiple functions in plants include enhancing the resistance to biotic and abiotic stresses as well as aiding pollination and seed dispersal (He and Giusti, 2010). They are the mail secondary compounds that contribute to fruits coloration. Anthocyanin are the terminal metabolite of the flavonoid pathway and are synthesised by a series of enzymes encoded by structural genes. The plant hormones play crucial roles in anthocyanin biosynthesis regulatory systems.

The plant growth regulator abscisic acid (ABA) has been reported to play an important role in promoting anthocyanin production and fruit ripening (Yin *et al.,* 2001; Luo *et al.,* 2013; Wang *et al.,* 2018). Many plants accumulate considerable amounts of anthocyanin as they mature. The most important hormone stimulating fruit ripening in climacteric fruits including apple, plum, and fig is ethylene. Contrarily, the ABA concentration rises as the fruit ripens in non-climacteric fruits like sweet cherries (Ren *et al.,* 2011). Through its own signalling system, ABA can control the formation of anthocyanins (Ni *et al.,* 2020). Exogenous ABA treatment modifies the MBW complex's transcriptional activity to further control the expression of structural genes. For instance, ABA directly activates the expression of PacMYBA, which can promote the expression of PacDFR and PacANS, to regulate the coloration of red-colored sweet cherries (Shen *et al.,* 2014). Similar to this, ABA controls anthocyanin production in strawberries by activating FaMYB10 (Kadomura-Ishikawa *et al.,* 2015). All these results indicate that MYB1/A/10 is the main transcription factor in anthocyanin formation in response to the ABA signal. MdABI5, an important ABA signal regulator in apples, functioned as a positive regulator to improve the connection between MdMYB1 and MdbHLH3 (An *et al.,* 2021). Aside from controlling MBW complex transcription, ABA also affects the biosynthesis of anthocyanins that are influenced by environmental factors (*e.g.*, light, temperature, drought

and sugar). In bilberry, all the major anthocyanin structural genes, the key transcription factor MYBA1 and ABA biosynthetic genes are upregulated in both red and blue light treatments, whose expression levels are relatively higher in red light treatment (Samkumar *et al.,* 2021).

Anthocyanin accumulation is one of the manifestations of fruit ripening and ethylene is known as "maturity hormone", so ethylene is usually considered as colour enhancer for climacteric fruits. Fruit colouring and ethylene release go hand in hand throughout the ripening phase of these fruits (Ni *et al.,* 2020). In several species, the signalling system and ethylene production have been extensively explored. It has been suggested that ethylene-induced anthocyanin accumulation involves ethylene signalling pathway components. MdEIL1 increased the expression of MdMYB1, which interacted with the promoter of MdERF3 to generate positive feedback for ethylene biosynthesis control (An *et al.,* (2018). It is notable that the ERF TF members potentially affect the production of anthocyanins both favourably and unfavourably (Ni *et al.,* 2020). Evidence on promotion of anthocyanin synthesis regulated by ERF TFs has been mainly demonstrated in apple (An *et al.,* 2018c; Zhang *et al.,* 2018, 2020; Ma *et al.,* 2021). These identified ERFs interact with MYBs to primarily control anthocyanin accumulation. For example, MdERF1B interacts to the MdMYB9 and MdMYB11 promoters, boosting the expression of these genes. ERFs contribute to pigmentation in pear using a slightly different method. The ERFs-regulated biosynthesis of anthocyanins also needs bHLHs and MYBs in addition (Yao *et al.,* 2017). For instance, Pp4ERF24 and Pp12ERF96 interact with PpMYB114 and boost its interaction with PpbHLH3, which promotes the up-regulation of PpUFGT expression in blue light-induced anthocyanin biosynthesis (Ni *et al.,* 2019). However, Ni *et al.,* (2021) discovered that ethylene-induced PpERF105 transcriptionally stimulated the production of PpMYB140, which competes with PpMYB114 for the binding to PpbHLH3 and suppresses the expression of structural genes associated to anthocyanins, resulting in a reduction in anthocyanin content.

Jasmonate (JA) is an endogenous hormone in higher plants. It mainly includes jasmonic acid, methyl jasmonate (MeJA), jasmonate isoleucine and other cyclopentanone derivatives. JA is involved in many plants developmental processes including stomatal closure, leaf senescence, synthesis of secondary metabolites and sugar transport and so on (Browse, 2009). JAZ generally inhibits the MBW complex from forming by interacting with bHLH and MYB, which prevents the expression of genes involved in anthocyanin biosynthesis (Ni et al 2020). A dynamic modulator of JA-mediated anthocyanin accumulation in apples is JAZ1-TRB1-MYB9. MdJAZ1 interacts with MdTRB1 to interrupt the interaction between MdTRB1 and MdMYB9, adversely affecting the synthesis of anthocyanins (An *et al.,* 2021). Studies on strawberries showed that the molecular targets of FaJAZ repressors were FabHLH3, FabHLH33, and FaMYB10 (Garrido-Bigotes *et al.,* 2020). Additionally, Ni *et al.,* (2020b) discovered that during the colouring of red pears, ethylene reduced anthocyanin production whereas jasmonate increased anthocyanin and flavone synthesis. In the absence of ethylene, jasmonate promotes the synthesis of anthocyanin, but jasmonate also induces ethylene biosynthesis, which reduces anthocyanin synthesis and leads to more precursors transfer to the flavonoid biosynthesis pathway, ultimately causing fruit yellowing (Ni *et al.,* 2020b).

The anthocyanin composition of red pears was shown to be mainly cyanidin-3-O-galactoside (Francis 1970; Dussi *et al.,* 1995; Fischer *et al.,* 2007; Lin and Harnly 2008; Ngo *et al.,* 2009; Zhang *et al.,* 2012; Pierantoni *et al.,* 2010). Using TLC (Thin Layer Chromatography) and HPLC methods other anthocyanin were detected in minor quantity in several different cultivars. Sensation Red Bartlett, Red D'Anjou, D'Anjou and Seckel were identified as containing peonidin-3-O-galactoside (Dussi *et al.,* 1995; Lin, Harnly 2008). Cyanidin-3-O-arabinoside was analysed in *Pyrus communis* by Fischer *et al.,* (2007) and in 'Max Red Bartlett' fruit skin by Pierantoni et al (2010). The 'Red D'Anjou' fruit skin contains major cyanidin-3-O-galactoside, minor peonidin-3-O-galactoside and traces of cyanidin-3-O-arabinoside, cyanidin-

3-O-glucoside and peonidin-3-O-glucoside (Ngo *et al.*, 2009). Therefore, the anthocyanin component varies among different varieties of red pears (Zhang *et al.*, 2012).

In this chapter, three independent experiments made in consecutive vegetative seasons are reported. The level of anthocyanin accumulation during the development of the fruit were compared to the expression of the candidate genes detected by the QTL analysis (Chapter 4).

5.2. Materials and Methods

5.2.1. First trial: Anthocyanin accumulation during the development of the 'Cocomerina Precoce' fruit

Fruits of 'Cocomerina Precoce' (CP) were collected in 2021 at eleven time points during the fruit development season, starting from 2 to 17 weeks after full blooming (WAFB). Three biological replicas were made pooling 3 to 5 fruits harvested in three different trees located at the UNIBO experimental farm (Cadriano, Bologna, Italy). The harvested fruits were roughly chopped, immediately frozen in liquid nitrogen and stored at -80 °C. Part of the frozen samples was used for RNA extraction, another part, of the same sample, was freeze-dried and used for anthocyanin extraction and quantification by HPLC performed by CREA in Acireale, Catania, Italy.

5.2.2. Second trial: whole transcriptome sequencing (RNA seq) analysis of fruit flesh from red and white-fleshed genotypes in three early developmental stages

A comparison between CP and a white-fleshed offspring (genotype n°57 from the CP x C progeny) were performed in 2022. Fruits of the two genotypes were collected at three time points: 4, 6 and 8 WAFB. The trees of the two genotypes were hold by CREA (Forlì-Cesena, Italy). Three biological replicas were made pooling 2 to 5 pealed fruits from different trees, that were roughly chopped and immediately frozen in liquid nitrogen and then stored at -80 °C. A total of 18 RNA were isolated and, after the quality check, sent to an external company (Novogene Co, China) to perform the transcriptome sequencing (Table 5.1).

Table 5.1. Samples ID used for RNAseq analysis.

Sample ID	Sample description
N1	fruit flesh of CP at 4 weeks after full blooming
N2	fruit flesh of CP at 6 weeks after full blooming
N3	fruit flesh of CP at 8 weeks after full blooming
D1	fruit flesh of offspring 57 at 4 weeks after full blooming
D2	fruit flesh of offspring 57 at 6 weeks after full blooming
D3	fruit flesh of offspring 57 at 8 weeks after full blooming

Total RNA sequencing was carried out on Illumina platforms, based on the mechanism of SBS (sequencing by synthesis). Gene expression level was estimated by the abundance of transcripts (count of sequencing) that mapped to genome or exon. For alignment the *Pyrus communis* reference genome of 'Bartlett double haploid' was used (Linsmith *et al.,* 2019). Read counts is proportional to gene expression level, gene length and sequencing depth. FPKM (short for the expected number of Fragments Per Kilobase of transcript sequence per Millions base pairs sequenced) method was used to estimating gene expression levels, which takes the effects into consideration of both sequencing depth and gene length on counting of fragments (Mortazavi *et al.,* 2008). In order to analyse the differential gene expression nine different pairs comparison were set: N1vsN2, N1vsN3, N2vsN3, D1vsD2, D1vsD3, D2vsD3, D1vsN1, D2vsN2 and D3vsN3.

A Principal Component Analysis (PCA) was performed with the gene expression value (FPKM) of all samples to evaluate inter-group and intra-group differences. The adjusted p-value ≤ 0.05 and a Fold Change ≥ 1.0 were used to determine the differential genes (including up-regulation and down-regulation) for each compared group. Using the differential genes dataset, a Venn diagram was carried out to visualise the number of differentially expressed genes shared among the compared groups. The same dataset was used to obtain a heatmap

graph. A KEGG (Kyoto Encyclopaedia of Genes and Genomes) enrichment analysis were carried out in order to identified significantly enriched metabolic pathways or signal transduction pathways associated with differentially expressed genes, comparing the whole genome background. The adjusted p value < 0.05 were used as a threshold for significance (Kanehisa, 2008).

To date, the gene specific differential expression was analysed only for a few genes with the aim to investigate changing between white and red-fleshed genotypes. The attention was focused on the QTLs region (see chapter 4) and in plant hormones-related genes. For both of them the thresholds used to identify the candidate gene were: adjusted p value < 0.05 and Log Fold higher than 1.5 at least in one time point.

Additionally, the level of expression was analysed for the anthocyanin pathway genes (Table 5.2).

Table5.2. List of genes for which expression has been analysed.

Gene family	Gene ID	Chromosome	gene start	gene end	gene length	Reference
CHS	pycom04g00310	Chr4	309593	311421	1170	Pierantoni *et al.*, 2010
DFR	pycom15g02070	Chr15	1227711	1229380	510	Pierantoni *et al.*, 2010
ANS	pycom06g06810	Chr6	10931545	10933211	1473	Pierantoni *et al.*, 2010
UFGT	pycom07g27990	Chr7	27505226	27506892	1440	Pierantoni *et al.*, 2010
F3H	pycom02g10320	Chr2	7187743	7189830	1038	Pierantoni *et al.*, 2010
CHI	pycom01g14550	Chr1	14673969	14678327	1401	Pierantoni *et al.*, 2010
ABCC 2	pycom05g25670	Chr5	27000730	27010566	3393	This study
MYB114	pycom05g25770	Chr5	27101018	27103432	714	This study

5.2.3. Third trial: Anthocyanin-related genes expression in several red-fleshed genotypes in three early development stages

Six plants of the progeny obtained from the controlled cross 'R234 x R546', with very different red flesh phenotypes, were selected. The chosen phenotypes ranged from white flesh (Figure 5.1 C) to the most intense red in all the fruit tissues (Figure 5.1 B). The intermedia phenotypes were: anthocyanin only in the seed locules (Figure 5.1 A), in the seed locules and under the skin (Figure 5.1 F), mostly in the pulp without the red under the skin (Figure 5.1 E) and red

Figure 5.1. Pictures of the equatorial section of the fruits of the six different offsprings belonging the progeny P013.19 showing distinct colour distribution and intensity.

concentrated mostly in the fruit core (Figure 5.1 D). The progeny was hold by The New Zealand Institute for Plant and Food Research (PFR) in Motueka (Nelson, New Zealand). Three biological replicas were made pooling the flesh of 2-3 fruit collected from different parts of the

tree canopy. The selected fruits were peeled, chopped and immediately frozen in liquid nitrogen and stored at -80 °C. Part of the frozen samples was used for RNA extraction while, a second fraction, from the same pooled sample, was freeze-dried and used for anthocyanin extraction and quantification.

5.2.4. RNA extractions and qPCR DNA amplifications

RNA was isolated from approximately 0.1 g of fruit flesh tissue using the Spectrum™ Plant Total RNA Kit (Sigma-Aldrich, St. Louis, Missouri, US) following the manufacturer's instructions. The quality of the extracted RNA was tested by NanodropTM ND-1000 Spectrophotometer (Thermo Scientific, Wilmington, DE, USA). First-strand cDNA synthesis was carried out starting from 1 ug of RNA using oligo dT reaction by SuperScript III Kit (Invitrogen, Carlsbad, CA, USA) performed according to the manufacturer's instructions.

Real-time qPCR DNA amplification and analysis were carried out using the LightCycler 480 Real-Time PCR System (Roche Diagnostics, Mannheim, Germany), with LightCycler 480 software version 1.5. The LightCycler 480 SYBR Green I Master Mix (Roche Diagnostics, Mannheim, Germany) was used in 10 µL of total reaction volume was applied in all the reactions following the manufacturer's method. The qPCR conditions were 5 min at 95 °C, followed by 40 cycles of 5 s at 95 °C, 5 s at 60 °C and 10 s at 72 °C, followed by 65–95 °C melting curve detection.

Conserved regions of the various pear anthocyanin biosynthetic genes: chalcone synthase (CHS), dihydroflavonol-4-reductase (DFR), UDP-glucose:flavonoid-3-O-glycosyl transferase (UFGT) and transcription factor genes: MYB10 and MYB110a were identified using the NCBI 'Blast' program (https://www.ncbi.nlm.nih.gov). These sequences were used to generate qPCR primers (Table 5.1) using Primer 3 software (Rozen and Skaletsky, **202**0). The same method

was used to design the primers for the two major candidate genes MYB114 and ABCC2 identified by QTL analysis. The expression levels of all of the analysed genes were normalized to the expression of the pear actin gene (accession no. AF386514). The specificity of each reaction was verified by melting curve analysis.

Table 5.1. List of the primers used for qPCR DNA amplifications.

Gene	Forward	Reverse
ACTIN	TGAGACATTCAACACCCCGGCTAT	GATGGCATGTGGGAGGGCATA
MYB114	CCACGGAGAGCTAGAGTTGC	AGCGTTTTCTGTAGGTGGTGA
ABCC2	CCATTCAGTGCTTCACCAAA	GCAGCCTATCTCTATTATCAGAGCA
UFGT	CCACCAAAATCGAGCCACAA	GCATGAGTGGCAAAAGGGAA
DFR	TGGTATCATCAAGCAGGGCCAGTAT	CGTGTGACGAACAAATGTAGCGG
CHS	TCAAGCCTTGTTTGGTGACG	CGCCGAGACCAATTCAAACA
MYB10	ACAAACGTCGTCGTCAACAAAGAAC	TCAATGCTGGGACATGCAGCC
MYB110a	GTGATCAGACCTCAACCCCGAAGT	CACCAATCATTTCCATCGTTTGTCA

5.2.5. Anthocyanin extraction and HPLC analysis

Freeze-dried fruit flesh samples were powdered and around 100 mg of tissues was added of 700 µL of 0.1% HCl in methanol (v/v) solvent solution. The samples were vortexed every 30 minutes while being kept at room temperature in the dark for three hours. Then the micro-tubes were centrifuged for ten minutes at maximum speed (15’000 rpm). The supernatants were transferred in new tubes keeping the volume consistent between samples. After that, the extracted anthocyanin were dried using a Speed vac for about two hours. These dried samples were re-suspended in 500 µL 20% methanol and syringe filtered using 1 ml syringes on a regenerated cellulose membrane with pore size of 0.45 µm, (15 mm syringe filter, Phenomenex ®, Torrance, California, US). Undiluted samples were run as an HPLC (High Performance Liquid Chromatography) method without the mass spectrophotometric (MS; Acquity QDa

Detector, Waters, Milford, Massachusetts, US); however, for few samples, QDa MS analysis were performed to verify the identity of cyanidin 3-galactoside as a unique anthocyanin present in the pear fruit flesh.

5.3. Results and Discussion

5.3.1. First trial: Anthocyanin accumulation during the development of the 'Cocomerina Precoce' fruit

HPLC analysis was performed to identify and quantify the content of anthocyanin in 'Cocomerina Precoce' fruit flesh during its development. Only cyanidin-3-O-galactoside (Cyn-3-Gal) was detected by the MS analysis in all the tested samples. The accumulation of anthocyanin in the flesh increases from the fruit-set reaching the peak between 7 and 9 weeks after full blooming (WAFB) with a concentration of more than 40 µg/g of dry weight of Cyn-3-Gal (Table 5.2). Then the amount of anthocyanin starts to decrease rapidly possibly due to the stop of synthesis, the effect of dilution resulting from the cell distention and presumably also to their degradation. The content of Cyn-3-Gal at ripening time (17 WAFB) was very low (3.3 µg/g) and concentrated mostly in the fruit core, as showed in Figure 5.2 (bottom line).

The level of gene relative expression was examined during the 'Cocomerina Precoce' fruit development. Striking differences were observed in the analysed time frame. The anthocyanin pathway related genes, CHS (chalcone synthase), DFR (dihydroflavonol 4-reductase) and UFGT (uridine diphosphate (UDP)-glucose:flavonoid 3-O-glycosyltransferase), showed a similar expression trend during the fruit growth (Figure 5.2). All three of them had a peak of expression at 6 WAFB decreasing to almost zero at maturity stage (17 WAFB). These data are compatible with the data of anthocyanin accumulation (HPLC) that reached the maximum concentration at 7 WAFB. Regarding the relative expression level of the candidate genes, MYB114 and ABCC2, they registered different curve during the time. MYB114, similarly to the anthocyanin pathway genes, achieved the highest value at 6 WAFB, ABCC2, instead, showed a delay for the maximum expression, that was reached at 9 WAFB.

Table 5.2. Concentration of Cyanidin-3-O-Galactoside in µg/g of dry weight in fruit flesh of Cocomerina Precoce from the fruit-set to the ripening time. Time points expressed in weeks after full blooming (WAFB). Different letters mean statistically significant differences.

Time point	Cyn-3-Gal ug/g of dry weight
2 WAFB	3,2 f
3 WAFB	6,0 de
4 WAFB	6,8 d
5 WAFB	7,1 d
6 WAFB	15,6 c
7 WAFB	43,5 a
9 WAFB	42,9 a
11 WAFB	20,1 b
13 WAFB	4,9 e
15 WAFB	4,6 ef
17 WAFB	3,3 f

These results did not allowed excluding neither of the two candidate genes as a key gene for the explained phenotype. MYB114 is supposed to play a role in promoting the expression of the structural anthocyanin pathway genes (Yao *et al.,* 2017); actually, its peak of expression occurred immediately before the maximum accumulation of Cyn-3-Gal in the fruit flesh. In the same way, ABCC2 should be involved in the storage of anthocyanin in the vacuole (Behrens *et al.,* 2019); in fact, the peak of gene expression occurred at the maximum of anthocyanin accumulation at 9 WAFB. The anthocyanin accumulation pattern is completely different from that seen in red fleshed apples. In the early stages of fruit growth, almost simultaneously with the cessation of cell division, there is a maximum of synthesis and accumulation of Cyn-3-Gal in pear fruits, particularly in ‘Cocomerina Precoce’. The content of anthocyanins subsequently starts to decline until fruit is fully ripe. On the other hand, in apples, both types of red flesh (type 1 and 2) exhibit an increase in anthocyanin accumulation throughout the fruit's last stages of ripening (Espley *et al.,* 2007; Sato *et al.,* 2017).

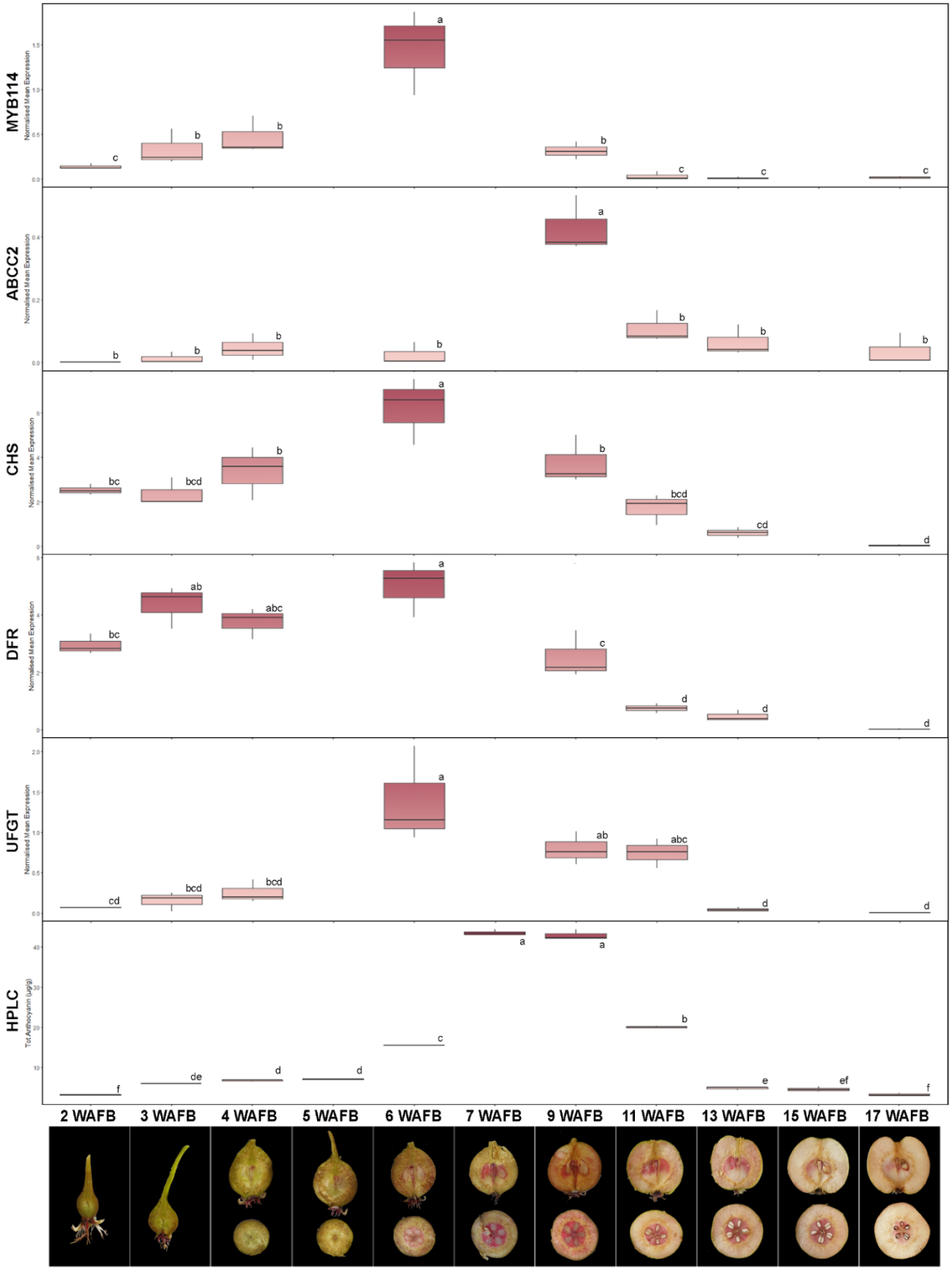

Figure 5.2. Expression profiling of pear anthocyanin genes and candidate genes identified by QTL analysis. Data from qPCR analysis of the CP fruit flesh in different development stages. CHS, DFR, UFGT. In the bottom-line fruit development series of CP fruits in the corresponding development stage.

The correlation between all the observations were generally high (Figure 5.3). The highest gene expression correlation was detected between ABCC2 and HPLC (0.90). On the other hand, ABCC2 expression showed the lowest correlations with the other genes.

Furthermore, MYB114 showed high correlation with DFR (0.75), CHS (0.84) and UFGT (0.73), in accordance with the results obtained by Yao *et al.*, (2017) that demonstrated that PyMYB114 is able, associated with PybHLH3, to promote the expression of PyDFR and PyUFGT.

Anthocyanin accumulation was highly correlated with the UFGT expression only, with a coefficient of 0.57, according to its function as last gene in the anthocyanin biosynthesis (Gerats *et al.*, 1983).

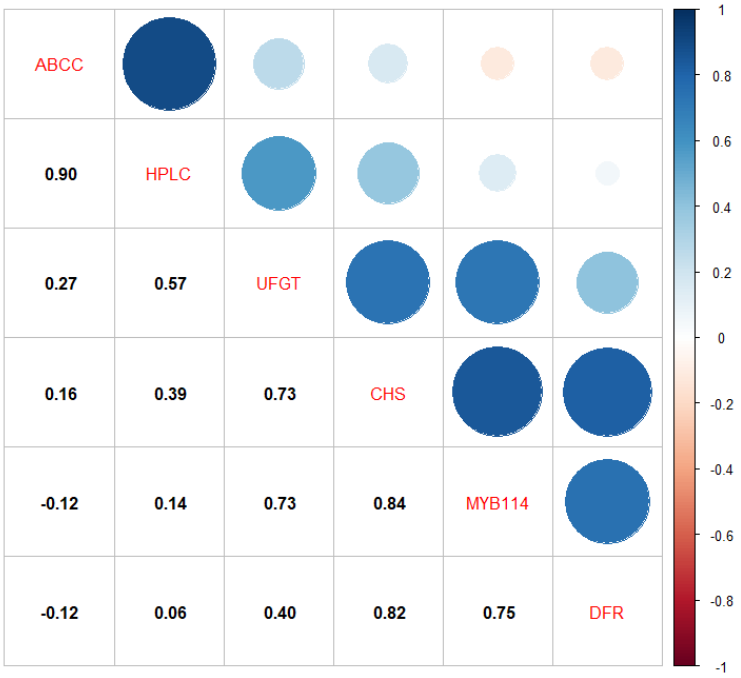

Figure 5.3. Correlation matrix of the gene expression levels and anthocyanin fruit concentration measured by HPLC.

5.3.2. Second trial: Entire transcriptome sequencing (RNA seq) analysis of fruit flesh from red and white-fleshed genotypes in three early developmental stages

5.3.2.1. General results of RNAseq analysis

RNAseq data obtained had generally high quality. The number of total reads per sample ranged between 40.8 to 46.9 million with more than 98% of clean reads for all the analysed samples (data non shown).

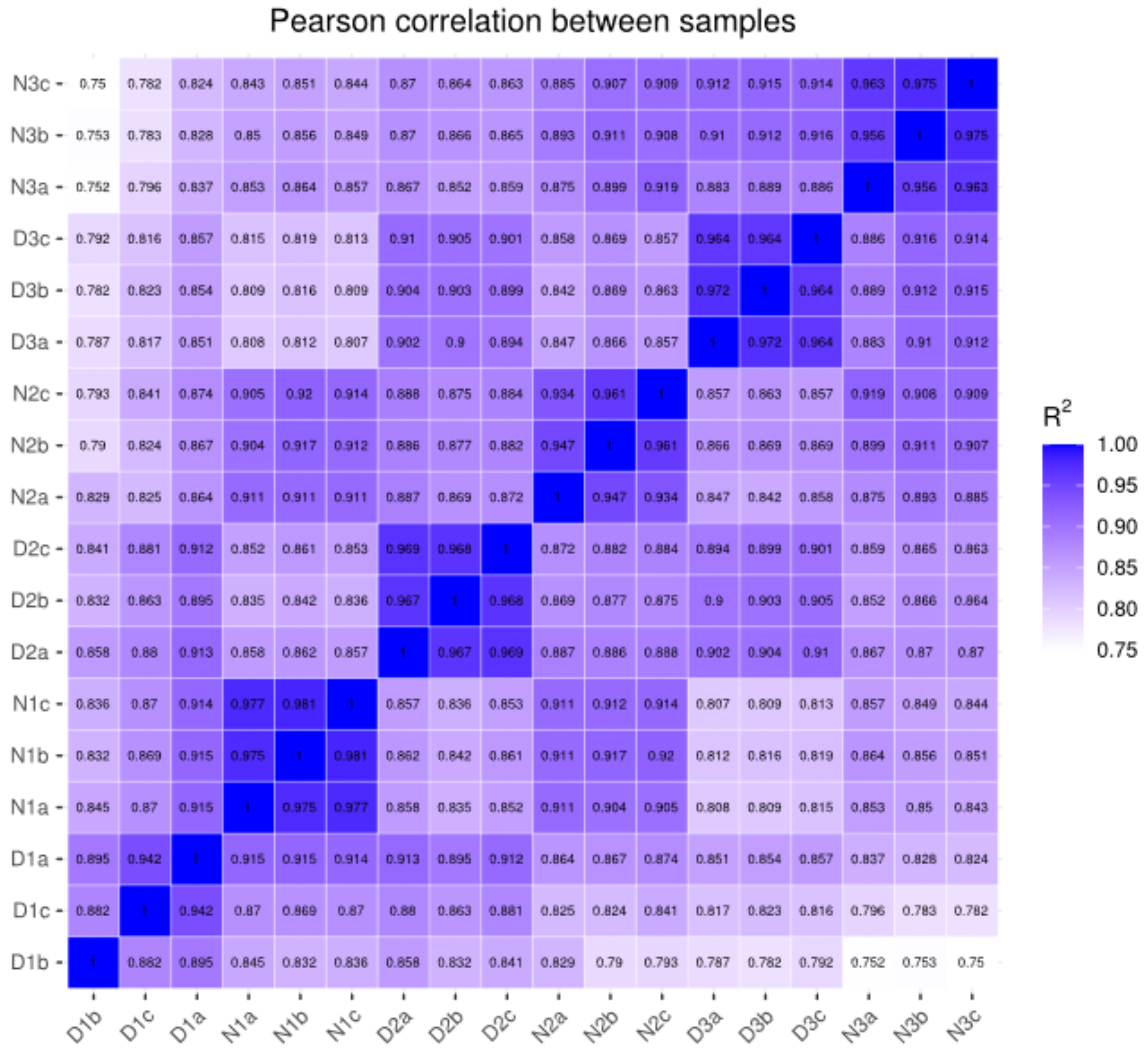

Figure 5.4. Inter-sample correlation matrix represents the R^2 of Pearson correlation coefficient according to gene expression levels (FPKM)

As expected, the highest level of gene expression correlation was found between the biological replicas of the same sample. Speaking of correlation between different samples, the combinations N1 / N2, N2 / N3 and D2 / D3 showed the highest correlation coefficients. Generally, the correlation between different genotype samples showed lower values, *i.e.*, N1 / D3 and N3 / D1 (Figure 5.4).

The principal component analysis (PCA) carried out on the gene expression value (FPKM) of all samples showed the ideal conditions: biological replicates of a genotype collected at a specific time point cluster together while the two samples of the two genotypes are well separated (Figure 5.5). In particular, the white-fleshed (D) in the upper part and the red-fleshed (N) in the lower part.

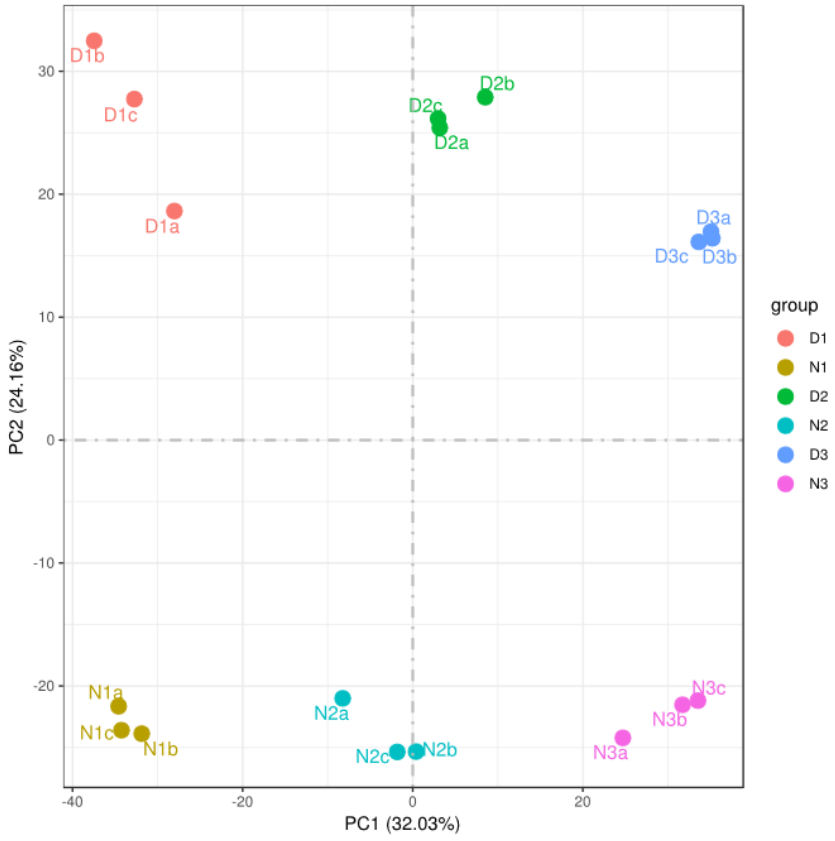

Figure 5.5. Principal component analysis (PCA) performed using the gene expression value (FPKM) of all samples.

Furthermore, the different time points were arranged in the same way for both the genotypes from left to right. The variability explained by the first two principal component was higher than 55%. The first Principal component was accounting for the 32% of the variability and was correlated with the development stage. The second principal component was accounting for the 24 % of the total variability and was related to the two genotypes.

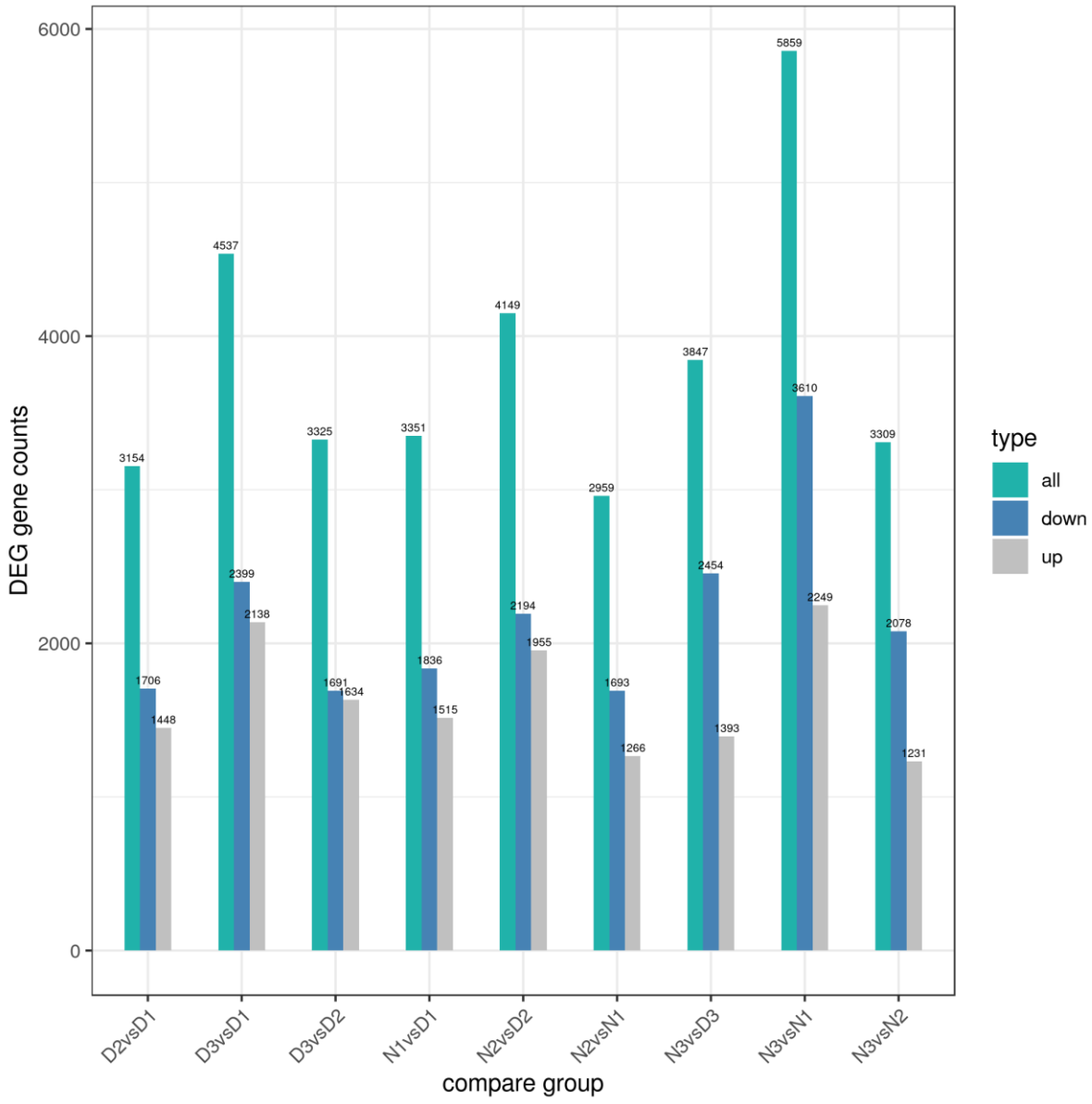

Figure 5.6. Histograms represents the number of total, down-regulated and up-regulated for each compare group.

From the analysis of the differential expressed genes for the compare groups, an enormous number of genes were identified (Figures 5.6 and 5.7). Focusing the attention on the red vs white compare groups, a total of 3351, 4149 and 3847 genes were identified having differential expression levels in N1vsD1, N2vsD2 and N3vsD3, respectively (Figure 5.6). Generally, the number of down-regulated genes was higher than the up-regulated ones. The high number of differential genes found was a demonstration of the complexity of the analysed system. In fact, most of the differences showed could be referenced to the two genotypes, *i.e.*, not only those due to the difference in colour.

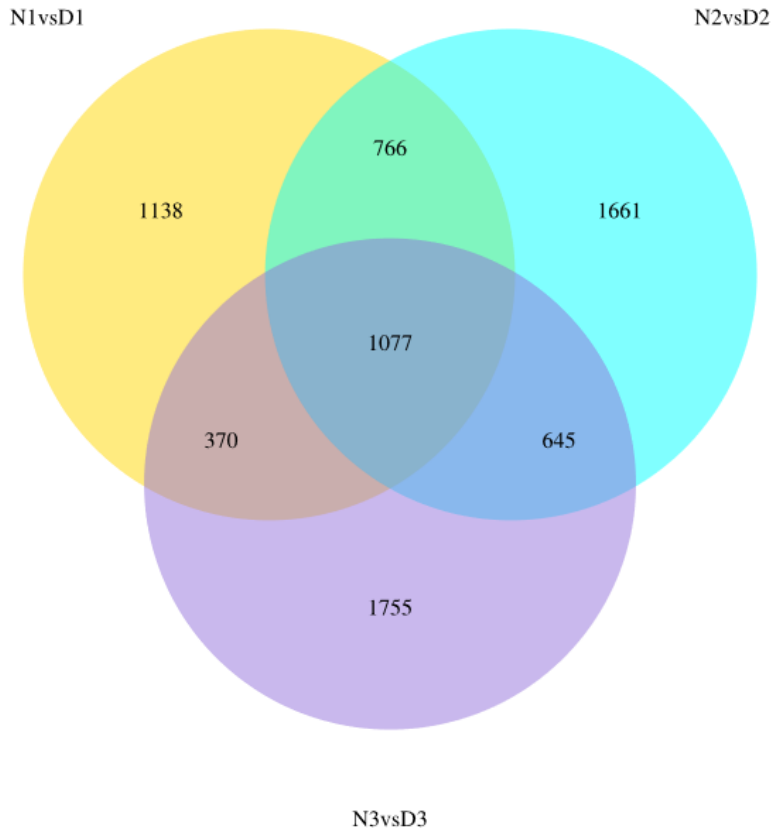

Figure 5.7. Differential Expression Venn diagram illustrates the number of differential genes of the compared treatment groups Red vs White in the three time points. The sum of all the numbers in the circle represents the total number in the compared groups, and the overlapping area indicates the number of differential genes shared between the groups.

A total of 1077 genes were found to have differential expression lever within the comparisons between N and D in all the three time points (Figure 5.7). The majority of the genes included were TF genes: NAC, BBOX, MYB, bHLH, JAZ were the most represented.

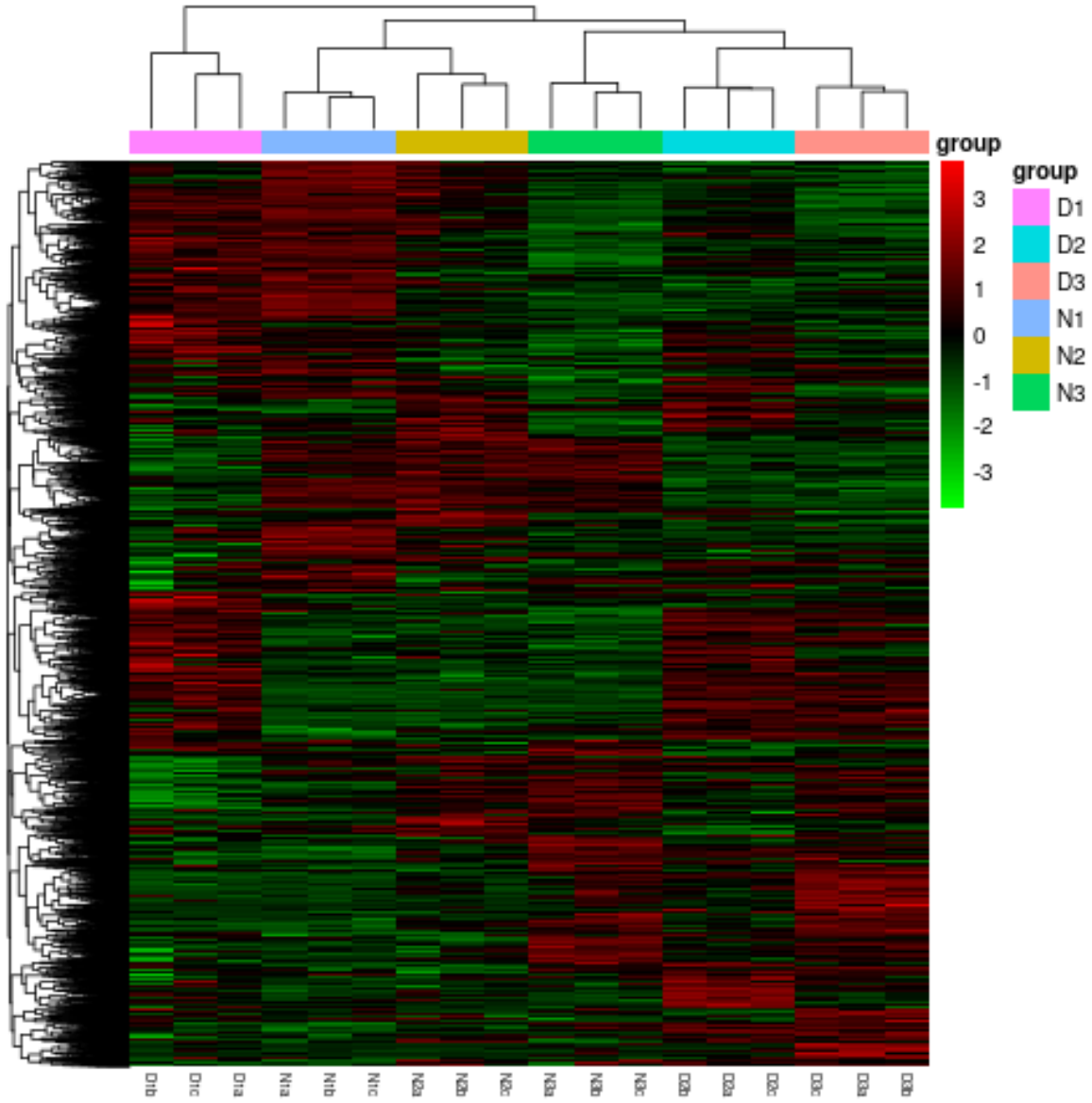

Figure 5.8. Heatmap representing the overall results of FPKM cluster analysis, clustered using the log2(FPKM+1) value. Red colour indicates genes with high expression levels, and green colour indicates genes with low expression levels. The colour ranging from red to green indicates that log2(FPKM+1) values where from large to small.

The heat map in Figure 5.8 showed a huge complexity level of the analysed system. The number of differential expressed genes was, as previously reported, over 5000. The KEGG pathways most represented and with the biggest significant differential expression were in the

three compare groups red vs white were reported (Figure 5.9). The Phenypropanoid and Flavonoid biosynthesis was the principal modified pathway in all the comparisons; moreover, Plant hormone signal transduction were always in the first 5 position. This confirm that pleiotropic interactions of plant hormones can play a crucial role in modulation of anthocyanin accumulation.

Figure 5.9. Histograms represent the 20 most significant differential expression KEGG pathways in comparison Red vs White: N1vsD1 (A), N2vsD2 (B) and N3vsD3 (C).

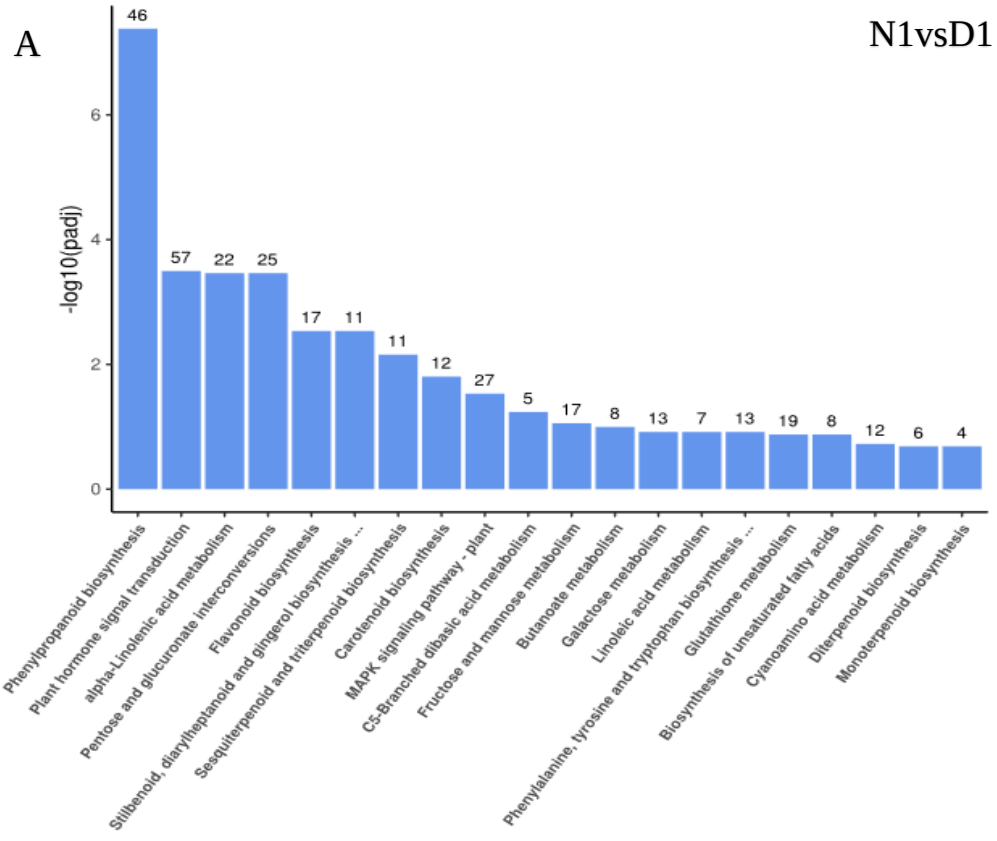

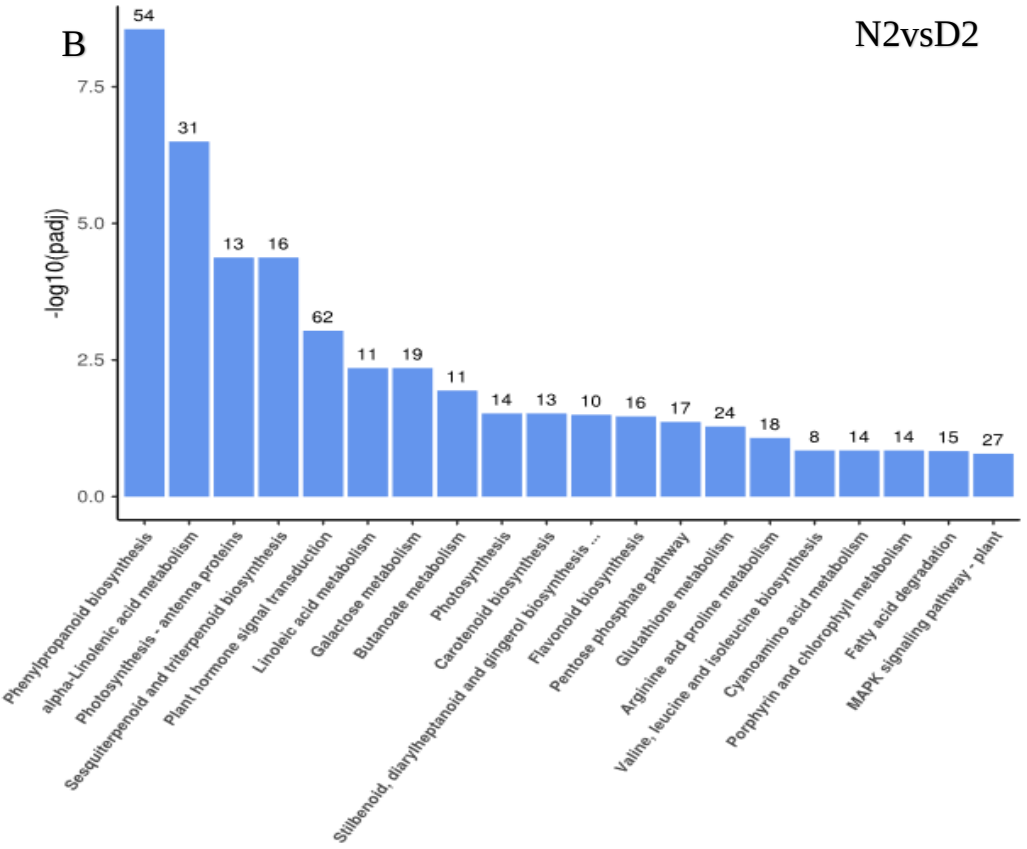
B
N2vsD2
-log10(padj)
7.5
5.0
2.5
0.0
54
31
13
16
62
11
19
11
14
13
10
16
17
24
18
8
14
14
15
27
Phenylpropanoid biosynthesis
alpha-Linolenic acid metabolism
Photosynthesis - antenna proteins
Sesquiterpenoid and triterpenoid biosynthesis
Plant hormone signal transduction
Linoleic acid metabolism
Galactose metabolism
Butanoate metabolism
Photosynthesis
Carotenoid biosynthesis
Stilbenoid, diarylheptanoid and gingerol biosynthesis ...
Flavonoid biosynthesis
Pentose phosphate pathway
Glutathione metabolism
Arginine and proline metabolism
Valine, leucine and isoleucine biosynthesis
Cyanoamino acid metabolism
Porphyrin and chlorophyll metabolism
Fatty acid degradation
MAPK signaling pathway - plant

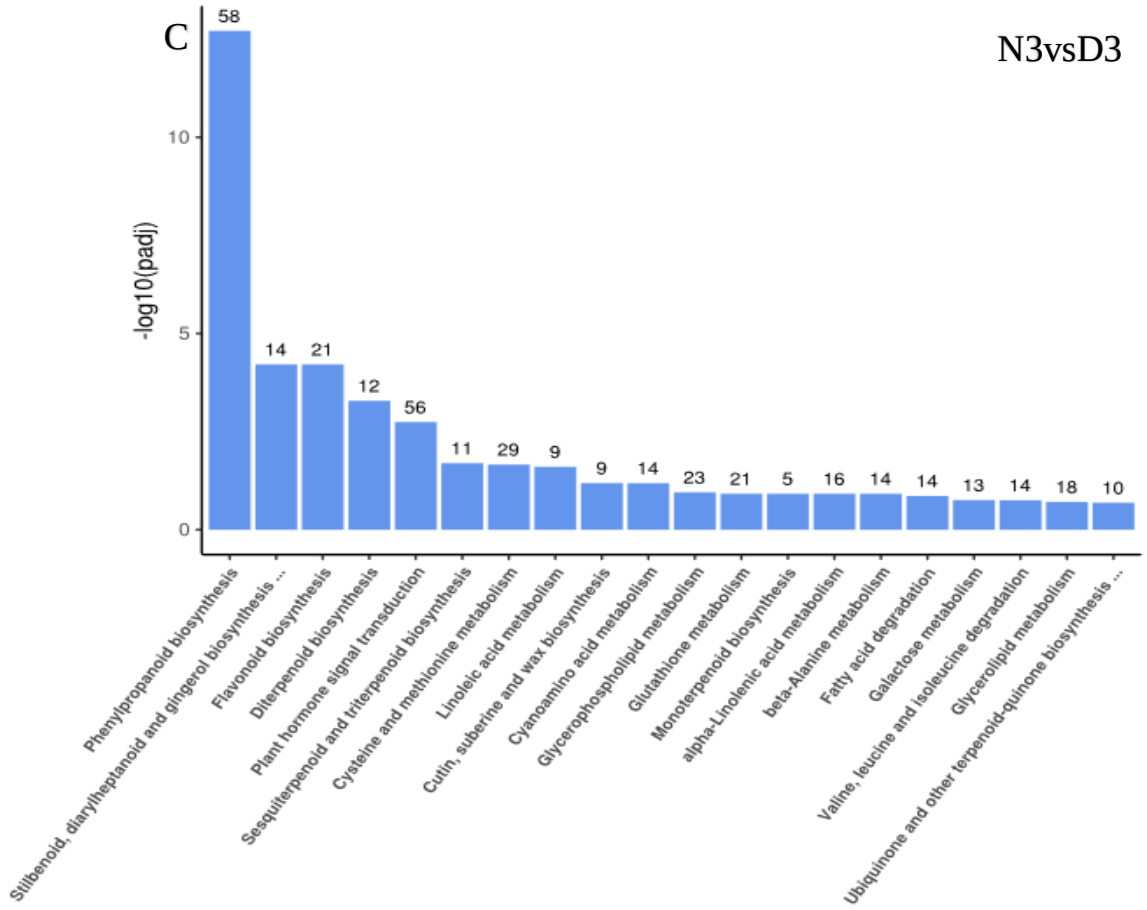
C
N3vsD3
-log10(padj)
10
5
0
58
14
21
12
56
11
29
9
9
14
23
21
5
16
14
14
13
14
18
10
Phenylpropanoid biosynthesis
Stilbenoid, diarylheptanoid and gingerol biosynthesis ...
Flavonoid biosynthesis
Diterpenoid biosynthesis
Plant hormone signal transduction
Sesquiterpenoid and triterpenoid biosynthesis
Cysteine and methionine metabolism
Linoleic acid metabolism
Cutin, suberine and wax biosynthesis
Cyanoamino acid metabolism
Glycerophospholipid metabolism
Glutathione metabolism
Monoterpenoid biosynthesis
alpha-Linolenic acid metabolism
beta-Alanine metabolism
Fatty acid degradation
Galactose metabolism
Valine, leucine and isoleucine degradation
Glycerolipid metabolism
Ubiquinone and other terpenoid-quinone biosynthesis ...

5.3.2.2. Phytohormones related gene differential expression

A total of 712 phytohormones related genes were found expressed in the analysed samples. 13 out of all showed a significant differential expression level in the three Red vs White compared groups (Table 5.4). In particular, two ABA hydroxylase genes, a SQUAMOSA Binding Protein gene (SBP), 6 jasmonate related genes (JAZ), three NAC TF genes and an ethylene responsing factor (ERF) were found having differential expression levels in the compared groups red vs white.

The SBP, located in chromosome (Chr) 16, was significantly down-regulated in red flesh fruit. In *Camelia synensis*, CsSBP8 had a positive effect on the anthocyanin accumulation during high temperature exposures and CsSBP12 showed a high correlation with anthocyanin accumulation during both high and low temperature (Zhang *et al.*, 2020). A role in anthocyanin accumulation were demonstrated for the gene MsSPL9 in *Medicago sativa* (Hanly *et al.*, 2020). Since the reported evidence affirms a positive regulation of the accumulation of anthocyanins, a direct involvement of this gene might be excluded. Moreover, 5 JAZ genes up-regulated in white-fleshed fruit were detected in several Chrs (9, 13, 14 and 15). JAZ genes generally inhibit the MBW complex from forming by interacting with bHLH and MYB, which prevents the expression of genes involved in anthocyanin biosynthesis (Ni et al 2020). In particular, in pear Premathilake *et al.*, (2020) demonstrated that PcMYB10 and PcMYC2 can directly interact with each other and bind to PcJAZ1 and PcJAZ2 repressors. In the same way in apple, a study concluded that MdJAZ2 inhibits the binding of MdbHLH3 to the MdMYB9 and MdMYB1 promoters. After jasmonate signals are perceived, MdbHLH3 is released to form the MBW complex involved in activating the downstream genes related to flavonoid biosynthesis (An *et al.*, 2015). As things stand, the lower expression level of these repressor genes could, hypothetically, boost the anthocyanin accumulation in red flesh fruit. In addition, in Chr5 a TPL binding protein gene showed up-regulation in white flesh fruit. Zheng *et al.*, (2019) found

in *A. thaliana* that HAT1 and TPL gene act as corepressor restrained anthocyanin accumulation by inhibiting the activities of MBW protein complex through blocking the formation of MBW protein complex. Similarly, to the JAZ repressor genes, low expression level of TPLs gene could enhance anthocyanin accumulation in red fruit.

Table 5.4. Phytohormones related genes with significant differential expression level in all the three Red vs White compare groups.

Gene ID	Chr	Gene description	N1vsD1 log2Fold Change	N1vsD1 padj	N2vsD2 log2Fold Change	N2vsD2 padj	N3vsD3 log2Fold Change	N3vsD3 padj
pycom16g10430	Chr16	SBP	-1,577	0,0050	-1,115	0,0340	-1,517	0,0002
pycom13g01830	Chr13	ZIM (JAZ)	-2,233	9,99E-20	-2,346	3,59E-16	-1,303	2,70E-05
pycom13g11020	Chr13	ZIM (JAZ)	-2,936	2,75E-13	-3,815	0,0003	-1,574	0,0002
pycom14g19920	Chr14	ZIM (JAZ)	-2,101	5,26E-12	-2,257	1,87E-09	-2,240	5,33E-09
pycom15g19540	Chr15	ZIM (JAZ)	-2,780	1,89E-05	-3,157	5,78E-15	-1,536	0,0016
pycom09g09690	Chr9	ZIM (JAZ)	-2,588	4,01E-11	-3,898	5,41E-13	-1,581	1,45E-08
pycom05g15750	Chr5	TPL binding protein	-3,290	3,52E-21	-3,417	1,93E-26	-1,207	1,63E-05
pycom15g12330	Chr15	NAC	-2,376	1,38E-10	-2,168	2,43E-16	-1,267	6,56E-07
pycom16g10690	Chr16	NAC	1,054	1,27E-06	1,215	3,46E-10	1,860	2,21E-46
pycom03g17130	Chr3	NAC	2,081	3,82E-13	1,072	3,72E-08	1,548	1,15E-51
pycom06g04520	Chr6	AP2 (ERF)	-1,463	1,20E-06	-1,040	1,29E-05	-1,440	1,88E-10
pycom02g13830	Chr2	ABA hydrox	-2,353	1,47E-26	-2,435	9,15E-28	-2,279	6,41E-08
pycom05g07510	Chr5	ABA hydrox	-1,862	1,69E-08	-1,903	6,58E-06	-1,103	0,0023

- SBP: SQUAMOSA Binding Protein; NAC: NAM, ATAF1/2, and CUC2; JAZ: Jasmonate related genes; ERF: Ethylene Responsing Factor; TPL: plant corepressor TOPLESS.

Additionally, three NAC TF genes were identified having differential expression level between red and white flesh fruit; the first one, located in Chr15 was down-regulated in red fruit, the other two, contrary, were up-regulate. NAC TFs are known actors in regulatory system of anthocyanin accumulation. For instance, in Arabidopsis the transcript levels of some genes related to flavonoid biosynthesis and the levels of anthocyanins were significantly increased in over expressed ANAC078 plants and reduced in knockout ANAC078 plants compared with wild-type plants under high-light stress (Morishita *et al.*, 2009) however ANAC032 suppressed

anthocyanin biosynthesis (Mahmood *et al.,* 2016). In red-fleshed apple, Zhang *et al.,* (2020) demonstrated than overexpression of MdNAC42 resulted in the up-regulation of flavonoid pathway genes thereby increasing the accumulation of anthocyanins. A NAC was found to be highly overexpressed in blood-fleshed peaches as compared to non-red-fleshed peaches and PpeNAC1 helped in anthocyanin accumulation by interacting with PpeMYB10 (Zhou *et al.,* 2015).

5.3.2.3. Expression level of the candidate genes detected by QTL analysis

The study of expression level of the 30 candidate genes detected by QTL mapping (see chapter 4), showed that three genes (MYB4, MYB114 and bHLH) were significantly differential expressed in red and white flesh. The MYB4 like gene (pycom05g18450), belonging the minor QTL in linkage group (LG), showed constantly a lower expression level in red flesh fruit (Table 5.3). MYB4 have been suggested to repress flavonoid biosynthesis (Jin *et al.,* 2000; Fornale *et al.,* 2014). MYB4 was also reported as a regulator of flavonoid biosynthesis in *Camellia sinensis* not only by repressing flavonoid biosynthetic genes but also by shikimate biosynthetic genes (Li *et al.,* 2017). In *Arabidopsis thaliana* MYB4 interact with the bHLH transcription factors TT8 (Transparent Testa), GL3 (Glabra) and EGL3 (Enhancer of Glabra) and thereby interfere with the transcriptional activity of the MBW complexes (Wang et al 2020). In addition, MYB4 was found also able to inhibit flavonoid accumulation by repressing expression of the gene encoding Arogenate Dehydratase 6 (ADT6), which catalyzes the final step in the biosynthesis of the precursor for flavonoid biosynthesis: phenylalanine (Wang *et al.,* 2020). Belonging the same QTL, a bHLH3 like gene was identified being up-regulated in red fleshed fruit (Fold Change 4,7 in N1vsD1 with adjusted p value = 0.01; Table 5.3). bHLH genes are widely known to interact with MYB and WD40 to promote anthocyanin accumulation (Espley *et al.*,2007; An *et al.,* 2012; Xie *et al.,* 2012). So far, two bHLH genes,

bHLH3 and bHLH33, have been identified as the regulators of anthocyanin synthesis in apples (Espley *et al.*, 2007; Peng and Moriguchi, 2013) and pear (Yao *et al.*, 2017).

Table 5.3. Candidate Genes identified by QTL analysis (see chapter 4) with significant differential expression level in at least two of the three Red vs White compare groups.

Gene ID	Chr	Gene description	N1vsD1 log2Fold Change	N1vsD1 padj	N2vsD2 log2Fold Change	N2vsD2 padj	N3vsD3 log2Fold Change	N3vsD3 padj
pycom05g18450	Chr5	MYB4 like	-2,69939	0,00423	-2,00924	0,01060	-0,78478	0,84358
pycom05g18900	Chr5	bHLH3 like	4,69137	0,01049	0,96443	0,49779	3,97925	0,00003
pycom04g14890	Chr4	WRKY 33 like	-3,25842	2,06E-06	-4,12398	1,53E-24	-1,39002	0,03329

Additionally, a WRKY33 like gene were found significantly down-regulate in red flesh samples in all the compare groups. Several WRKY genes are reported having an important role in the regulation of anthocyanin biosynthesis (Xu *et al.*, 2012; Duan *et al.*, 2018; An *et al.*, 2019). PyWRKY31 and PyWRKY26 interact with PyMYB10, PyMYB114 and PybHLH3 Asian pear (Li *et al.*, 2020), suggesting that it may have a role in upstream regulation of anthocyanin biosynthesis.

5.3.2.4. Differential expression level of structural genes of the anthocyanin pathway

The anthocyanin pathway related genes, CHS (chalcone synthase), CHI (Chalcone Isomerase), F3H (Flavanone 3-Hydroxylase), DFR (dihydroflavonol 4-reductase), and ANS (anthocyanidin synthase), showed a similar expression trend through the 3 time point analysed, 4, 6 and 8 weeks after full blooming (WAFB). All five of them had a peak of expression at 6 WAFB (Figure 5.4). Those genes are not only involved in anthocyanin pathway, but they are

known to act in other phenolic compounds pathways; actually, no significant differences were detected in the expression of these genes between the two genotypes with different flesh colour. On the other hand, the UFGT (uridine diphosphate (UDP)-glucose:flavonoid 3-O-glycosyltransferase) gene had a higher expression in CP compared to the white genotype and this could be related to its terminal role in anthocyanin biosynthesis. Shifting to the expression of the candidate genes, ABCC2 gene showed a similar expression level within the time points and between the two genotypes. MYB114 gene, instead, it was expressed in the red-fleshed fruits while resulted completely not expressed in the white flesh (Figure 5.4). From these results, the critical role of MYB114 gene in the anthocyanin accumulation in fruit flesh seems confirmed, while ABCC2 gene could be excluded as a key gene in determining red flesh phenotype.

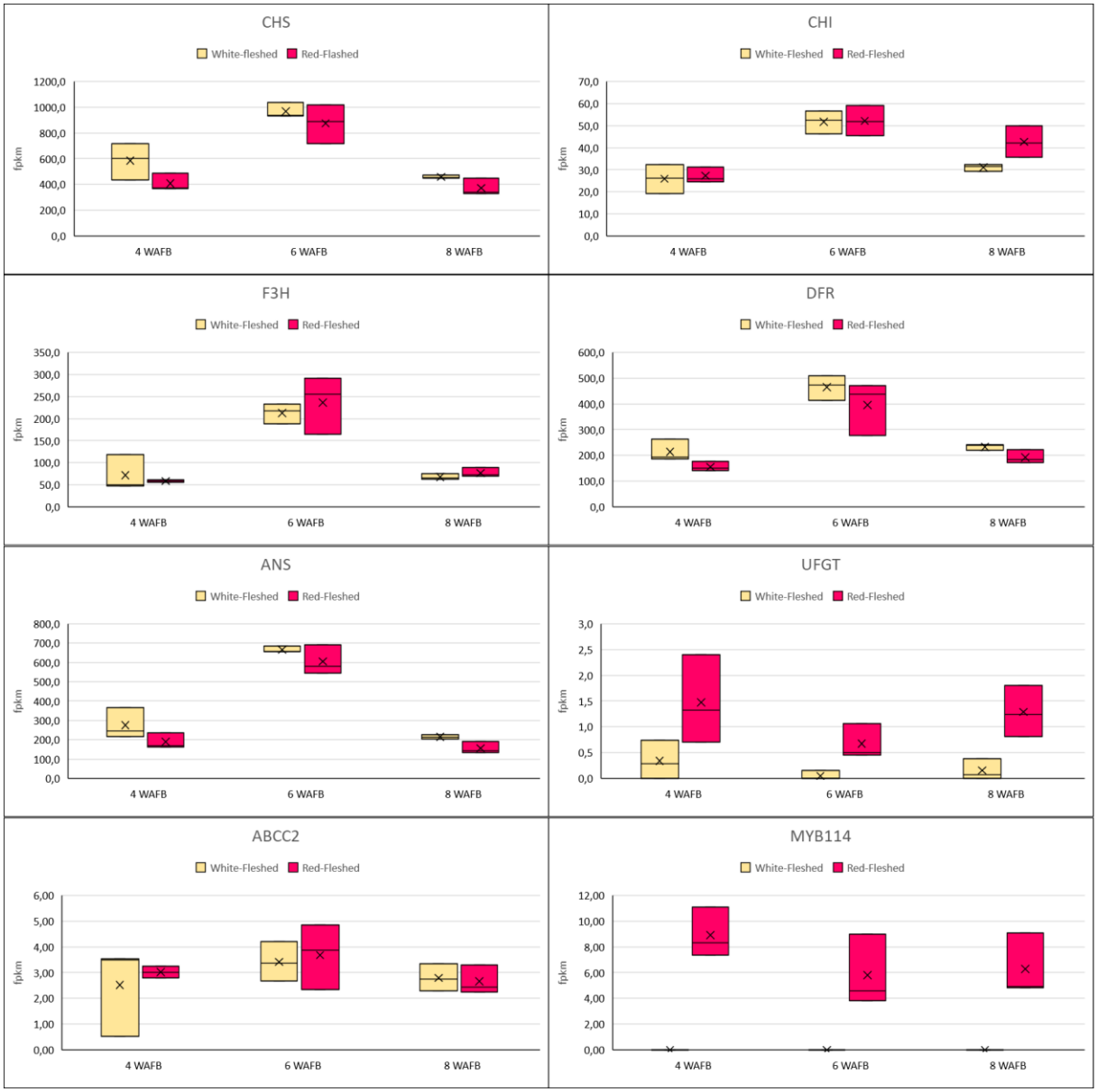

Figure 5.4. Comparison of expression levels of the anthocyanin related genes (from RNAseq) between the white and red-fleshed fruit pulp (seedling57 in yellow and Cocomerina Precoce in red).

5.3.6. Third trial: Anthocyanin-related genes expression in different red-fleshed fruit during the early developmental stage

5.3.6.1. Anthocyanin content detection in fruit flesh

HPLC analysis was performed to identify and quantify the different content of anthocyanin among 6 genotypes, belonging to the same progeny (P013.019, hold in Motueka, Nelson, NZ), chosen because they have different distributions of red in the fruit. Three different development stages 6, 8 and 10 weeks after full blooming (WAFB) were examined. Only cyanidin-3-O-galactoside (C-3-G) was detected by the MS analysis in all the tested samples. The concentration ranged from around 200 µg/g in the genotype F to 0 µg/g detected in genotype A (Table 5.3). An increasing of anthocyanin accumulation through the time points was found in genotypes B, C and E.

Table 5.3. Content of Cyanidin-3-O-galactoside (µg/g of dry weight) detected in 6 different genotypes and three time points.

Genotype	Time point	µg/g Cyn-3-Gal
A	4 WAFB	0,00
White	6 WAFB	0,00
	8 WAFB	0,00
B	4 WAFB	0,00
Only SL	6 WAFB	0,00
	8 WAFB	11,79
C	4 WAFB	11,23
SL and US	6 WAFB	11,30
	8 WAFB	15,73
D	4 WAFB	49,59
Mostly TF	6 WAFB	23,28
	8 WAFB	39,91
E	4 WAFB	48,82
Mostly FF	6 WAFB	32,15
	8 WAFB	70,71
F	4 WAFB	197,27
Reddest	6 WAFB	169,44
	8 WAFB	188,17

*SL: Seed Locules; TF: True Fruit; FF: False Fruit; US: Under the fruit skin; WAFB: week after full bloom.

Figure5.5a. Expression profiling of pear anthocyanin genes and candidate genes identified by QTL analysis in genotypes A, B and C. Data from qPCR analysis of the CP fruit flesh in different development stages. CHS, chalcone synthase; DFR, dihydroflavonol 4-reductase. In the bottom line fruit development series of fruits in the corresponding development stage.

Figure5.5b. Expression profiling of pear anthocyanin genes and candidate genes identified by QTL analysis in genotypes D, E and F. Data from qPCR analysis of the CP fruit flesh in different development stages. CHS, chalcone synthase; DFR, dihydroflavonol 4-reductase. In the bottom line fruit development series of fruits in the corresponding development stage.

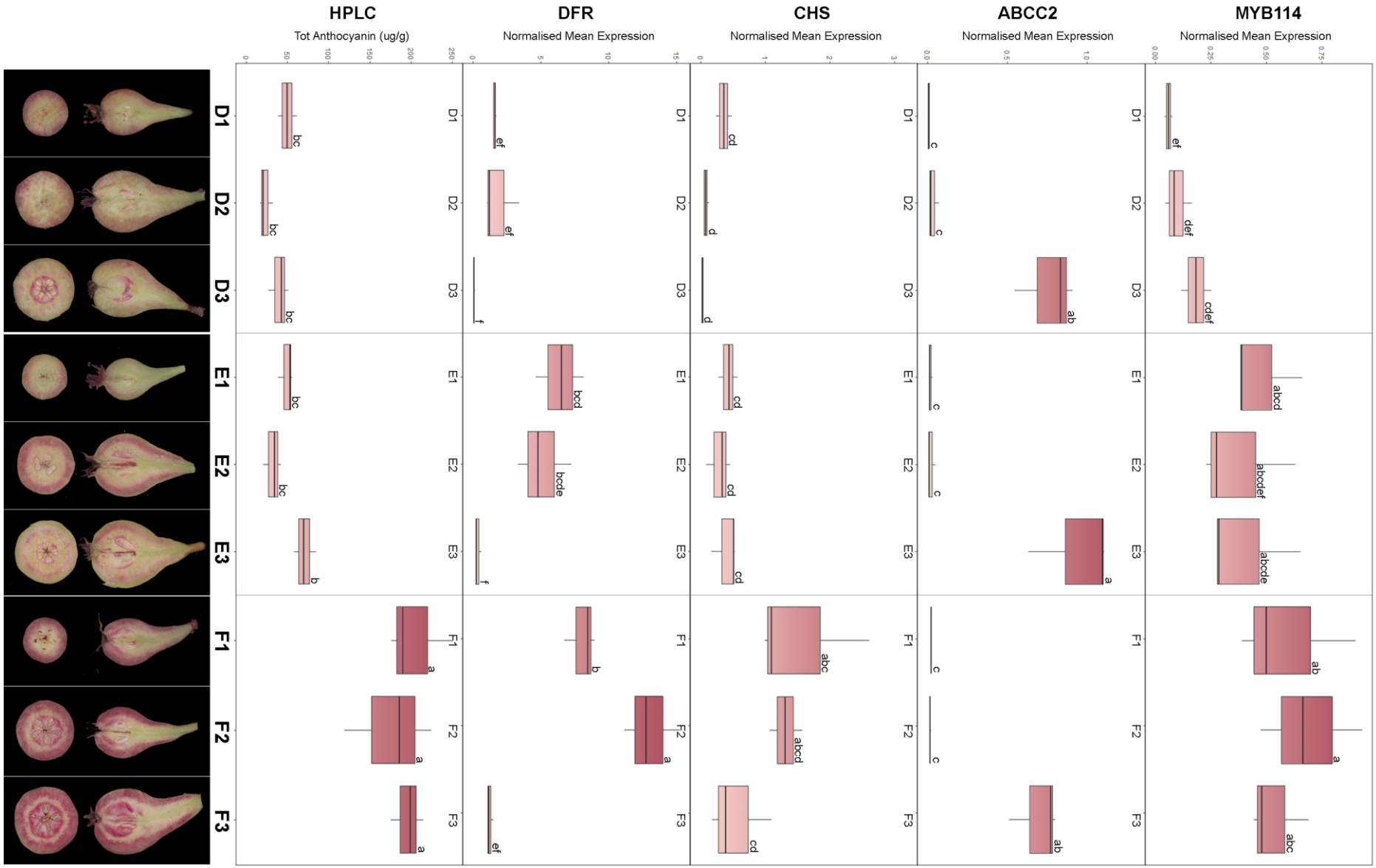

5.3.6.2. Relative gene expression analysis

The relative expression level tested in early stage development pear fruit flesh samples showed significant differences in most of the tested genes. No amplifications were detected for UFGT, MYB10 and MYB110a (data not showed).

The CHS gene showed differential level of expressions among the six genotypes (Figure 5.5 a and b). In C, D and E the level of relative expression was constantly very low throughout the three time points; in contrast, in B, C and F the expression was higher, especially in A, with a decreasing at 10 WAFB. In a similar way, the relative expression level of DFR in A, C and D was low and tendentially decreasing during time. On the other hand, B and E had a higher value in the first two time points falling down in the third one. Dissimilarly, the genotype F, had a peak of expression at 8 WAFB followed by a noticeable drop in the last time point.

Moving to the candidate genes relative expression levels, the ABCC2 gene had no expression in all the tested genotypes in the first two sampling time followed by a comparable increment of expression at 10 WAFB. Moreover, MYB114 showed a differential expression level among the genotypes. The highest expression level was registered in the reddest genotype F and no expression was detected in the white-fleshed genotype A. The level of expression, even if variable among genotypes, were tendentially constant during the examined time.

By comparing the expression levels and anthocyanin content data of the six analysed genotypes (Figure 5.6), the highest correlation was detected between MYB114 expression and HPLC data (0.75), consolidating the previous results that connect the activity of the MYB114 with the anthocyanin accumulation in fruit flesh. Nevertheless, a good level of correlation was also observed for DFR and CHS (0.44), MYB114 and DFR (0.49) and HPLC/DFR data (0.39). On the other hand, ABCC2 expression showed a negative correlation with the DFR genes (-0.60).

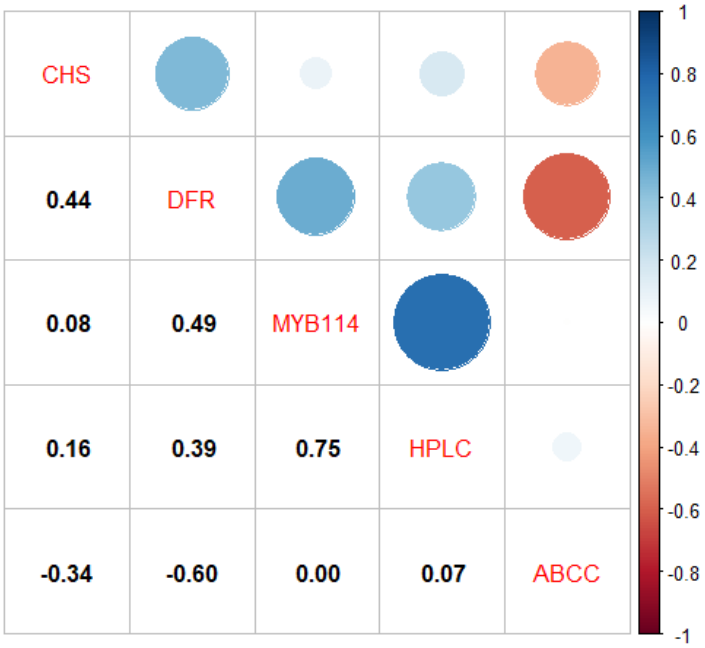

Figure 5.6. Correlation matrix of the gene expression levels and anthocyanin fruit concentration measured by HPLC.

5.4. Conclusions

These three different trials led to a better comprehension of the genetic control of the anthocyanin accumulation in pear fruit flesh. A complete growing season of 'Cocomerina Precoce' fruit were examined finding the pattern of synthesis and accumulation of anthocyanin during the fruit development, finding crucial differences from red-fleshed apple, even if their close botanical relationship. A peak of expression of the anthocyanin pathway genes CHS, DFR, and UFGT was found just before the maximum accumulation of cyaniding-3-O-galactoside in the fruit flesh. The same peak of expression was found around 6 WAFB in two different seasons in 'Cocomerina Precoce' using qPCR and RNAseq data. In all the experiments conducted in different growing season and with different source of red ('Cocomerina Precoce' in the first two, and 'Sanguinole' for the third one) the expression level of the candidate gene MYB114 was highly correlated with the red flesh phenotype, proving its key role for the appearance of the trait.

Regarding the modulatory system of anthocyanin accumulation, several TF genes were found having differential expression between red and white flesh fruits. An upstream regulation of the pathway seems to be acted by plant hormone-related genes. Further investigation is needed to clarify the putative specific genes interaction. The transcriptomic data obtained in this work could give more evidence with additional analysis.

References

- An XH, Tian Y, Chen KQ, Wang XF, Hao YJ (2012) The apple WD40 protein MdTTG1 interacts with bHLH but not MYB proteins to regulate anthocyanin accumulation. J Plant Physiol 169:710–717
- An, X. H., Tian, Y., Chen, K. Q., Liu, X. J., Liu, D. D., Xie, X. B., ... & Hao, Y. J. (2015). MdMYB9 and MdMYB11 are involved in the regulation of the JA-induced biosynthesis of anthocyanin and proanthocyanidin in apples. Plant and Cell Physiology, 56(4), 650-662.
- An, J. P., Wang, X. F., Li, Y. Y., Song, L. Q., Zhao, L. L., You, C. X., & Hao, Y. J. (2018). EIN3-LIKE1, MYB1, and ETHYLENE RESPONSE FACTOR3 act in a regulatory loop that synergistically modulates ethylene biosynthesis and anthocyanin accumulation. Plant Physiology, 178(2), 808-823.
- An, J. P., Zhang, X. W., Bi, S. Q., You, C. X., Wang, X. F., & Hao, Y. J. (2020). The ERF transcription factor MdERF38 promotes drought stress-induced anthocyanin biosynthesis in apple. The Plant Journal, 101(3), 573-589.
- An, J. P., Zhang, X. W., Liu, Y. J., Wang, X. F., You, C. X., & Hao, Y. J. (2021). ABI5 regulates ABA-induced anthocyanin biosynthesis by modulating the MYB1-bHLH3 complex in apple. Journal of Experimental Botany, 72(4), 1460-1472.
- An, J. P., Xu, R. R., Liu, X., Zhang, J. C., Wang, X. F., You, C. X., & Hao, Y. J. (2021). Jasmonate induces biosynthesis of anthocyanin and proanthocyanidin in apple by mediating the JAZ1–TRB1–MYB9 complex. The Plant Journal, 106(5), 1414-1430.
- Behrens, C. E., Smith, K. E., Iancu, C. V., Choe, J. Y., & Dean, J. V. (2019). Transport of anthocyanins and other flavonoids by the Arabidopsis ATP-binding cassette transporter AtABCC2. Scientific Reports, 9(1), 1-15.
- Browse, J. (2009). Jasmonate passes muster: a receptor and targets for the defense hormone. Annual Review of Plant Biology, 60, 183-205.
- Dussi M.C., Sugar D., Wrolstad R.E., 1995. Characterizing and quantifying anthocyanins in red pears and the effect of light quality on fruit color. Journal of the American Society for Horticultural Science, 120: 785–789.
- Espley, R. V., Hellens, R. P., Putterill, J., Stevenson, D. E., Kutty-Amma, S., & Allan, A. C. (2007). Red colouration in apple fruit is due to the activity of the MYB transcription factor, MdMYB10. The Plant Journal, 49(3), 414-427.

- Fischer T.C., Gosch C., Pfeiffer J., Halbwirth H., Halle C., Stich K., Forkmann G., 2007. Flavonoid genes of pear (Pyrus communis). Trees-Structure and Function, 21: 521–529
- Fornale, S., Lopez, E., Salazar-Henao, J.E., Fernandez-Nohales, P., Rigau, J. and Caparros-Ruiz, D. (2014) AtMYB7, a new player in the regulation of UV-sunscreens in Arabidopsis thaliana. Plant Cell Physiol. 55, 507–516.
- Francis F.J., 1970. Anthocyanins in pears. HortScience, 5: 42
- Garrido-Bigotes, A., Torrejón, M., Solano, R., & Figueroa, C. R. (2020). Interactions of JAZ repressors with anthocyanin biosynthesis-related transcription factors of Fragaria× ananassa. Agronomy, 10(10), 1586.
- Gerats, A. G. M., Wallroth, M., Donker-Koopman, W., Groot, S. P. C., & Schram, A. W. (1983). The genetic control of the enzyme UDP-glucose: 3-0-flavonoid-glucosyltransferase in flowers of Petunia hybrida. Theoretical and Applied Genetics, 65, 349-352.
- Hanly, A., Karagiannis, J., Lu, Q. S. M., Tian, L., & Hannoufa, A. (2020). Characterization of the Role of SPL9 in Drought Stress Tolerance in Medicago sativa. International Journal of Molecular Sciences, 21(17), 6003.
- Jin, H., Cominelli, E., Bailey, P., Parr, A., Mehrtens, F., Jones, J., Tonelli, C., Weisshaar, B. and Martin, C. (2000) Transcriptional repression by AtMYB4 controls production of UV-protecting sunscreens in Arabidopsis. EMBO J. 19, 6150–6161.
- Kadomura-Ishikawa, Y., Miyawaki, K., Takahashi, A., Masuda, T., & Noji, S. (2015). Light and abscisic acid independently regulated FaMYB10 in Fragaria× ananassa fruit. Planta, 241, 953-965.
- Kanehisa M, Goto S. KEGG: kyoto encyclopedia of genes and genomes. Nucleic acids research, 2000, 28(1): 27-30.
- Li, M., Li, Y., Guo, L., Gong, N., Pang, Y., Jiang, W., ... & Xia, T. (2017). Functional characterization of tea (Camellia sinensis) MYB4a transcription factor using an integrative approach. Frontiers in plant science, 8, 943.
- Lin L.Z., Harnly J.M., 2008. Phenolic compounds and chromatographic profiles of pear skins (Pyrus spp.). Journal of Agricultural and Food Chemistry, 56: 9094–9101.
- Linsmith, G., Rombauts, S., Montanari, S., Deng, C. H., Celton, J. M., Guérif, P., ... & Bianco, L. (2019). Pseudo-chromosome–length genome assembly of a double haploid “Bartlett” pear (Pyrus communis L.). Gigascience, 8(12), giz138.

- Luo, H., Dai, S., Ren, J., Zhang, C., Ding, Y., Li, Z., ... & Leng, P. (2014). The role of ABA in the maturation and postharvest life of a nonclimacteric sweet cherry fruit. Journal of Plant Growth Regulation, 33, 373-383.
- Ma, H., Yang, T., Li, Y., Zhang, J., Wu, T., Song, T., ... & Tian, J. (2021). The long noncoding RNA MdLNC499 bridges MdWRKY1 and MdERF109 function to regulate early-stage light-induced anthocyanin accumulation in apple fruit. The Plant Cell, 33(10), 3309-3330.
- Morishita, T., Kojima, Y., Maruta, T., Nishizawa-Yokoi, A., Yabuta, Y., & Shigeoka, S. (2009). Arabidopsis NAC transcription factor, ANAC078, regulates flavonoid biosynthesis under high-light. Plant and Cell Physiology, 50(12), 2210-2222.
- Mortazavi, A., Williams, B. A., McCue, K., Schaeffer, L., & Wold, B. (2008). Mapping and quantifying mammalian transcriptomes by RNA-Seq. Nature methods, 5(7), 621-628.
- Ngo T., Zhao Y.Y., 2009. Stabilization of anthocyanins on thermally processed red D'Anjou pears through complexation and polymerization. LWT-Food Science and Technology, 42: 1144–1152
- Ni, J., Bai, S., Zhao, Y., Qian, M., Tao, R., Yin, L., ... & Teng, Y. (2019). Ethylene response factors Pp4ERF24 and Pp12ERF96 regulate blue light-induced anthocyanin biosynthesis in 'Red Zaosu'pear fruits by interacting with MYB114. Plant molecular biology, 99, 67-78.
- Ni, J., Premathilake, A. T., Gao, Y., Yu, W., Tao, R., Teng, Y., & Bai, S. (2021). Ethylene-activated PpERF105 induces the expression of the repressor-type R2R3-MYB gene PpMYB140 to inhibit anthocyanin biosynthesis in red pear fruit. The Plant Journal, 105(1), 167-181.
- Peng T, Moriguchi T (2013) The molecular network regulating the coloration in apple. Sci Hortic 163:1–9
- Pierantoni, L., Dondini, L., De Franceschi, P., Musacchi, S., Winkel, B. S., & Sansavini, S. (2010). Mapping of an anthocyanin-regulating MYB transcription factor and its expression in red and green pear, Pyrus communis. Plant Physiology and Biochemistry, 48(12), 1020-1026.
- Premathilake, A. T., Ni, J., Shen, J., Bai, S., & Teng, Y. (2020). Transcriptome analysis provides new insights into the transcriptional regulation of methyl jasmonate-induced flavonoid biosynthesis in pear calli. BMC Plant Biology, 20(1), 1-14.

- Ren, J., Chen, P., Dai, S. J., Li, P., Li, Q., Ji, K., ... & Leng, P. (2011). Role of abscisic acid and ethylene in sweet cherry fruit maturation: molecular aspects. New Zealand Journal of Crop and Horticultural Science, 39(3), 161-174.
- Rozen, S. and Skaletsky, H. (2020). “Primer3 on the WWW for general users and for biologist programmers” Methods Mol. Biol., 132 (2000), pp. 365-386
- Samkumar, A., Jones, D., Karppinen, K., Dare, A. P., Sipari, N., Espley, R. V., ... & Jaakola, L. (2021). Red and blue light treatments of ripening bilberry fruits reveal differences in signalling through abscisic acid-regulated anthocyanin biosynthesis. Plant, Cell & Environment, 44(10), 3227-3245.
- Sato, H., Otagaki, S., Saelai, P., Kondo, S., Shiratake, K., & Matsumoto, S. (2017). Varietal differences in phenolic compounds metabolism of type 2 red-fleshed apples. Scientia Horticulturae, 219, 1-9.
- Shen, X., Zhao, K., Liu, L., Zhang, K., Yuan, H., Liao, X., ... & Li, T. (2014). A role for PacMYBA in ABA-regulated anthocyanin biosynthesis in red-colored sweet cherry cv. Hong Deng (Prunus avium L.). Plant and Cell Physiology, 55(5), 862-880.
- Wang, Y. C., Wang, N., Xu, H. F., Jiang, S. H., Fang, H. C., Su, M. Y., ... & Chen, X. S. (2018). Auxin regulates anthocyanin biosynthesis through the Aux/IAA–ARF signaling pathway in apple. Horticulture Research, 5.
- Wang, X. C., Wu, J., Guan, M. L., Zhao, C. H., Geng, P., & Zhao, Q. (2020). Arabidopsis MYB4 plays dual roles in flavonoid biosynthesis. The Plant Journal, 101(3), 637-652.
- Xie X, Li S, Zhang R, Zhao J, Che Y, Zhao Q, Yao Y, You C, Zhang X, Hao Y (2012) The bHLH transcription factor MdbHLH3 promotes anthocyanin accumulation and fruit colouration in response to low temperature in apples. Plant Cell Environ 35:1884–1897
- Yao, G., Ming, M., Allan, A. C., Gu, C., Li, L., Wu, X., ... & Wu, J. (2017). Map-based cloning of the pear gene MYB 114 identifies an interaction with other transcription factors to coordinately regulate fruit anthocyanin biosynthesis. The Plant Journal, 92(3), 437-451.
- Yin, J. H., Gao, F. F., Hu, G. B., & Zhu, S. H. (2001). regulation of litchi maturation and coloration by abscisic acid and ethylene. Acta horticulturae.

- Zhang, X. D., Allan, A. C., Chen, X. Q., Fan, L., Chen, L. M., Shu, Q., ... & Li, K. Z. (2012). Coloration, anthocyanin profile and metal element content of Yunnan Red Pear (Pyrus pyrifolia). Horticultural Science, 39(4), 164-171.
- Zhang, J., Xu, H., Wang, N., Jiang, S., Fang, H., Zhang, Z., ... & Chen, X. (2018). The ethylene response factor MdERF1B regulates anthocyanin and proanthocyanidin biosynthesis in apple. Plant Molecular Biology, 98, 205-218.
- Zhang, D., Han, Z., Li, J., Qin, H., Zhou, L., Wang, Y., ... & Fang, W. (2020). Genome-wide analysis of the SBP-box gene family transcription factors and their responses to abiotic stresses in tea (Camellia sinensis). Genomics, 112(3), 2194-2202.
- Zheng, T., Tan, W., Yang, H., Zhang, L. E., Li, T., Liu, B., ... & Lin, H. (2019). Regulation of anthocyanin accumulation via MYB75/HAT1/TPL-mediated transcriptional repression. PLoS Genetics, 15(3), e1007993.

6. General Conclusions and Future Prospective

The results obtained from these studies provided a better understanding of the anthocyanin accumulation in pear fruit flesh. A small genomic region in LG5 related to the red flesh fruit trait was found by QTL analysis performed on the CP x C pear cross population. The candidate gene MYB114 was found in this region supporting the hypothesis of its involvement in the appearance of this phenotype in European pear. Nevertheless, from the best knowledge achieved in this study, this QTL does not explain all the variability showed among the progenies examined. MYB114 could explain only the presence/absence of the anthocyanin accumulation in fruit flesh but not its content level. The transcriptomic analysis provides the identification of secondary candidate genes putatively involved in the regulatory system. Several TFs were found having differential expression levels between red and white-fleshed fruits. JAZ, bHLH, MYB, WRKY and NAC are the most represented TF families. This knowledge can be the basis for new studies that can lead to a better understanding of the genetic mechanisms behind this process. For example, data of RNAseq provide clear evidence that MYB114 is a key factor in activating anthocyanin synthesis in pear fruit pulp however, further investigations and analysis on these data, for instance a gene network analysis, could provide possible interactions between MYB114 and other TF genes or structural genes in the anthocyanin pathway.

The finding of the relationship between the allele 202 of the molecular marker SSR114 and the red flesh phenotype might be a fundamental tool for boosting the ongoing breeding programs of red-fleshed pear. It plausible that a particular allelic variant of the MYB114 could be present in ‘Cocomerina Precoce’, and in other red-fleshed accessions, associated to the allele 202 detected with the marker SSR114.

Concerning the origin of this fascinating trait in pear, it should be advisable to analyse more samples collected in different areas, for example, made a genetic diversity analysis with more European red-fleshed landraces could further shed light about the origin of the trait. As well as test more red-fleshed genotypes with the SSR114 marker to determine the presence of the 202 allele and eventually discover new genetic sources of the trait.

The allelic sequences of the ‘Cocomerina Precoce’ MYB114 gene and its promoter region are under investigations to explain the differential functionality of the gene. The two alleles were cloned in recent days, and functional assays involving transient changes in tobacco, callus of apple and pear are now being conducted. The final findings are not yet obtained; however, the first sequencing showed some differences in the coding sequence that could affect the functionality of the protein.

Appendix 1.

1.1. Linkage groups of Carmen

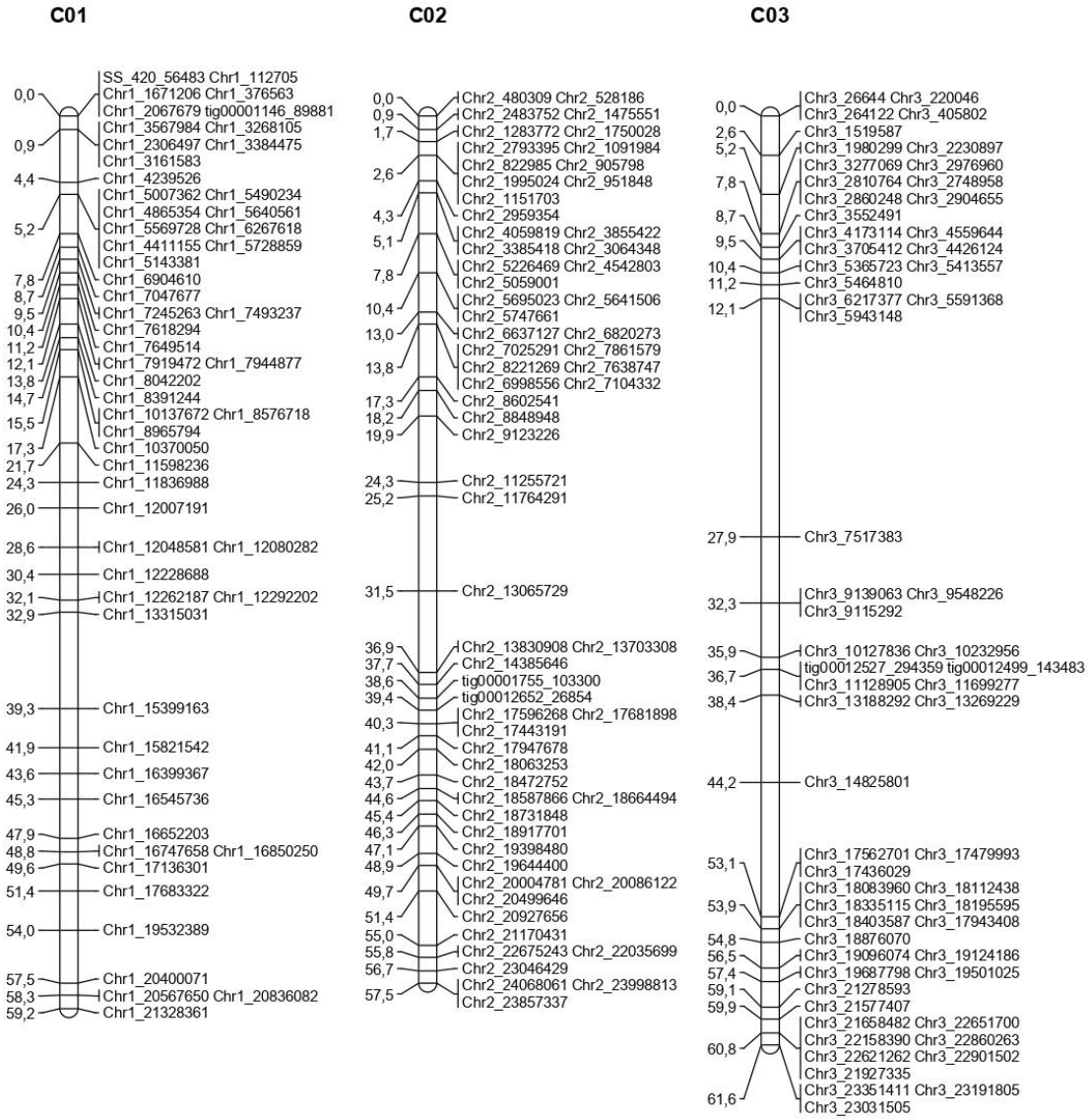

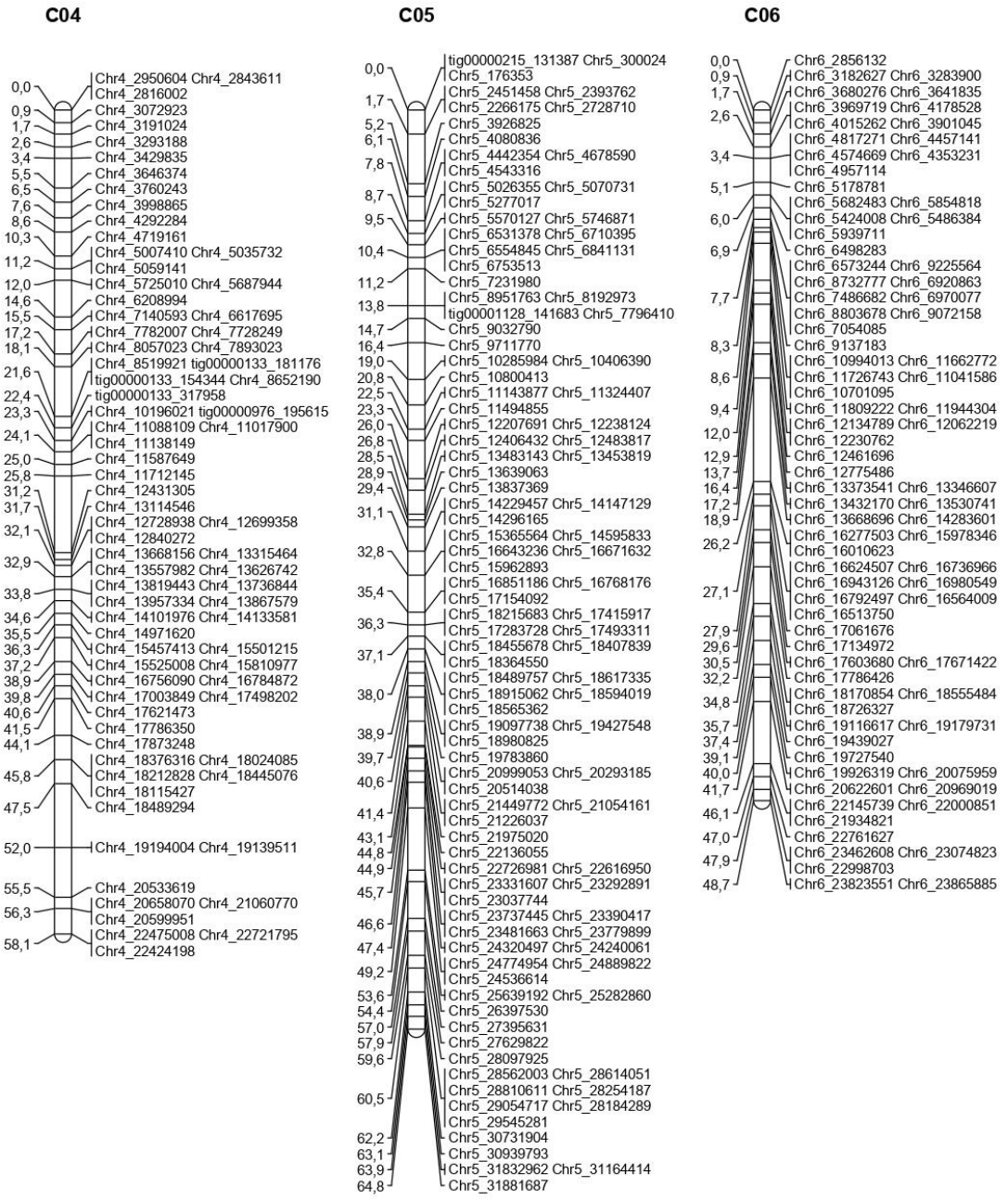
C04
0,0 Chr4_2950604 Chr4_2843611
Chr4_2816002
0,9 Chr4_3072923
1,7 Chr4_3191024
2,6 Chr4_3293188
3,4 Chr4_3429835
5,5 Chr4_3646374
6,5 Chr4_3760243
7,6 Chr4_3998865
8,6 Chr4_4292284
10,3 Chr4_4719161
11,2 Chr4_5007410 Chr4_5035732
Chr4_5059141
12,0 Chr4_5725010 Chr4_5687944
14,6 Chr4_6208994
15,5 Chr4_7140593 Chr4_6617695
17,2 Chr4_7782007 Chr4_7728249
18,1 Chr4_8057023 Chr4_7893023
21,6 Chr4_8519921 tig00000133_181176
tig00000133_154344 Chr4_8652190
22,4 tig00000133_317958
23,3 Chr4_10196021 tig00000976_195615
24,1 Chr4_11088109 Chr4_11017900
Chr4_11138149
25,0 Chr4_11587649
25,8 Chr4_11712145
31,2 Chr4_12431305
31,7 Chr4_13114546
32,1 Chr4_12728938 Chr4_12699358
Chr4_12840272
32,9 Chr4_13668156 Chr4_13315464
Chr4_13557982 Chr4_13626742
33,8 Chr4_13819443 Chr4_13736844
Chr4_13957334 Chr4_13867579
34,6 Chr4_14101976 Chr4_14133581
35,5 Chr4_14971620
36,3 Chr4_15457413 Chr4_15501215
37,2 Chr4_15525008 Chr4_15810977
38,9 Chr4_16756090 Chr4_16784872
39,8 Chr4_17003849 Chr4_17498202
40,6 Chr4_17621473
41,5 Chr4_17786350
44,1 Chr4_17873248
45,8 Chr4_18376316 Chr4_18024085
Chr4_18212828 Chr4_18445076
Chr4_18115427
47,5 Chr4_18489294
52,0 Chr4_19194004 Chr4_19139511
55,5 Chr4_20533619
56,3 Chr4_20658070 Chr4_21060770
Chr4_20599951
58,1 Chr4_22475008 Chr4_22721795
Chr4_22424198
C05
0,0 tig00000215_131387 Chr5_300024
Chr5_176353
1,7 Chr5_2451458 Chr5_2393762
Chr5_2266175 Chr5_2728710
5,2 Chr5_3926825
6,1 Chr5_4080836
7,8 Chr5_4442354 Chr5_4678590
Chr5_4543316
8,7 Chr5_5026355 Chr5_5070731
Chr5_5277017
9,5 Chr5_5570127 Chr5_5746871
Chr5_6531378 Chr5_6710395
10,4 Chr5_6554845 Chr5_6841131
Chr5_6753513
11,2 Chr5_7231980
13,8 Chr5_8951763 Chr5_8192973
tig00001128_141683 Chr5_7796410
14,7 Chr5_9032790
16,4 Chr5_9711770
19,0 Chr5_10285984 Chr5_10406390
20,8 Chr5_10800413
22,5 Chr5_11143877 Chr5_11324407
23,3 Chr5_11494855
26,0 Chr5_12207691 Chr5_12238124
26,8 Chr5_12406432 Chr5_12483817
28,5 Chr5_13483143 Chr5_13453819
28,9 Chr5_13639063
29,4 Chr5_13837369
31,1 Chr5_14229457 Chr5_14147129
Chr5_14296165
32,8 Chr5_15365564 Chr5_14595833
Chr5_16643236 Chr5_16671632
Chr5_15962893
35,4 Chr5_16851186 Chr5_16768176
Chr5_17154092
36,3 Chr5_18215683 Chr5_17415917
37,1 Chr5_17283728 Chr5_17493311
Chr5_18455678 Chr5_18407839
Chr5_18364550
38,0 Chr5_18489757 Chr5_18617335
Chr5_18915062 Chr5_18594019
Chr5_18565362
38,9 Chr5_19097738 Chr5_19427548
Chr5_18980825
39,7 Chr5_19783860
40,6 Chr5_20999053 Chr5_20293185
Chr5_20514038
41,4 Chr5_21449772 Chr5_21054161
Chr5_21226037
43,1 Chr5_21975020
44,8 Chr5_22136055
44,9 Chr5_22726981 Chr5_22616950
45,7 Chr5_23331607 Chr5_23292891
Chr5_23037744
46,6 Chr5_23737445 Chr5_23390417
47,4 Chr5_23481663 Chr5_23779899
Chr5_24320497 Chr5_24240061
49,2 Chr5_24774954 Chr5_24889822
Chr5_24536614
53,6 Chr5_25639192 Chr5_25282860
54,4 Chr5_26397530
57,0 Chr5_27395631
57,9 Chr5_27629822
59,6 Chr5_28097925
60,5 Chr5_28562003 Chr5_28614051
Chr5_28810611 Chr5_28254187
Chr5_29054717 Chr5_28184289
Chr5_29545281
62,2 Chr5_30731904
63,1 Chr5_30939793
63,9 Chr5_31832962 Chr5_31164414
64,8 Chr5_31881687
C06
0,0 Chr6_2856132
0,9 Chr6_3182627 Chr6_3283900
1,7 Chr6_3680276 Chr6_3641835
2,6 Chr6_3969719 Chr6_4178528
Chr6_4015262 Chr6_3901045
Chr6_4817271 Chr6_4457141
3,4 Chr6_4574669 Chr6_4353231
Chr6_4957114
5,1 Chr6_5178781
6,0 Chr6_5682483 Chr6_5854818
Chr6_5424008 Chr6_5486384
Chr6_5939711
6,9 Chr6_6498283
Chr6_6573244 Chr6_9225564
7,7 Chr6_8732777 Chr6_6920863
Chr6_7486682 Chr6_6970077
Chr6_8803678 Chr6_9072158
Chr6_7054085
8,3 Chr6_9137183
8,6 Chr6_10994013 Chr6_11662772
Chr6_11726743 Chr6_11041586
Chr6_10701095
9,4 Chr6_11809222 Chr6_11944304
12,0 Chr6_12134789 Chr6_12062219
Chr6_12230762
12,9 Chr6_12461696
13,7 Chr6_12775486
16,4 Chr6_13373541 Chr6_13346607
17,2 Chr6_13432170 Chr6_13530741
18,9 Chr6_13668696 Chr6_14283601
26,2 Chr6_16277503 Chr6_15978346
Chr6_16010623
Chr6_16624507 Chr6_16736966
27,1 Chr6_16943126 Chr6_16980549
Chr6_16792497 Chr6_16564009
Chr6_16513750
27,9 Chr6_17061676
29,6 Chr6_17134972
30,5 Chr6_17603680 Chr6_17671422
32,2 Chr6_17786426
34,8 Chr6_18170854 Chr6_18555484
Chr6_18726327
35,7 Chr6_19116617 Chr6_19179731
37,4 Chr6_19439027
39,1 Chr6_19727540
40,0 Chr6_19926319 Chr6_20075959
41,7 Chr6_20622601 Chr6_20969019
46,1 Chr6_22145739 Chr6_22000851
Chr6_21934821
47,0 Chr6_22761627
47,9 Chr6_23462608 Chr6_23074823
Chr6_22998703
48,7 Chr6_23823551 Chr6_23865885

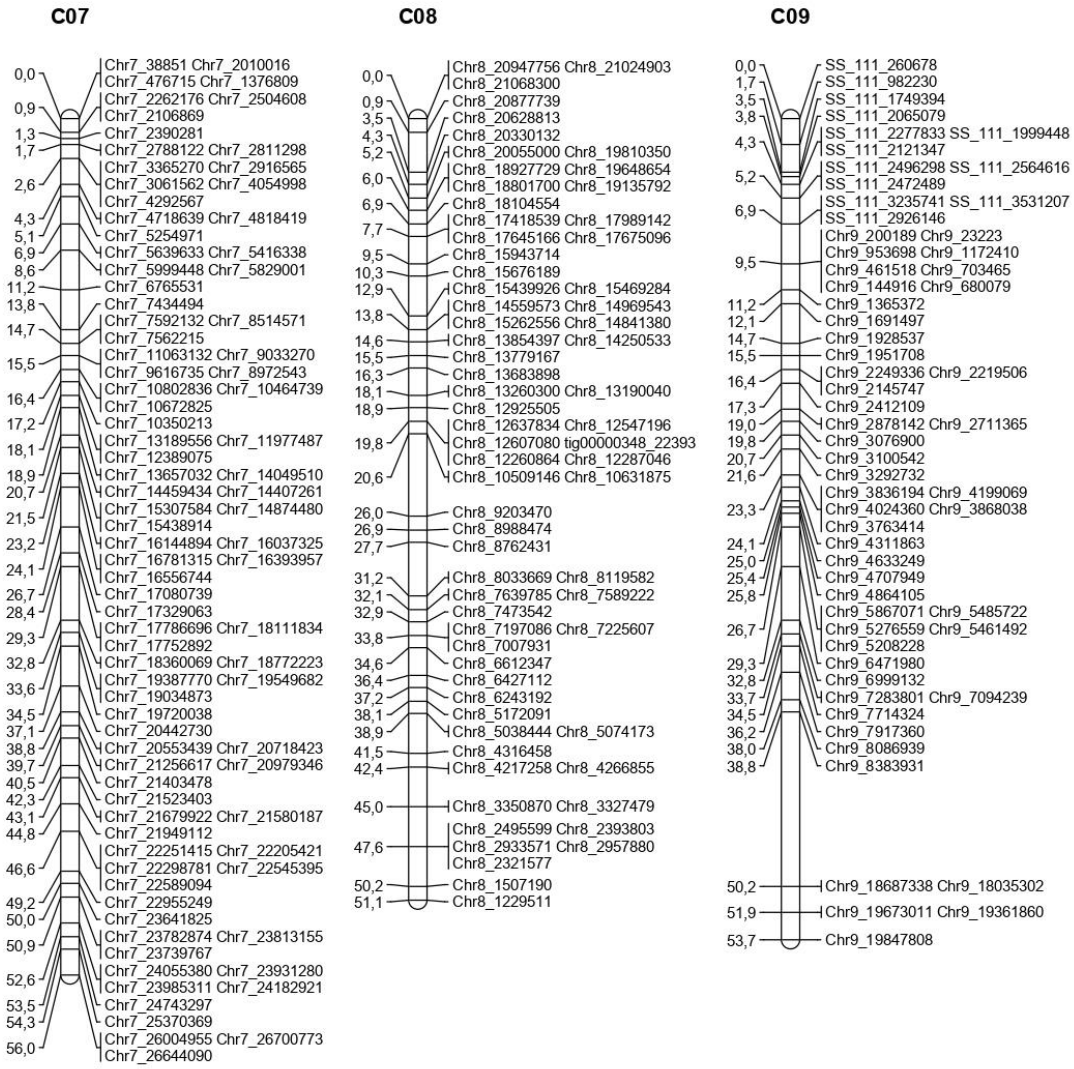
C07
0,0 Chr7_38851 Chr7_2010016
Chr7_476715 Chr7_1376809
0,9 Chr7_2262176 Chr7_2504608
Chr7_2106869
1,3 Chr7_2390281
1,7 Chr7_2788122 Chr7_2811298
2,6 Chr7_3365270 Chr7_2916565
Chr7_3061562 Chr7_4054998
Chr7_4292567
4,3 Chr7_4718639 Chr7_4818419
5,1 Chr7_5254971
6,9 Chr7_5639633 Chr7_5416338
8,6 Chr7_5999448 Chr7_5829001
11,2 Chr7_6765531
13,8 Chr7_7434494
14,7 Chr7_7592132 Chr7_8514571
Chr7_7562215
15,5 Chr7_11063132 Chr7_9033270
Chr7_9616735 Chr7_8972543
16,4 Chr7_10802836 Chr7_10464739
Chr7_10672825
17,2 Chr7_10350213
18,1 Chr7_13189556 Chr7_11977487
Chr7_12389075
18,9 Chr7_13657032 Chr7_14049510
20,7 Chr7_14459434 Chr7_14407261
21,5 Chr7_15307584 Chr7_14874480
Chr7_15438914
23,2 Chr7_16144894 Chr7_16037325
24,1 Chr7_16781315 Chr7_16393957
Chr7_16556744
26,7 Chr7_17080739
28,4 Chr7_17329063
29,3 Chr7_17786696 Chr7_18111834
Chr7_17752892
32,8 Chr7_18360069 Chr7_18772223
33,6 Chr7_19387770 Chr7_19549682
Chr7_19034873
34,5 Chr7_19720038
37,1 Chr7_20442730
38,8 Chr7_20553439 Chr7_20718423
39,7 Chr7_21256617 Chr7_20979346
40,5 Chr7_21403478
42,3 Chr7_21523403
43,1 Chr7_21679922 Chr7_21580187
44,8 Chr7_21949112
46,6 Chr7_22251415 Chr7_22205421
Chr7_22298781 Chr7_22545395
Chr7_22589094
49,2 Chr7_22955249
50,0 Chr7_23641825
50,9 Chr7_23782874 Chr7_23813155
Chr7_23739767
52,6 Chr7_24055380 Chr7_23931280
Chr7_23985311 Chr7_24182921
53,5 Chr7_24743297
54,3 Chr7_25370369
56,0 Chr7_26004955 Chr7_26700773
Chr7_26644090
C08
0,0 Chr8_20947756 Chr8_21024903
Chr8_21068300
0,9 Chr8_20877739
3,5 Chr8_20628813
4,3 Chr8_20330132
5,2 Chr8_20055000 Chr8_19810350
6,0 Chr8_18927729 Chr8_19648654
Chr8_18801700 Chr8_19135792
6,9 Chr8_18104554
7,7 Chr8_17418539 Chr8_17989142
Chr8_17645166 Chr8_17675096
9,5 Chr8_15943714
10,3 Chr8_15676189
12,9 Chr8_15439926 Chr8_15469284
13,8 Chr8_14559573 Chr8_14969543
Chr8_15262556 Chr8_14841380
14,6 Chr8_13854397 Chr8_14250533
15,5 Chr8_13779167
16,3 Chr8_13683898
18,1 Chr8_13260300 Chr8_13190040
18,9 Chr8_12925505
19,8 Chr8_12637834 Chr8_12547196
Chr8_12607080 tig00000348_22393
Chr8_12260864 Chr8_12287046
20,6 Chr8_10509146 Chr8_10631875
26,0 Chr8_9203470
26,9 Chr8_8988474
27,7 Chr8_8762431
31,2 Chr8_8033669 Chr8_8119582
32,1 Chr8_7639785 Chr8_7589222
32,9 Chr8_7473542
33,8 Chr8_7197086 Chr8_7225607
Chr8_7007931
34,6 Chr8_6612347
36,4 Chr8_6427112
37,2 Chr8_6243192
38,1 Chr8_5172091
38,9 Chr8_5038444 Chr8_5074173
41,5 Chr8_4316458
42,4 Chr8_4217258 Chr8_4266855
45,0 Chr8_3350870 Chr8_3327479
47,6 Chr8_2495599 Chr8_2393803
Chr8_2933571 Chr8_2957880
Chr8_2321577
50,2 Chr8_1507190
51,1 Chr8_1229511
C09
0,0 SS_111_260678
1,7 SS_111_982230
3,5 SS_111_1749394
3,8 SS_111_2065079
4,3 SS_111_2277833 SS_111_1999448
SS_111_2121347
5,2 SS_111_2496298 SS_111_2564616
SS_111_2472489
6,9 SS_111_3235741 SS_111_3531207
SS_111_2926146
Chr9_200189 Chr9_23223
9,5 Chr9_953698 Chr9_1172410
Chr9_461518 Chr9_703465
Chr9_144916 Chr9_680079
11,2 Chr9_1365372
12,1 Chr9_1691497
14,7 Chr9_1928537
15,5 Chr9_1951708
16,4 Chr9_2249336 Chr9_2219506
Chr9_2145747
17,3 Chr9_2412109
19,0 Chr9_2878142 Chr9_2711365
19,8 Chr9_3076900
20,7 Chr9_3100542
21,6 Chr9_3292732
23,3 Chr9_3836194 Chr9_4199069
Chr9_4024360 Chr9_3868038
Chr9_3763414
24,1 Chr9_4311863
25,0 Chr9_4633249
25,4 Chr9_4707949
25,8 Chr9_4864105
26,7 Chr9_5867071 Chr9_5485722
Chr9_5276559 Chr9_5461492
Chr9_5208228
29,3 Chr9_6471980
32,8 Chr9_6999132
33,7 Chr9_7283801 Chr9_7094239
34,5 Chr9_7714324
36,2 Chr9_7917360
38,0 Chr9_8086939
38,8 Chr9_8383931
50,2 Chr9_18687338 Chr9_18035302
51,9 Chr9_19673011 Chr9_19361860
53,7 Chr9_19847808

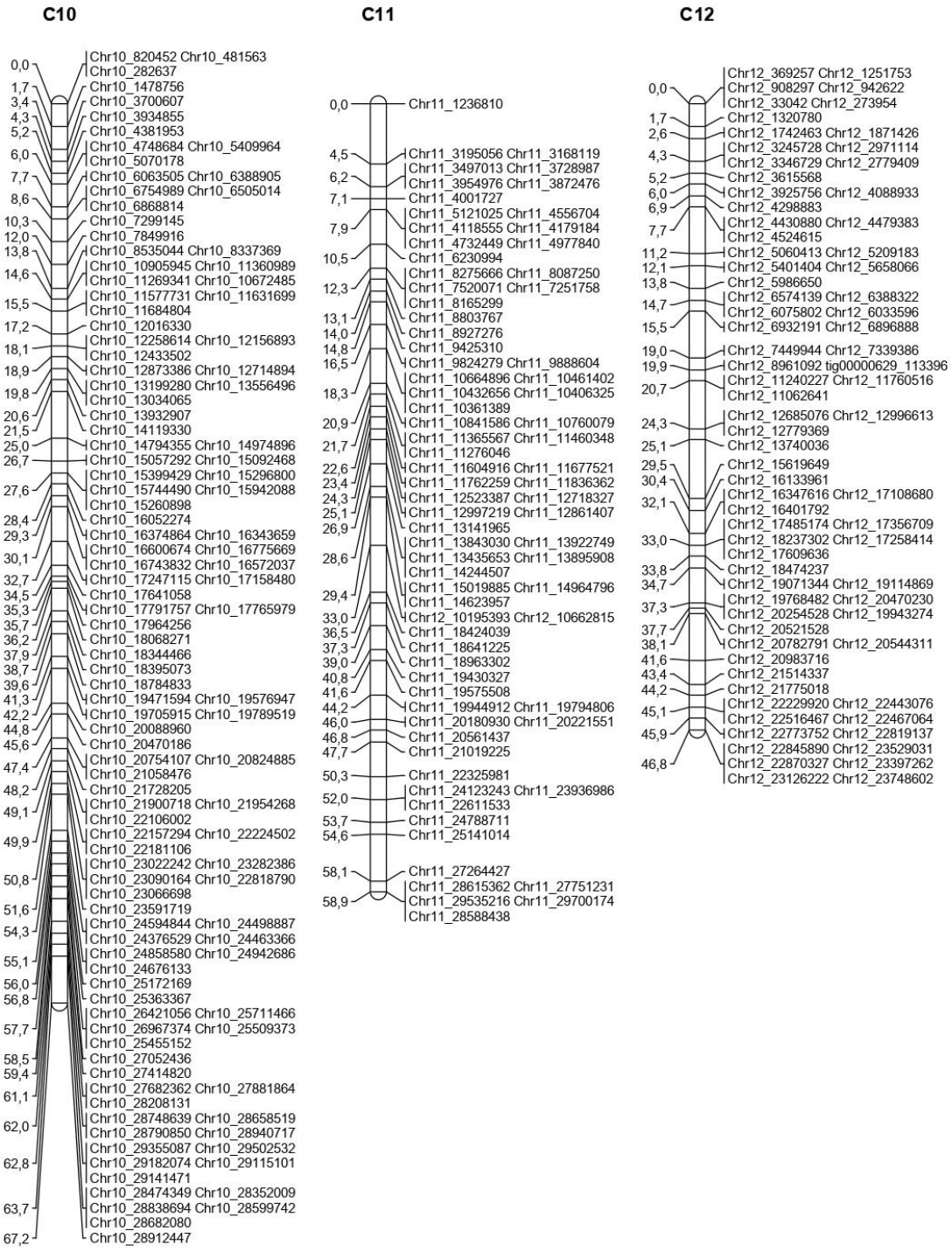
C10
0,0 Chr10_820452 Chr10_481563
1,7 Chr10_282637
3,4 Chr10_1478756
4,3 Chr10_3700607
5,2 Chr10_3934855
Chr10_4381953
6,0 Chr10_4748684 Chr10_5409964
Chr10_5070178
7,7 Chr10_6063505 Chr10_6388905
8,6 Chr10_6754989 Chr10_6505014
Chr10_6868814
10,3 Chr10_7299145
12,0 Chr10_7849916
13,8 Chr10_8535044 Chr10_8337369
14,6 Chr10_10905945 Chr10_11360989
Chr10_11269341 Chr10_10672485
15,5 Chr10_11577731 Chr10_11631699
Chr10_11684804
17,2 Chr10_12016330
18,1 Chr10_12258614 Chr10_12156893
Chr10_12433502
18,9 Chr10_12873386 Chr10_12714894
19,8 Chr10_13199280 Chr10_13556496
Chr10_13034065
20,6 Chr10_13932907
21,5 Chr10_14119330
25,0 Chr10_14794355 Chr10_14974896
26,7 Chr10_15057292 Chr10_15092468
Chr10_15399429 Chr10_15296800
27,6 Chr10_15744490 Chr10_15942088
Chr10_15260898
28,4 Chr10_16052274
29,3 Chr10_16374864 Chr10_16343659
Chr10_16600674 Chr10_16775669
30,1 Chr10_16743832 Chr10_16572037
32,7 Chr10_17247115 Chr10_17158480
34,5 Chr10_17641058
35,3 Chr10_17791757 Chr10_17765979
35,7 Chr10_17964256
36,2 Chr10_18068271
37,9 Chr10_18344466
38,7 Chr10_18395073
39,6 Chr10_18784833
41,3 Chr10_19471594 Chr10_19576947
42,2 Chr10_19705915 Chr10_19789519
44,8 Chr10_20088960
45,6 Chr10_20470186
47,4 Chr10_20754107 Chr10_20824885
Chr10_21058476
48,2 Chr10_21728205
49,1 Chr10_21900718 Chr10_21954268
Chr10_22106002
49,9 Chr10_22157294 Chr10_22224502
Chr10_22181106
Chr10_23022242 Chr10_23282386
50,8 Chr10_23090164 Chr10_22818790
Chr10_23066698
51,6 Chr10_23591719
54,3 Chr10_24594844 Chr10_24498887
Chr10_24376529 Chr10_24463366
55,1 Chr10_24858580 Chr10_24942686
Chr10_24676133
56,0 Chr10_25172169
56,8 Chr10_25363367
Chr10_26421056 Chr10_25711466
57,7 Chr10_26967374 Chr10_25509373
Chr10_25455152
58,5 Chr10_27052436
59,4 Chr10_27414820
61,1 Chr10_27682362 Chr10_27881864
Chr10_28208131
62,0 Chr10_28748639 Chr10_28658519
Chr10_28790850 Chr10_28940717
Chr10_29355087 Chr10_29502532
62,8 Chr10_29182074 Chr10_29115101
Chr10_29141471
Chr10_28474349 Chr10_28352009
63,7 Chr10_28838694 Chr10_28599742
Chr10_28682080
67,2 Chr10_28912447
C11
0,0 Chr11_1236810
4,5 Chr11_3195056 Chr11_3168119
6,2 Chr11_3497013 Chr11_3728987
Chr11_3954976 Chr11_3872476
7,1 Chr11_4001727
Chr11_5121025 Chr11_4556704
7,9 Chr11_4118555 Chr11_4179184
Chr11_4732449 Chr11_4977840
10,5 Chr11_6230994
Chr11_8275666 Chr11_8087250
12,3 Chr11_7520071 Chr11_7251758
Chr11_8165299
13,1 Chr11_8803767
14,0 Chr11_8927276
14,8 Chr11_9425310
16,5 Chr11_9824279 Chr11_9888604
Chr11_10664896 Chr11_10461402
18,3 Chr11_10432656 Chr11_10406325
Chr11_10361389
20,9 Chr11_10841586 Chr11_10760079
21,7 Chr11_11365567 Chr11_11460348
Chr11_11276046
22,6 Chr11_11604916 Chr11_11677521
23,4 Chr11_11762259 Chr11_11836362
24,3 Chr11_12523387 Chr11_12718327
25,1 Chr11_12997219 Chr11_12861407
26,9 Chr11_13141965
Chr11_13843030 Chr11_13922749
28,6 Chr11_13435653 Chr11_13895908
Chr11_14244507
Chr11_15019885 Chr11_14964796
29,4 Chr11_14623957
33,0 Chr12_10195393 Chr12_10662815
36,5 Chr11_18424039
37,3 Chr11_18641225
39,0 Chr11_18963302
40,8 Chr11_19430327
41,6 Chr11_19575508
44,2 Chr11_19944912 Chr11_19794806
46,0 Chr11_20180930 Chr11_20221551
46,8 Chr11_20561437
47,7 Chr11_21019225
50,3 Chr11_22325981
52,0 Chr11_24123243 Chr11_23936986
Chr11_22611533
53,7 Chr11_24788711
54,6 Chr11_25141014
58,1 Chr11_27264427
Chr11_28615362 Chr11_27751231
58,9 Chr11_29535216 Chr11_29700174
Chr11_28588438
C12
Chr12_369257 Chr12_1251753
0,0 Chr12_908297 Chr12_942622
Chr12_33042 Chr12_273954
1,7 Chr12_1320780
2,6 Chr12_1742463 Chr12_1871426
4,3 Chr12_3245728 Chr12_2971114
Chr12_3346729 Chr12_2779409
5,2 Chr12_3615568
6,0 Chr12_3925756 Chr12_4088933
6,9 Chr12_4298883
7,7 Chr12_4430880 Chr12_4479383
Chr12_4524615
11,2 Chr12_5060413 Chr12_5209183
12,1 Chr12_5401404 Chr12_5658066
13,8 Chr12_5986650
14,7 Chr12_6574139 Chr12_6388322
Chr12_6075802 Chr12_6033596
15,5 Chr12_6932191 Chr12_6896888
19,0 Chr12_7449944 Chr12_7339386
19,9 Chr12_8961092 tig00000629_113396
20,7 Chr12_11240227 Chr12_11760516
Chr12_11062641
24,3 Chr12_12685076 Chr12_12996613
Chr12_12779369
25,1 Chr12_13740036
29,5 Chr12_15619649
30,4 Chr12_16133961
32,1 Chr12_16347616 Chr12_17108680
Chr12_16401792
Chr12_17485174 Chr12_17356709
33,0 Chr12_18237302 Chr12_17258414
Chr12_17609636
33,8 Chr12_18474237
34,7 Chr12_19071344 Chr12_19114869
37,3 Chr12_19768482 Chr12_20470230
Chr12_20254528 Chr12_19943274
37,7 Chr12_20521528
38,1 Chr12_20782791 Chr12_20544311
41,6 Chr12_20983716
43,4 Chr12_21514337
44,2 Chr12_21775018
45,1 Chr12_22229920 Chr12_22443076
Chr12_22516467 Chr12_22467064
45,9 Chr12_22773752 Chr12_22819137
Chr12_22845890 Chr12_23529031
46,8 Chr12_22870327 Chr12_23397262
Chr12_23126222 Chr12_23748602

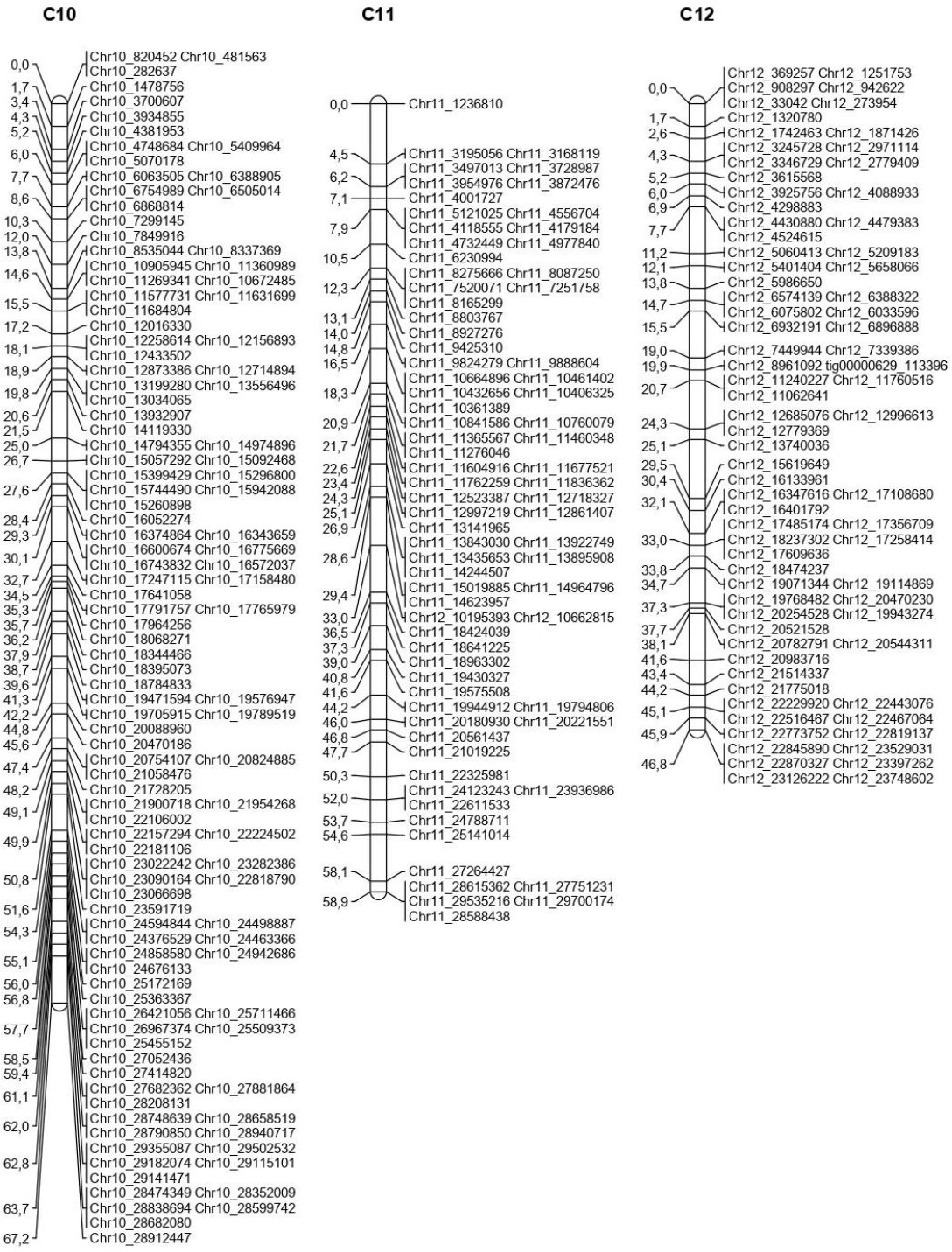
C10
0,0 Chr10_820452 Chr10_481563
1,7 Chr10_282637
3,4 Chr10_1478756
4,3 Chr10_3700607
5,2 Chr10_3934855
6,0 Chr10_4381953
7,7 Chr10_4748684 Chr10_5409964
8,6 Chr10_5070178
10,3 Chr10_6063505 Chr10_6388905
12,0 Chr10_6754989 Chr10_6505014
13,8 Chr10_6868814
14,6 Chr10_7299145
15,5 Chr10_7849916
17,2 Chr10_8535044 Chr10_8337369
18,1 Chr10_10905945 Chr10_11360989
18,9 Chr10_11269341 Chr10_10672485
19,8 Chr10_11577731 Chr10_11631699
20,6 Chr10_11684804
21,5 Chr10_12016330
25,0 Chr10_12258614 Chr10_12156893
26,7 Chr10_12433502
27,6 Chr10_12873386 Chr10_12714894
28,4 Chr10_13199280 Chr10_13556496
29,3 Chr10_13034065
30,1 Chr10_13932907
32,7 Chr10_14119330
34,5 Chr10_14794355 Chr10_14974896
35,3 Chr10_15057292 Chr10_15092468
35,7 Chr10_15399429 Chr10_15296800
36,2 Chr10_15744490 Chr10_15942088
37,9 Chr10_15260898
38,7 Chr10_16052274
39,6 Chr10_16374864 Chr10_16343659
41,3 Chr10_16600674 Chr10_16775669
42,2 Chr10_16743832 Chr10_16572037
44,8 Chr10_17247115 Chr10_17158480
45,6 Chr10_17641058
47,4 Chr10_17791757 Chr10_17765979
48,2 Chr10_17964256
49,1 Chr10_18068271
49,9 Chr10_18344466
50,8 Chr10_18395073
51,6 Chr10_18784833
54,3 Chr10_19471594 Chr10_19576947
55,1 Chr10_19705915 Chr10_19789519
56,0 Chr10_20088960
56,8 Chr10_20470186
57,7 Chr10_20754107 Chr10_20824885
58,5 Chr10_21058476
59,4 Chr10_21728205
61,1 Chr10_21900718 Chr10_21954268
62,0 Chr10_22106002
62,8 Chr10_22157294 Chr10_22224502
63,7 Chr10_22181106
67,2 Chr10_23022242 Chr10_23282386
Chr10_23090164 Chr10_22818790
Chr10_23066698
Chr10_23591719
Chr10_24594844 Chr10_24498887
Chr10_24376529 Chr10_24463366
Chr10_24858580 Chr10_24942686
Chr10_24676133
Chr10_25172169
Chr10_25363367
Chr10_26421056 Chr10_25711466
Chr10_26967374 Chr10_25509373
Chr10_25455152
Chr10_27052436
Chr10_27414820
Chr10_27682362 Chr10_27881864
Chr10_28208131
Chr10_28748639 Chr10_28658519
Chr10_28790850 Chr10_28940717
Chr10_29355087 Chr10_29502532
Chr10_29182074 Chr10_29115101
Chr10_29141471
Chr10_28474349 Chr10_28352009
Chr10_28838694 Chr10_28599742
Chr10_28682080
Chr10_28912447
C11
0,0 Chr11_1236810
4,5 Chr11_3195056 Chr11_3168119
6,2 Chr11_3497013 Chr11_3728987
7,1 Chr11_3954976 Chr11_3872476
7,9 Chr11_4001727
10,5 Chr11_5121025 Chr11_4556704
12,3 Chr11_4118555 Chr11_4179184
13,1 Chr11_4732449 Chr11_4977840
14,0 Chr11_6230994
14,8 Chr11_8275666 Chr11_8087250
16,5 Chr11_7520071 Chr11_7251758
18,3 Chr11_8165299
20,9 Chr11_8803767
21,7 Chr11_8927276
22,6 Chr11_9425310
23,4 Chr11_9824279 Chr11_9888604
24,3 Chr11_10664896 Chr11_10461402
25,1 Chr11_10432656 Chr11_10406325
26,9 Chr11_10361389
28,6 Chr11_10841586 Chr11_10760079
29,4 Chr11_11365567 Chr11_11460348
33,0 Chr11_11276046
36,5 Chr11_11604916 Chr11_11677521
37,3 Chr11_11762259 Chr11_11836362
39,0 Chr11_12523387 Chr11_12718327
40,8 Chr11_12997219 Chr11_12861407
41,6 Chr11_13141965
44,2 Chr11_13843030 Chr11_13922749
46,0 Chr11_13435653 Chr11_13895908
46,8 Chr11_14244507
47,7 Chr11_15019885 Chr11_14964796
50,3 Chr11_14623957
52,0 Chr12_10195393 Chr12_10662815
53,7 Chr11_18424039
54,6 Chr11_18641225
58,1 Chr11_18963302
58,9 Chr11_19430327
Chr11_19575508
Chr11_19944912 Chr11_19794806
Chr11_20180930 Chr11_20221551
Chr11_20561437
Chr11_21019225
Chr11_22325981
Chr11_24123243 Chr11_23936986
Chr11_22611533
Chr11_24788711
Chr11_25141014
Chr11_27264427
Chr11_28615362 Chr11_27751231
Chr11_29535216 Chr11_29700174
Chr11_28588438
C12
0,0 Chr12_369257 Chr12_1251753
1,7 Chr12_908297 Chr12_942622
2,6 Chr12_33042 Chr12_273954
4,3 Chr12_1320780
5,2 Chr12_1742463 Chr12_1871426
6,0 Chr12_3245728 Chr12_2971114
6,9 Chr12_3346729 Chr12_2779409
7,7 Chr12_3615568
11,2 Chr12_3925756 Chr12_4088933
12,1 Chr12_4298883
13,8 Chr12_4430880 Chr12_4479383
14,7 Chr12_4524615
15,5 Chr12_5060413 Chr12_5209183
19,0 Chr12_5401404 Chr12_5658066
19,9 Chr12_5986650
20,7 Chr12_6574139 Chr12_6388322
24,3 Chr12_6075802 Chr12_6033596
25,1 Chr12_6932191 Chr12_6896888
29,5 Chr12_7449944 Chr12_7339386
30,4 Chr12_8961092 tig00000629_113396
32,1 Chr12_11240227 Chr12_11760516
33,0 Chr12_11062641
33,8 Chr12_12685076 Chr12_12996613
34,7 Chr12_12779369
37,3 Chr12_13740036
37,7 Chr12_15619649
38,1 Chr12_16133961
41,6 Chr12_16347616 Chr12_17108680
43,4 Chr12_16401792
44,2 Chr12_17485174 Chr12_17356709
45,1 Chr12_18237302 Chr12_17258414
45,9 Chr12_17609636
46,8 Chr12_18474237
Chr12_19071344 Chr12_19114869
Chr12_19768482 Chr12_20470230
Chr12_20254528 Chr12_19943274
Chr12_20521528
Chr12_20782791 Chr12_20544311
Chr12_20983716
Chr12_21514337
Chr12_21775018
Chr12_22229920 Chr12_22443076
Chr12_22516467 Chr12_22467064
Chr12_22773752 Chr12_22819137
Chr12_22845890 Chr12_23529031
Chr12_22870327 Chr12_23397262
Chr12_23126222 Chr12_23748602

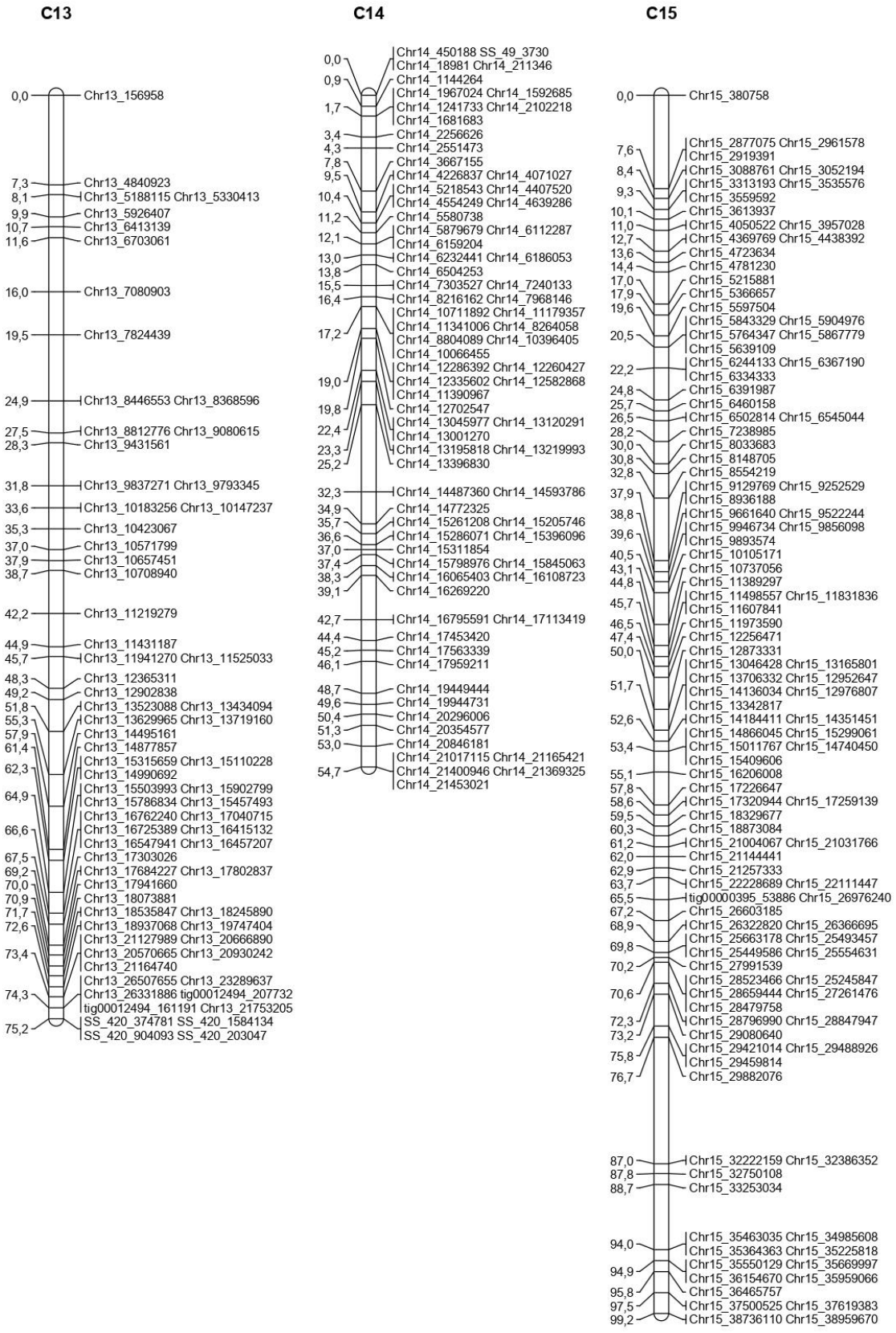
C13
0,0 Chr13_156958
7,3 Chr13_4840923
8,1 Chr13_5188115 Chr13_5330413
9,9 Chr13_5926407
10,7 Chr13_6413139
11,6 Chr13_6703061
16,0 Chr13_7080903
19,5 Chr13_7824439
24,9 Chr13_8446553 Chr13_8368596
27,5 Chr13_8812776 Chr13_9080615
28,3 Chr13_9431561
31,8 Chr13_9837271 Chr13_9793345
33,6 Chr13_10183256 Chr13_10147237
35,3 Chr13_10423067
37,0 Chr13_10571799
37,9 Chr13_10657451
38,7 Chr13_10708940
42,2 Chr13_11219279
44,9 Chr13_11431187
45,7 Chr13_11941270 Chr13_11525033
48,3 Chr13_12365311
49,2 Chr13_12902838
51,8 Chr13_13523088 Chr13_13434094
55,3 Chr13_13629965 Chr13_13719160
57,9 Chr13_14495161
61,4 Chr13_14877857
62,3 Chr13_15315659 Chr13_15110228
Chr13_14990692
64,9 Chr13_15503993 Chr13_15902799
Chr13_15786834 Chr13_15457493
Chr13_16762240 Chr13_17040715
66,6 Chr13_16725389 Chr13_16415132
Chr13_16547941 Chr13_16457207
67,5 Chr13_17303026
69,2 Chr13_17684227 Chr13_17802837
70,0 Chr13_17941660
70,9 Chr13_18073881
71,7 Chr13_18535847 Chr13_18245890
72,6 Chr13_18937068 Chr13_19747404
Chr13_21127989 Chr13_20666890
73,4 Chr13_20570665 Chr13_20930242
Chr13_21164740
Chr13_26507655 Chr13_23289637
74,3 Chr13_26331886 tig00012494_207732
tig00012494_161191 Chr13_21753205
75,2 SS_420_374781 SS_420_1584134
SS_420_904093 SS_420_203047
C14
0,0 Chr14_450188 SS_49_3730
Chr14_18981 Chr14_211346
0,9 Chr14_1144264
Chr14_1967024 Chr14_1592685
1,7 Chr14_1241733 Chr14_2102218
Chr14_1681683
3,4 Chr14_2256626
4,3 Chr14_2551473
7,8 Chr14_3667155
9,5 Chr14_4226837 Chr14_4071027
10,4 Chr14_5218543 Chr14_4407520
Chr14_4554249 Chr14_4639286
11,2 Chr14_5580738
12,1 Chr14_5879679 Chr14_6112287
Chr14_6159204
13,0 Chr14_6232441 Chr14_6186053
13,8 Chr14_6504253
15,5 Chr14_7303527 Chr14_7240133
16,4 Chr14_8216162 Chr14_7968146
Chr14_10711892 Chr14_11179357
17,2 Chr14_11341006 Chr14_8264058
Chr14_8804089 Chr14_10396405
Chr14_10066455
Chr14_12286392 Chr14_12260427
19,0 Chr14_12335602 Chr14_12582868
Chr14_11390967
19,8 Chr14_12702547
Chr14_13045977 Chr14_13120291
22,4 Chr14_13001270
23,3 Chr14_13195818 Chr14_13219993
25,2 Chr14_13396830
32,3 Chr14_14487360 Chr14_14593786
34,9 Chr14_14772325
35,7 Chr14_15261208 Chr14_15205746
36,6 Chr14_15286071 Chr14_15396096
37,0 Chr14_15311854
37,4 Chr14_15798976 Chr14_15845063
38,3 Chr14_16065403 Chr14_16108723
39,1 Chr14_16269220
42,7 Chr14_16795591 Chr14_17113419
44,4 Chr14_17453420
45,2 Chr14_17563339
46,1 Chr14_17959211
48,7 Chr14_19449444
49,6 Chr14_19944731
50,4 Chr14_20296006
51,3 Chr14_20354577
53,0 Chr14_20846181
Chr14_21017115 Chr14_21165421
54,7 Chr14_21400946 Chr14_21369325
Chr14_21453021
C15
0,0 Chr15_380758
Chr15_2877075 Chr15_2961578
7,6 Chr15_2919391
8,4 Chr15_3088761 Chr15_3052194
Chr15_3313193 Chr15_3535576
9,3 Chr15_3559592
10,1 Chr15_3613937
11,0 Chr15_4050522 Chr15_3957028
12,7 Chr15_4369769 Chr15_4438392
13,6 Chr15_4723634
14,4 Chr15_4781230
17,0 Chr15_5215881
17,9 Chr15_5366657
19,6 Chr15_5597504
Chr15_5843329 Chr15_5904976
20,5 Chr15_5764347 Chr15_5867779
Chr15_5639109
Chr15_6244133 Chr15_6367190
22,2 Chr15_6334333
24,8 Chr15_6391987
25,7 Chr15_6460158
26,5 Chr15_6502814 Chr15_6545044
28,2 Chr15_7238985
30,0 Chr15_8033683
30,8 Chr15_8148705
32,8 Chr15_8554219
Chr15_9129769 Chr15_9252529
37,9 Chr15_8936188
38,8 Chr15_9661640 Chr15_9522244
Chr15_9946734 Chr15_9856098
39,6 Chr15_9893574
40,5 Chr15_10105171
43,1 Chr15_10737056
44,8 Chr15_11389297
Chr15_11498557 Chr15_11831836
45,7 Chr15_11607841
46,5 Chr15_11973590
47,4 Chr15_12256471
50,0 Chr15_12873331
Chr15_13046428 Chr15_13165801
Chr15_13706332 Chr15_12952647
51,7 Chr15_14136034 Chr15_12976807
Chr15_13342817
52,6 Chr15_14184411 Chr15_14351451
Chr15_14866045 Chr15_15299061
53,4 Chr15_15011767 Chr15_14740450
Chr15_15409606
55,1 Chr15_16206008
57,8 Chr15_17226647
58,6 Chr15_17320944 Chr15_17259139
59,5 Chr15_18329677
60,3 Chr15_18873084
61,2 Chr15_21004067 Chr15_21031766
62,0 Chr15_21144441
62,9 Chr15_21257333
63,7 Chr15_22228689 Chr15_22111447
65,5 tig00000395_53886 Chr15_26976240
67,2 Chr15_26603185
68,9 Chr15_26322820 Chr15_26366695
Chr15_25663178 Chr15_25493457
69,8 Chr15_25449586 Chr15_25554631
70,2 Chr15_27991539
Chr15_28523466 Chr15_25245847
70,6 Chr15_28659444 Chr15_27261476
Chr15_28479758
72,3 Chr15_28796990 Chr15_28847947
73,2 Chr15_29080640
Chr15_29421014 Chr15_29488926
75,8 Chr15_29459814
76,7 Chr15_29882076
87,0 Chr15_32222159 Chr15_32386352
87,8 Chr15_32750108
88,7 Chr15_33253034
94,0 Chr15_35463035 Chr15_34985608
Chr15_35364363 Chr15_35225818
94,9 Chr15_35550129 Chr15_35669997
Chr15_36154670 Chr15_35959066
95,8 Chr15_36465757
97,5 Chr15_37500525 Chr15_37619383
99,2 Chr15_38736110 Chr15_38959670

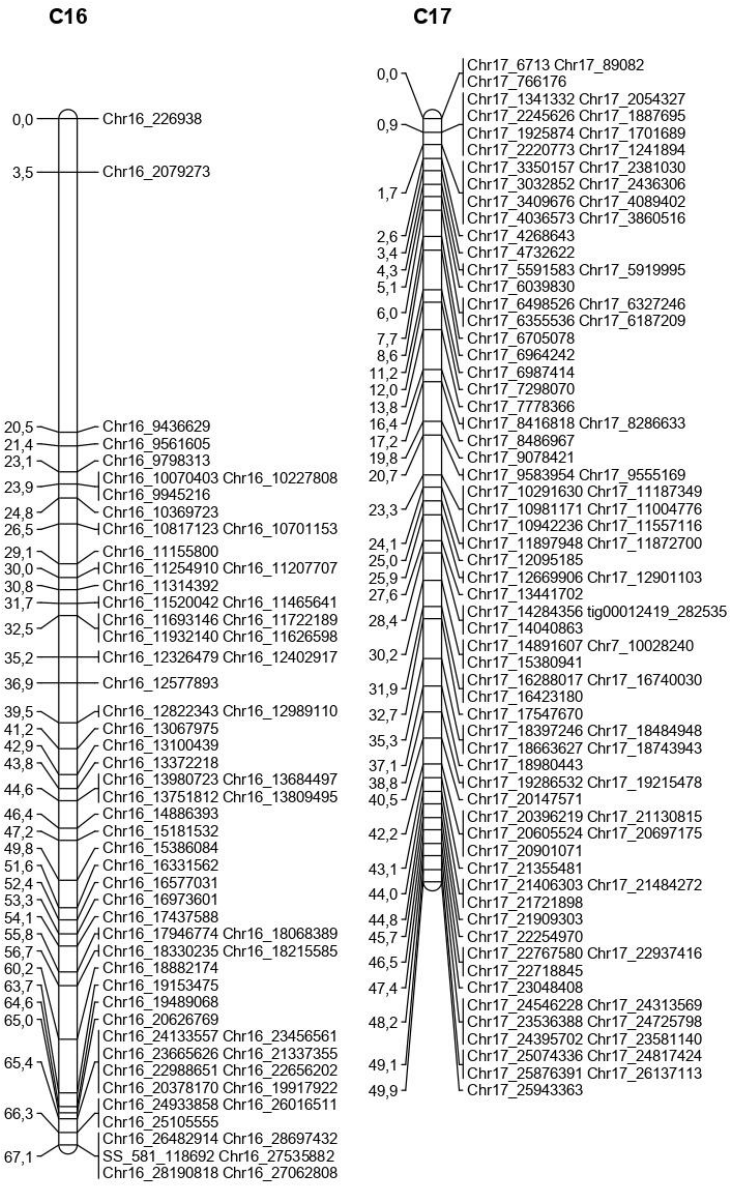
C16
C17
0,0 Chr16_226938
3,5 Chr16_2079273
20,5 Chr16_9436629
21,4 Chr16_9561605
23,1 Chr16_9798313
23,9 Chr16_10070403 Chr16_10227808
Chr16_9945216
24,8 Chr16_10369723
26,5 Chr16_10817123 Chr16_10701153
29,1 Chr16_11155800
30,0 Chr16_11254910 Chr16_11207707
30,8 Chr16_11314392
31,7 Chr16_11520042 Chr16_11465641
32,5 Chr16_11693146 Chr16_11722189
Chr16_11932140 Chr16_11626598
35,2 Chr16_12326479 Chr16_12402917
36,9 Chr16_12577893
39,5 Chr16_12822343 Chr16_12989110
41,2 Chr16_13067975
42,9 Chr16_13100439
43,8 Chr16_13372218
44,6 Chr16_13980723 Chr16_13684497
Chr16_13751812 Chr16_13809495
46,4 Chr16_14886393
47,2 Chr16_15181532
49,8 Chr16_15386084
51,6 Chr16_16331562
52,4 Chr16_16577031
53,3 Chr16_16973601
54,1 Chr16_17437588
55,8 Chr16_17946774 Chr16_18068389
56,7 Chr16_18330235 Chr16_18215585
60,2 Chr16_18882174
63,7 Chr16_19153475
64,6 Chr16_19489068
65,0 Chr16_20626769
65,4 Chr16_24133557 Chr16_23456561
Chr16_23665626 Chr16_21337355
Chr16_22988651 Chr16_22656202
Chr16_20378170 Chr16_19917922
66,3 Chr16_24933858 Chr16_26016511
Chr16_25105555
67,1 Chr16_26482914 Chr16_28697432
SS_581_118692 Chr16_27535882
Chr16_28190818 Chr16_27062808
0,0 Chr17_6713 Chr17_89082
Chr17_766176
0,9 Chr17_1341332 Chr17_2054327
Chr17_2245626 Chr17_1887695
Chr17_1925874 Chr17_1701689
Chr17_2220773 Chr17_1241894
1,7 Chr17_3350157 Chr17_2381030
Chr17_3032852 Chr17_2436306
Chr17_3409676 Chr17_4089402
Chr17_4036573 Chr17_3860516
2,6 Chr17_4268643
3,4 Chr17_4732622
4,3 Chr17_5591583 Chr17_5919995
5,1 Chr17_6039830
6,0 Chr17_6498526 Chr17_6327246
Chr17_6355536 Chr17_6187209
7,7 Chr17_6705078
8,6 Chr17_6964242
11,2 Chr17_6987414
12,0 Chr17_7298070
13,8 Chr17_7778366
16,4 Chr17_8416818 Chr17_8286633
17,2 Chr17_8486967
19,8 Chr17_9078421
20,7 Chr17_9583954 Chr17_9555169
23,3 Chr17_10291630 Chr17_11187349
Chr17_10981171 Chr17_11004776
Chr17_10942236 Chr17_11557116
24,1 Chr17_11897948 Chr17_11872700
25,0 Chr17_12095185
25,9 Chr17_12669906 Chr17_12901103
27,6 Chr17_13441702
28,4 Chr17_14284356 tig00012419_282535
Chr17_14040863
30,2 Chr17_14891607 Chr7_10028240
Chr17_15380941
31,9 Chr17_16288017 Chr17_16740030
Chr17_16423180
32,7 Chr17_17547670
35,3 Chr17_18397246 Chr17_18484948
37,1 Chr17_18663627 Chr17_18743943
Chr17_18980443
38,8 Chr17_19286532 Chr17_19215478
40,5 Chr17_20147571
42,2 Chr17_20396219 Chr17_21130815
Chr17_20605524 Chr17_20697175
Chr17_20901071
43,1 Chr17_21355481
44,0 Chr17_21406303 Chr17_21484272
Chr17_21721898
44,8 Chr17_21909303
45,7 Chr17_22254970
46,5 Chr17_22767580 Chr17_22937416
Chr17_22718845
47,4 Chr17_23048408
48,2 Chr17_24546228 Chr17_24313569
Chr17_23536388 Chr17_24725798
Chr17_24395702 Chr17_23581140
49,1 Chr17_25074336 Chr17_24817424
Chr17_25876391 Chr17_26137113
49,9 Chr17_25943363

1.2. Linkage groups of Cocomerina Precoce

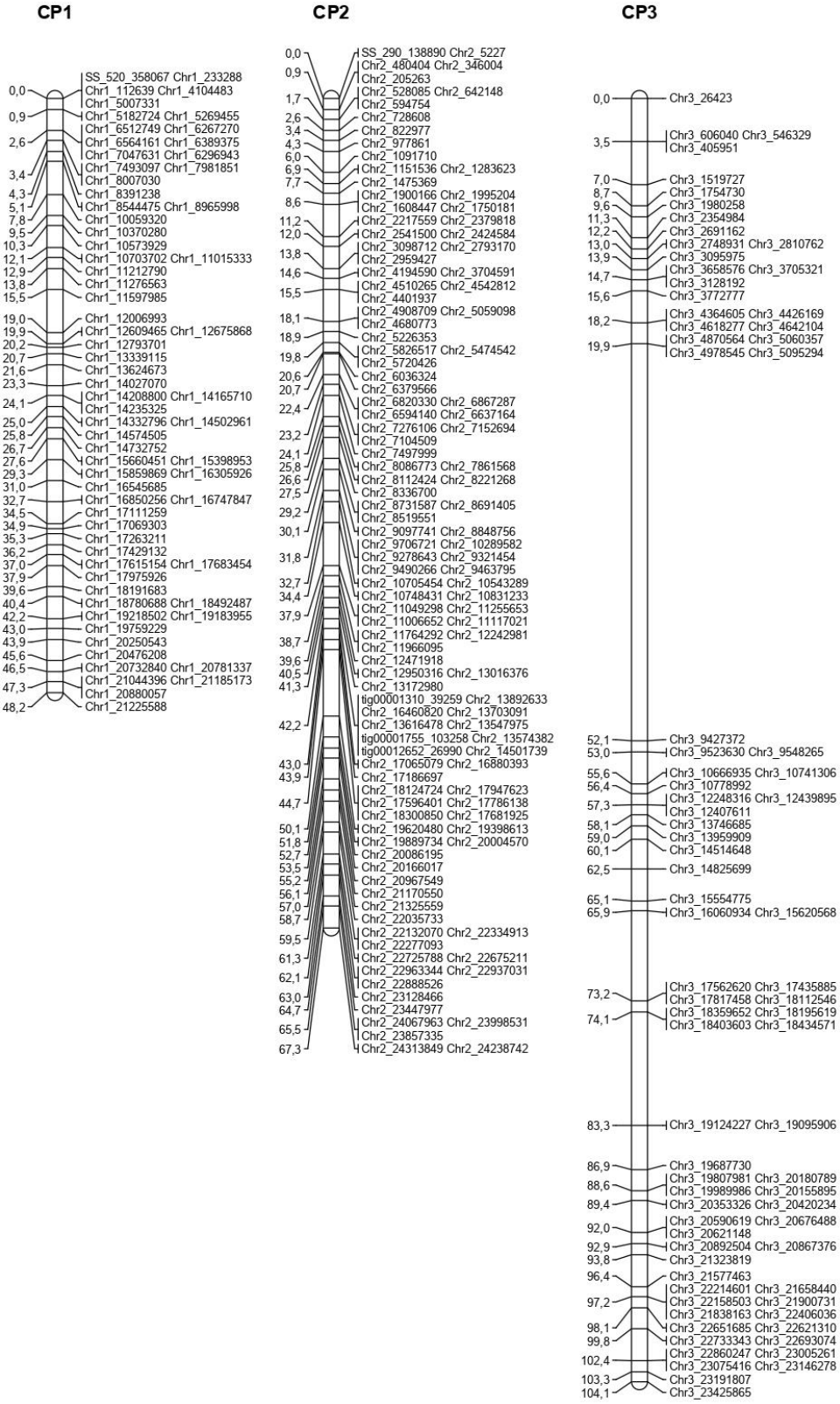

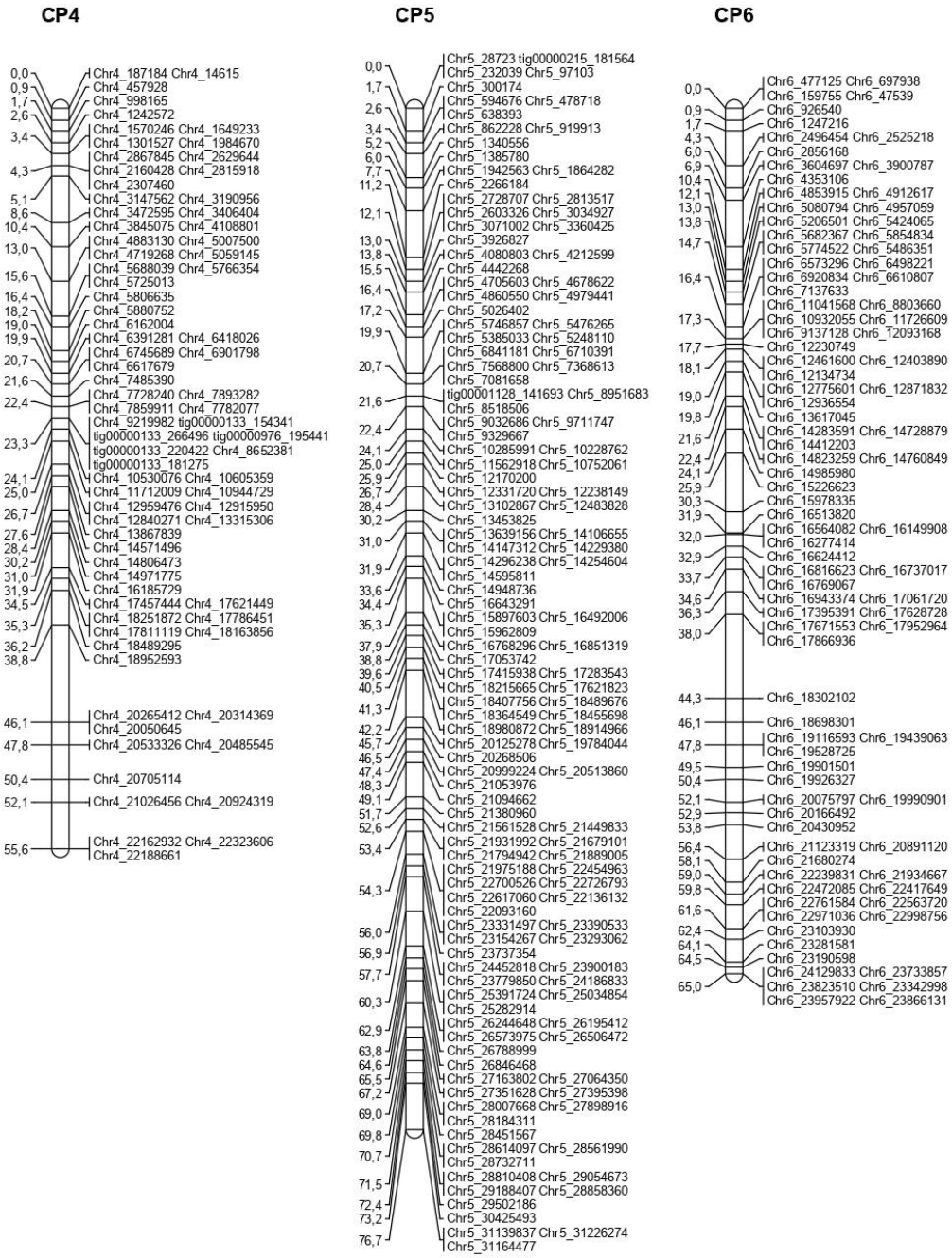
CP4
0,0 Chr4_187184 Chr4_14615
0,9 Chr4_457928
1,7 Chr4_998165
2,6 Chr4_1242572
3,4 Chr4_1570246 Chr4_1649233
Chr4_1301527 Chr4_1984670
Chr4_2867845 Chr4_2629644
4,3 Chr4_2160428 Chr4_2815918
Chr4_2307460
5,1 Chr4_3147562 Chr4_3190956
8,6 Chr4_3472595 Chr4_3406404
10,4 Chr4_3845075 Chr4_4108801
13,0 Chr4_4883130 Chr4_5007500
Chr4_4719268 Chr4_5059145
15,6 Chr4_5688039 Chr4_5766354
Chr4_5725013
16,4 Chr4_5806635
18,2 Chr4_5880752
19,0 Chr4_6162004
19,9 Chr4_6391281 Chr4_6418026
20,7 Chr4_6745689 Chr4_6901798
Chr4_6617679
21,6 Chr4_7485390
22,4 Chr4_7728240 Chr4_7893282
Chr4_7859911 Chr4_7782077
Chr4_9219982 tig00000133_154341
23,3 tig00000133_266496 tig00000976_195441
tig00000133_220422 Chr4_8652381
tig00000133_181275
24,1 Chr4_10530076 Chr4_10605359
25,0 Chr4_11712009 Chr4_10944729
26,7 Chr4_12959476 Chr4_12915950
Chr4_12840271 Chr4_13315306
27,6 Chr4_13867839
28,4 Chr4_14571496
30,2 Chr4_14806473
31,0 Chr4_14971775
31,9 Chr4_16185729
34,5 Chr4_17457444 Chr4_17621449
35,3 Chr4_18251872 Chr4_17786451
Chr4_17811119 Chr4_18163856
36,2 Chr4_18489295
38,8 Chr4_18952593
46,1 Chr4_20265412 Chr4_20314369
Chr4_20050645
47,8 Chr4_20533326 Chr4_20485545
50,4 Chr4_20705114
52,1 Chr4_21026456 Chr4_20924319
55,6 Chr4_22162932 Chr4_22323606
Chr4_22188661
CP5
0,0 Chr5_28723 tig00000215_181564
Chr5_232039 Chr5_97103
1,7 Chr5_300174
2,6 Chr5_594676 Chr5_478718
3,4 Chr5_638393
5,2 Chr5_862228 Chr5_919913
6,0 Chr5_1340556
7,7 Chr5_1385780
11,2 Chr5_1942563 Chr5_1864282
Chr5_2266184
12,1 Chr5_2728707 Chr5_2813517
Chr5_2603326 Chr5_3034927
Chr5_3071002 Chr5_3360425
13,0 Chr5_3926827
13,8 Chr5_4080803 Chr5_4212599
15,5 Chr5_4442268
16,4 Chr5_4705603 Chr5_4678622
17,2 Chr5_4860550 Chr5_4979441
Chr5_5026402
19,9 Chr5_5746857 Chr5_5476265
Chr5_5385033 Chr5_5248110
20,7 Chr5_6841181 Chr5_6710391
Chr5_7568800 Chr5_7368613
Chr5_7081658
21,6 tig00001128_141693 Chr5_8951683
Chr5_8518506
22,4 Chr5_9032686 Chr5_9711747
Chr5_9329667
24,1 Chr5_10285991 Chr5_10228762
25,0 Chr5_11562918 Chr5_10752061
25,9 Chr5_12170200
26,7 Chr5_12331720 Chr5_12238149
28,4 Chr5_13102867 Chr5_12483828
30,2 Chr5_13453825
31,0 Chr5_13639156 Chr5_14106655
Chr5_14147312 Chr5_14229380
31,9 Chr5_14296238 Chr5_14254604
Chr5_14595811
33,6 Chr5_14948736
34,4 Chr5_16643291
35,3 Chr5_15897603 Chr5_16492006
Chr5_15962809
37,9 Chr5_16768296 Chr5_16851319
38,8 Chr5_17053742
39,6 Chr5_17415938 Chr5_17283543
40,5 Chr5_18215665 Chr5_17621823
41,3 Chr5_18407756 Chr5_18489676
Chr5_18364549 Chr5_18455698
42,2 Chr5_18980872 Chr5_18914966
45,7 Chr5_20125278 Chr5_19784044
46,5 Chr5_20268506
47,4 Chr5_20999224 Chr5_20513860
48,3 Chr5_21053976
49,1 Chr5_21094662
51,7 Chr5_21380960
52,6 Chr5_21561528 Chr5_21449833
53,4 Chr5_21931992 Chr5_21679101
Chr5_21794942 Chr5_21889005
54,3 Chr5_21975188 Chr5_22454963
Chr5_22700526 Chr5_22726793
Chr5_22617060 Chr5_22136132
Chr5_22093160
56,0 Chr5_23331497 Chr5_23390533
56,9 Chr5_23154267 Chr5_23293062
Chr5_23737354
57,7 Chr5_24452818 Chr5_23900183
60,3 Chr5_23779850 Chr5_24186833
Chr5_25391724 Chr5_25034854
Chr5_25282914
62,9 Chr5_26244648 Chr5_26195412
63,8 Chr5_26573975 Chr5_26506472
64,6 Chr5_26788999
65,5 Chr5_26846468
67,2 Chr5_27163802 Chr5_27064350
Chr5_27351628 Chr5_27395398
69,0 Chr5_28007668 Chr5_27898916
69,8 Chr5_28184311
Chr5_28451567
70,7 Chr5_28614097 Chr5_28561990
Chr5_28732711
71,5 Chr5_28810408 Chr5_29054673
Chr5_29188407 Chr5_28858360
72,4 Chr5_29502186
73,2 Chr5_30425493
76,7 Chr5_31139837 Chr5_31226274
Chr5_31164477
CP6
0,0 Chr6_477125 Chr6_697938
Chr6_159755 Chr6_47539
0,9 Chr6_926540
1,7 Chr6_1247216
4,3 Chr6_2496454 Chr6_2525218
6,0 Chr6_2856168
6,9 Chr6_3604697 Chr6_3900787
10,4 Chr6_4353106
12,1 Chr6_4853915 Chr6_4912617
13,0 Chr6_5080794 Chr6_4957059
13,8 Chr6_5206501 Chr6_5424065
Chr6_5682367 Chr6_5854834
14,7 Chr6_5774522 Chr6_5486351
Chr6_6573296 Chr6_6498221
16,4 Chr6_6920834 Chr6_6610807
Chr6_7137633
Chr6_11041568 Chr6_8803660
17,3 Chr6_10932055 Chr6_11726609
Chr6_9137128 Chr6_12093168
17,7 Chr6_12230749
18,1 Chr6_12461600 Chr6_12403890
Chr6_12134734
19,0 Chr6_12775601 Chr6_12871832
Chr6_12936554
19,8 Chr6_13617045
21,6 Chr6_14283591 Chr6_14728879
Chr6_14412203
22,4 Chr6_14823259 Chr6_14760849
24,1 Chr6_14985980
25,9 Chr6_15226623
30,3 Chr6_15978335
31,9 Chr6_16513820
32,0 Chr6_16564082 Chr6_16149908
Chr6_16277414
32,9 Chr6_16624412
33,7 Chr6_16816623 Chr6_16737017
Chr6_16769067
34,6 Chr6_16943374 Chr6_17061720
36,3 Chr6_17395391 Chr6_17628728
38,0 Chr6_17671553 Chr6_17952964
Chr6_17866936
44,3 Chr6_18302102
46,1 Chr6_18698301
47,8 Chr6_19116593 Chr6_19439063
Chr6_19528725
49,5 Chr6_19901501
50,4 Chr6_19926327
52,1 Chr6_20075797 Chr6_19990901
52,9 Chr6_20166492
53,8 Chr6_20430952
56,4 Chr6_21123319 Chr6_20891120
58,1 Chr6_21680274
59,0 Chr6_22239831 Chr6_21934667
59,8 Chr6_22472085 Chr6_22417649
61,6 Chr6_22761584 Chr6_22563720
Chr6_22971036 Chr6_22998756
62,4 Chr6_23103930
64,1 Chr6_23281581
64,5 Chr6_23190598
65,0 Chr6_24129833 Chr6_23733857
Chr6_23823510 Chr6_23342998
Chr6_23957922 Chr6_23866131

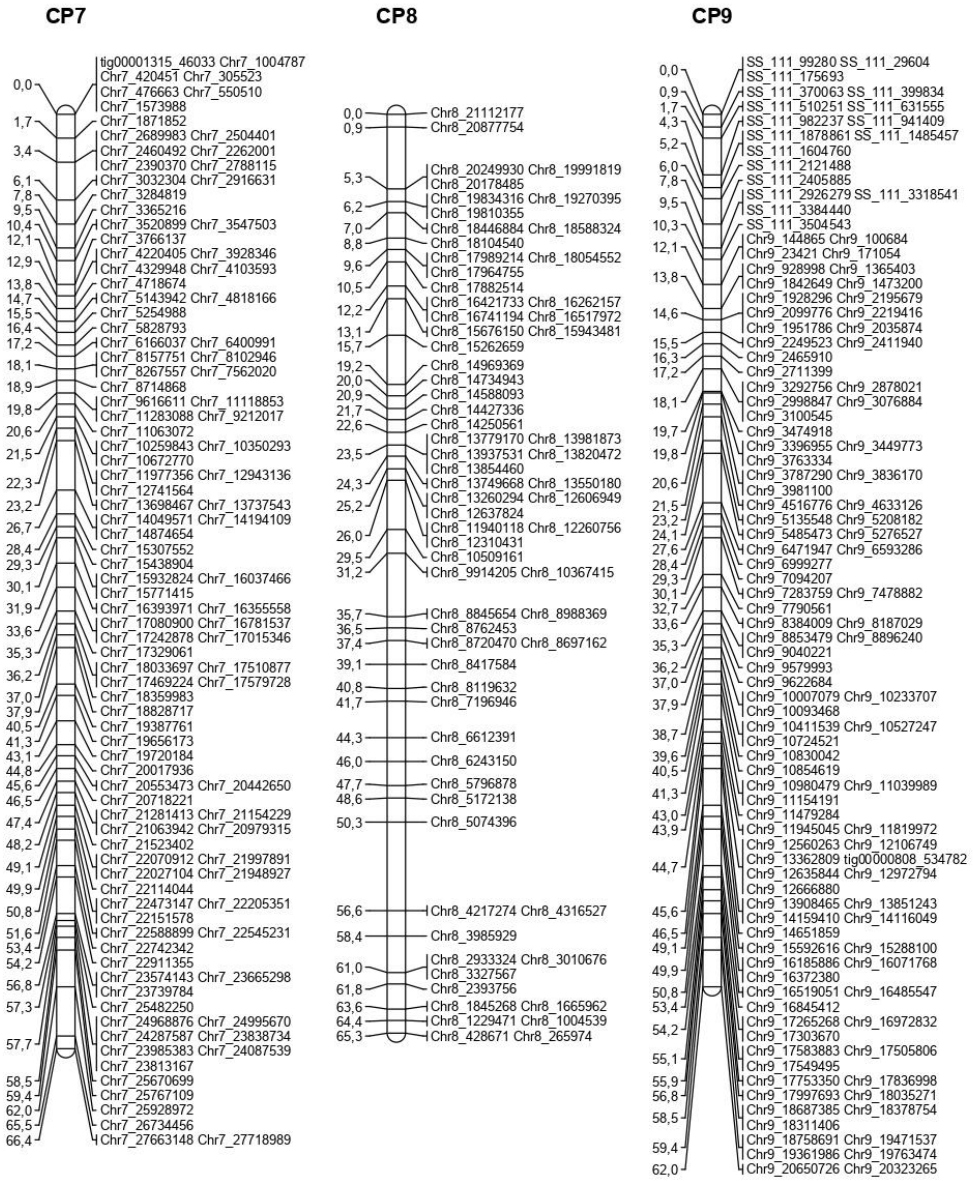
CP7
CP8
CP9
0,0 tig00001315_46033 Chr7_1004787
Chr7_420451 Chr7_305523
Chr7_476663 Chr7_550510
Chr7_1573988
1,7 Chr7_1871852
Chr7_2689983 Chr7_2504401
3,4 Chr7_2460492 Chr7_2262001
Chr7_2390370 Chr7_2788115
6,1 Chr7_3032304 Chr7_2916631
7,8 Chr7_3284819
9,5 Chr7_3365216
10,4 Chr7_3520899 Chr7_3547503
12,1 Chr7_3766137
Chr7_4220405 Chr7_3928346
12,9 Chr7_4329948 Chr7_4103593
13,8 Chr7_4718674
14,7 Chr7_5143942 Chr7_4818166
15,5 Chr7_5254988
16,4 Chr7_5828793
17,2 Chr7_6166037 Chr7_6400991
18,1 Chr7_8157751 Chr7_8102946
Chr7_8267557 Chr7_7562020
18,9 Chr7_8714868
19,8 Chr7_9616611 Chr7_11118853
Chr7_11283088 Chr7_9212017
20,6 Chr7_11063072
21,5 Chr7_10259843 Chr7_10350293
Chr7_10672770
22,3 Chr7_11977356 Chr7_12943136
Chr7_12741564
23,2 Chr7_13698467 Chr7_13737543
26,7 Chr7_14049571 Chr7_14194109
Chr7_14874654
28,4 Chr7_15307552
29,3 Chr7_15438904
30,1 Chr7_15932824 Chr7_16037466
Chr7_15771415
31,9 Chr7_16393971 Chr7_16355558
33,6 Chr7_17080900 Chr7_16781537
Chr7_17242878 Chr7_17015346
35,3 Chr7_17329061
36,2 Chr7_18033697 Chr7_17510877
Chr7_17469224 Chr7_17579728
37,0 Chr7_18359983
37,9 Chr7_18828717
40,5 Chr7_19387761
41,3 Chr7_19656173
43,1 Chr7_19720184
44,8 Chr7_20017936
45,6 Chr7_20553473 Chr7_20442650
46,5 Chr7_20718221
47,4 Chr7_21281413 Chr7_21154229
Chr7_21063942 Chr7_20979315
48,2 Chr7_21523402
49,1 Chr7_22070912 Chr7_21997891
Chr7_22027104 Chr7_21948927
49,9 Chr7_22114044
50,8 Chr7_22473147 Chr7_22205351
51,6 Chr7_22151578
53,4 Chr7_22588899 Chr7_22545231
54,2 Chr7_22742342
Chr7_22911355
56,8 Chr7_23574143 Chr7_23665298
57,3 Chr7_23739784
Chr7_25482250
57,7 Chr7_24968876 Chr7_24995670
Chr7_24287587 Chr7_23838734
Chr7_23985383 Chr7_24087539
Chr7_23813167
58,5 Chr7_25670699
59,4 Chr7_25767109
62,0 Chr7_25928972
65,5 Chr7_26734456
66,4 Chr7_27663148 Chr7_27718989
0,0 Chr8_21112177
0,9 Chr8_20877754
5,3 Chr8_20249930 Chr8_19991819
Chr8_20178485
6,2 Chr8_19834316 Chr8_19270395
Chr8_19810355
7,0 Chr8_18446884 Chr8_18588324
8,8 Chr8_18104540
9,6 Chr8_17989214 Chr8_18054552
Chr8_17964755
10,5 Chr8_17882514
12,2 Chr8_16421733 Chr8_16262157
Chr8_16741194 Chr8_16517972
13,1 Chr8_15676150 Chr8_15943481
15,7 Chr8_15262659
19,2 Chr8_14969369
20,0 Chr8_14734943
20,9 Chr8_14588093
21,7 Chr8_14427336
22,6 Chr8_14250561
23,5 Chr8_13779170 Chr8_13981873
Chr8_13937531 Chr8_13820472
Chr8_13854460
24,3 Chr8_13749668 Chr8_13550180
25,2 Chr8_13260294 Chr8_12606949
Chr8_12637824
26,0 Chr8_11940118 Chr8_12260756
Chr8_12310431
29,5 Chr8_10509161
31,2 Chr8_9914205 Chr8_10367415
35,7 Chr8_8845654 Chr8_8988369
36,5 Chr8_8762453
37,4 Chr8_8720470 Chr8_8697162
39,1 Chr8_8417584
40,8 Chr8_8119632
41,7 Chr8_7196946
44,3 Chr8_6612391
46,0 Chr8_6243150
47,7 Chr8_5796878
48,6 Chr8_5172138
50,3 Chr8_5074396
56,6 Chr8_4217274 Chr8_4316527
58,4 Chr8_3985929
61,0 Chr8_2933324 Chr8_3010676
Chr8_3327567
61,8 Chr8_2393756
63,6 Chr8_1845268 Chr8_1665962
64,4 Chr8_1229471 Chr8_1004539
65,3 Chr8_428671 Chr8_265974
0,0 SS_111_99280 SS_111_29604
SS_111_175693
0,9 SS_111_370063 SS_111_399834
1,7 SS_111_510251 SS_111_631555
4,3 SS_111_982237 SS_111_941409
5,2 SS_111_1878861 SS_111_1485457
SS_111_1604760
6,0 SS_111_2121488
7,8 SS_111_2405885
9,5 SS_111_2926279 SS_111_3318541
SS_111_3384440
10,3 SS_111_3504543
12,1 Chr9_144865 Chr9_100684
Chr9_23421 Chr9_171054
13,8 Chr9_928998 Chr9_1365403
Chr9_1842649 Chr9_1473200
14,6 Chr9_1928296 Chr9_2195679
Chr9_2099776 Chr9_2219416
Chr9_1951786 Chr9_2035874
15,5 Chr9_2249523 Chr9_2411940
16,3 Chr9_2465910
17,2 Chr9_2711399
18,1 Chr9_3292756 Chr9_2878021
Chr9_2998847 Chr9_3076884
Chr9_3100545
19,7 Chr9_3474918
19,8 Chr9_3396955 Chr9_3449773
Chr9_3763334
20,6 Chr9_3787290 Chr9_3836170
Chr9_3981100
21,5 Chr9_4516776 Chr9_4633126
23,2 Chr9_5135548 Chr9_5208182
24,1 Chr9_5485473 Chr9_5276527
27,6 Chr9_6471947 Chr9_6593286
28,4 Chr9_6999277
29,3 Chr9_7094207
30,1 Chr9_7283759 Chr9_7478882
32,7 Chr9_7790561
33,6 Chr9_8384009 Chr9_8187029
Chr9_8853479 Chr9_8896240
35,3 Chr9_9040221
36,2 Chr9_9579993
37,0 Chr9_9622684
37,9 Chr9_10007079 Chr9_10233707
Chr9_10093468
38,7 Chr9_10411539 Chr9_10527247
39,6 Chr9_10724521
40,5 Chr9_10830042
Chr9_10854619
41,3 Chr9_10980479 Chr9_11039989
43,0 Chr9_11154191
43,9 Chr9_11479284
Chr9_11945045 Chr9_11819972
44,7 Chr9_12560263 Chr9_12106749
Chr9_13362809 tig00000808_534782
Chr9_12635844 Chr9_12972794
Chr9_12666880
45,6 Chr9_13908465 Chr9_13851243
46,5 Chr9_14159410 Chr9_14116049
49,1 Chr9_14651859
Chr9_15592616 Chr9_15288100
49,9 Chr9_16185886 Chr9_16071768
Chr9_16372380
50,8 Chr9_16519051 Chr9_16485547
53,4 Chr9_16845412
54,2 Chr9_17265268 Chr9_16972832
Chr9_17303670
55,1 Chr9_17583883 Chr9_17505806
Chr9_17549495
55,9 Chr9_17753350 Chr9_17836998
56,8 Chr9_17997693 Chr9_18035271
58,5 Chr9_18687385 Chr9_18378754
Chr9_18311406
59,4 Chr9_18758691 Chr9_19471537
Chr9_19361986 Chr9_19763474
62,0 Chr9_20650726 Chr9_20323265

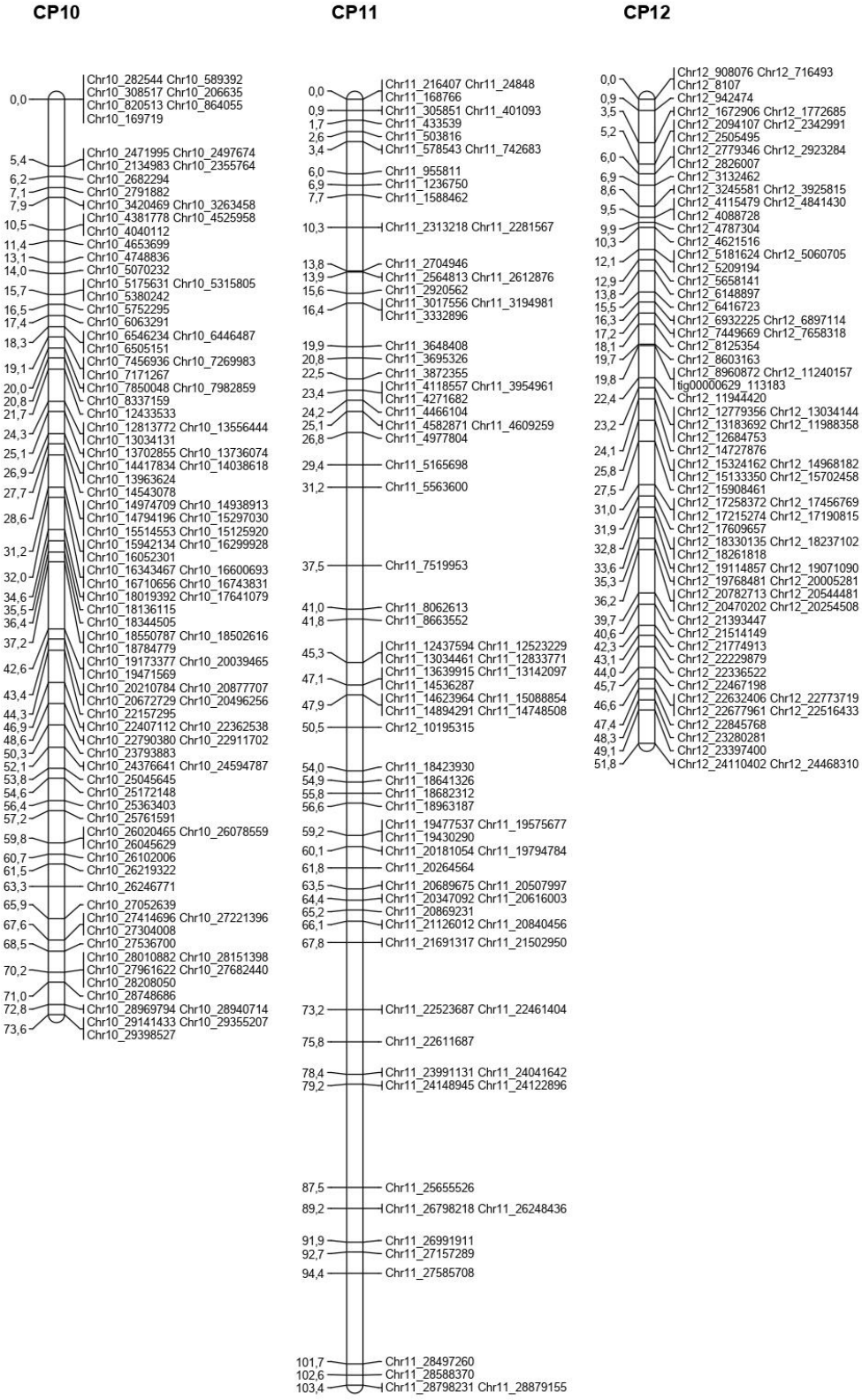
CP10
0,0 Chr10_282544 Chr10_589392 Chr10_308517 Chr10_206635 Chr10_820513 Chr10_864055 Chr10_169719
5,4 Chr10_2471995 Chr10_2497674 Chr10_2134983 Chr10_2355764
6,2 Chr10_2682294
7,1 Chr10_2791882
7,9 Chr10_3420469 Chr10_3263458
10,5 Chr10_4381778 Chr10_4525958 Chr10_4040112
11,4 Chr10_4653699
13,1 Chr10_4748836
14,0 Chr10_5070232
15,7 Chr10_5175631 Chr10_5315805 Chr10_5380242
16,5 Chr10_5752295
17,4 Chr10_6063291
18,3 Chr10_6546234 Chr10_6446487 Chr10_6505151
19,1 Chr10_7456936 Chr10_7269983 Chr10_7171267
20,0 Chr10_7850048 Chr10_7982859
20,8 Chr10_8337159
21,7 Chr10_12433533
24,3 Chr10_12813772 Chr10_13556444 Chr10_13034131
25,1 Chr10_13702855 Chr10_13736074
26,9 Chr10_14417834 Chr10_14038618 Chr10_13963624
27,7 Chr10_14543078
28,6 Chr10_14974709 Chr10_14938913 Chr10_14794196 Chr10_15297030 Chr10_15514553 Chr10_15125920
31,2 Chr10_15942134 Chr10_16299928 Chr10_16052301
32,0 Chr10_16343467 Chr10_16600693 Chr10_16710656 Chr10_16743831
34,6 Chr10_18019392 Chr10_17641079
35,5 Chr10_18136115
36,4 Chr10_18344505
37,2 Chr10_18550787 Chr10_18502616 Chr10_18784779
42,6 Chr10_19173377 Chr10_20039465 Chr10_19471569
43,4 Chr10_20210784 Chr10_20877707 Chr10_20672729 Chr10_20496256 Chr10_22157295
44,3 Chr10_22407112 Chr10_22362538
46,9 Chr10_22790380 Chr10_22911702 Chr10_23793883
48,6 Chr10_24376641 Chr10_24594787
50,3 Chr10_25045645
52,1 Chr10_25172148
53,8 Chr10_25363403
54,6 Chr10_25761591
56,4 Chr10_26020465 Chr10_26078559 Chr10_26045629
57,2 Chr10_26102006
59,8 Chr10_26219322
60,7 Chr10_26246771
61,5 Chr10_27052639
63,3 Chr10_27414696 Chr10_27221396 Chr10_27304008
65,9 Chr10_27536700
67,6 Chr10_28010882 Chr10_28151398 Chr10_27961622 Chr10_27682440 Chr10_28208050
68,5 Chr10_28748686
70,2 Chr10_28969794 Chr10_28940714 Chr10_29141433 Chr10_29355207 Chr10_29398527
71,0
72,8
73,6
CP11
0,0 Chr11_216407 Chr11_24848 Chr11_168766
0,9 Chr11_305851 Chr11_401093
1,7 Chr11_433539
2,6 Chr11_503816
3,4 Chr11_578543 Chr11_742683
6,0 Chr11_955811
6,9 Chr11_1236750
7,7 Chr11_1588462
10,3 Chr11_2313218 Chr11_2281567
13,8 Chr11_2704946
13,9 Chr11_2564813 Chr11_2612876
15,6 Chr11_2920562
16,4 Chr11_3017556 Chr11_3194981 Chr11_3332896
19,9 Chr11_3648408
20,8 Chr11_3695326
22,5 Chr11_3872355
23,4 Chr11_4118557 Chr11_3954961 Chr11_4271682
24,2 Chr11_4466104
25,1 Chr11_4582871 Chr11_4609259
26,8 Chr11_4977804
29,4 Chr11_5165698
31,2 Chr11_5563600
37,5 Chr11_7519953
41,0 Chr11_8062613
41,8 Chr11_8663552
45,3 Chr11_12437594 Chr11_12523229 Chr11_13034461 Chr11_12833771
47,1 Chr11_13639915 Chr11_13142097 Chr11_14536287
47,9 Chr11_14623964 Chr11_15088854 Chr11_14894291 Chr11_14748508
50,5 Chr12_10195315
54,0 Chr11_18423930
54,9 Chr11_18641326
55,8 Chr11_18682312
56,6 Chr11_18963187
59,2 Chr11_19477537 Chr11_19575677 Chr11_19430290
60,1 Chr11_20181054 Chr11_19794784
61,8 Chr11_20264564
63,5 Chr11_20689675 Chr11_20507997
64,4 Chr11_20347092 Chr11_20616003
65,2 Chr11_20869231
66,1 Chr11_21126012 Chr11_20840456
67,8 Chr11_21691317 Chr11_21502950
73,2 Chr11_22523687 Chr11_22461404
75,8 Chr11_22611687
78,4 Chr11_23991131 Chr11_24041642
79,2 Chr11_24148945 Chr11_24122896
87,5 Chr11_25655526
89,2 Chr11_26798218 Chr11_26248436
91,9 Chr11_26991911
92,7 Chr11_27157289
94,4 Chr11_27585708
101,7 Chr11_28497260
102,6 Chr11_28588370
103,4 Chr11_28798231 Chr11_28879155
CP12
0,0 Chr12_908076 Chr12_716493 Chr12_8107
0,9 Chr12_942474
3,5 Chr12_1672906 Chr12_1772685
5,2 Chr12_2094107 Chr12_2342991 Chr12_2505495
6,0 Chr12_2779346 Chr12_2923284 Chr12_2826007
6,9 Chr12_3132462
8,6 Chr12_3245581 Chr12_3925815
9,5 Chr12_4115479 Chr12_4841430 Chr12_4088728
9,9 Chr12_4787304
10,3 Chr12_4621516
12,1 Chr12_5181624 Chr12_5060705 Chr12_5209194
12,9 Chr12_5658141
13,8 Chr12_6148897
15,5 Chr12_6416723
16,3 Chr12_6932225 Chr12_6897114
17,2 Chr12_7449669 Chr12_7658318
18,1 Chr12_8125354
19,7 Chr12_8603163
19,8 Chr12_8960872 Chr12_11240157 tig00000629_113183
22,4 Chr12_11944420
23,2 Chr12_12779356 Chr12_13034144 Chr12_13183692 Chr12_11988358 Chr12_12684753
24,1 Chr12_14727876
25,8 Chr12_15324162 Chr12_14968182 Chr12_15133350 Chr12_15702458 Chr12_15908461
27,5 Chr12_17258372 Chr12_17456769 Chr12_17215274 Chr12_17190815 Chr12_17609657
31,0 Chr12_18330135 Chr12_18237102 Chr12_18261818
31,9 Chr12_19114857 Chr12_19071090 Chr12_19768481 Chr12_20005281
32,8 Chr12_20782713 Chr12_20544481 Chr12_20470202 Chr12_20254508
33,6 Chr12_21393447
35,3 Chr12_21514149
36,2 Chr12_21774913
39,7 Chr12_22229879
40,6 Chr12_22336522
42,3 Chr12_22467198
43,1 Chr12_22632406 Chr12_22773719 Chr12_22677961 Chr12_22516433
44,0 Chr12_22845768
45,7 Chr12_23280281
46,6 Chr12_23397400
47,4 Chr12_24110402 Chr12_24468310
48,3
49,1
51,8

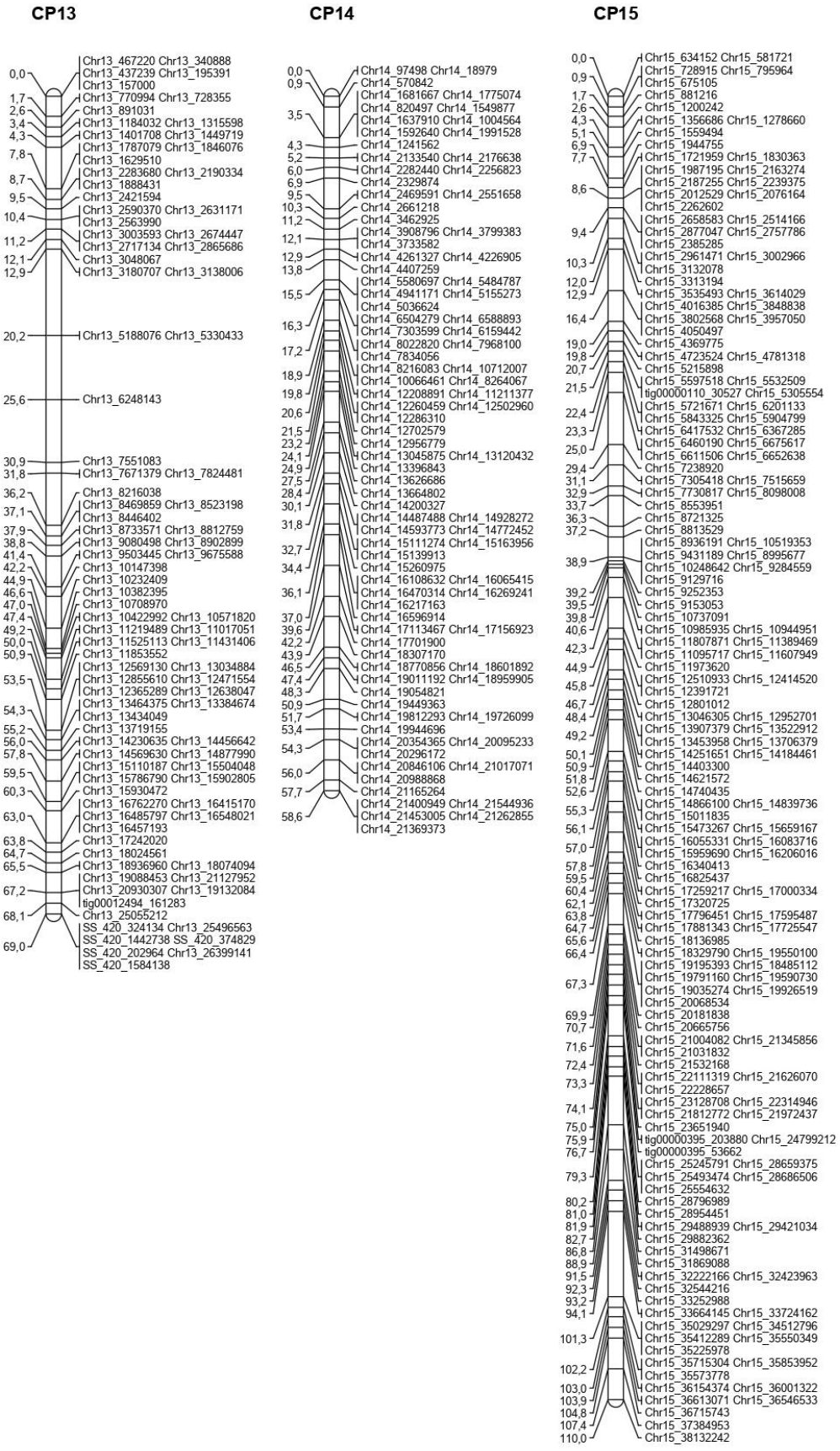
CP13
0,0 Chr13_467220 Chr13_340888
Chr13_437239 Chr13_195391
Chr13_157000
1,7 Chr13_770994 Chr13_728355
2,6 Chr13_891031
3,4 Chr13_1184032 Chr13_1315598
4,3 Chr13_1401708 Chr13_1449719
7,8 Chr13_1787079 Chr13_1846076
Chr13_1629510
8,7 Chr13_2283680 Chr13_2190334
Chr13_1888431
9,5 Chr13_2421594
10,4 Chr13_2590370 Chr13_2631171
Chr13_2563990
11,2 Chr13_3003593 Chr13_2674447
Chr13_2717134 Chr13_2865686
12,1 Chr13_3048067
12,9 Chr13_3180707 Chr13_3138006
20,2 Chr13_5188076 Chr13_5330433
25,6 Chr13_6248143
30,9 Chr13_7551083
31,8 Chr13_7671379 Chr13_7824481
36,2 Chr13_8216038
37,1 Chr13_8469859 Chr13_8523198
Chr13_8446402
37,9 Chr13_8733571 Chr13_8812759
38,8 Chr13_9080498 Chr13_8902899
41,4 Chr13_9503445 Chr13_9675588
42,2 Chr13_10147398
44,9 Chr13_10232409
46,6 Chr13_10382395
47,0 Chr13_10708970
47,4 Chr13_10422992 Chr13_10571820
49,2 Chr13_11219489 Chr13_11017051
50,0 Chr13_11525113 Chr13_11431406
50,9 Chr13_11853552
53,5 Chr13_12569130 Chr13_13034884
Chr13_12855610 Chr13_12471554
Chr13_12365289 Chr13_12638047
54,3 Chr13_13464375 Chr13_13384674
Chr13_13434049
55,2 Chr13_13719155
56,0 Chr13_14230635 Chr13_14456642
57,8 Chr13_14569630 Chr13_14877990
59,5 Chr13_15110187 Chr13_15504048
Chr13_15786790 Chr13_15902805
60,3 Chr13_15930472
63,0 Chr13_16762270 Chr13_16415170
Chr13_16485797 Chr13_16548021
Chr13_16457193
63,8 Chr13_17242020
64,7 Chr13_18024561
65,5 Chr13_18936960 Chr13_18074094
67,2 Chr13_19088453 Chr13_21127952
Chr13_20930307 Chr13_19132084
tig00012494_161283
68,1 Chr13_25055212
69,0 SS_420_324134 Chr13_25496563
SS_420_1442738 SS_420_374829
SS_420_202964 Chr13_26399141
SS_420_1584138
CP14
0,0 Chr14_97498 Chr14_18979
0,9 Chr14_570842
Chr14_1681667 Chr14_1775074
3,5 Chr14_820497 Chr14_1549877
Chr14_1637910 Chr14_1004564
Chr14_1592640 Chr14_1991528
4,3 Chr14_1241562
5,2 Chr14_2133540 Chr14_2176638
6,0 Chr14_2282440 Chr14_2256823
6,9 Chr14_2329874
9,5 Chr14_2469591 Chr14_2551658
10,3 Chr14_2661218
11,2 Chr14_3462925
12,1 Chr14_3908796 Chr14_3799383
Chr14_3733582
12,9 Chr14_4261327 Chr14_4226905
13,8 Chr14_4407259
15,5 Chr14_5580697 Chr14_5484787
Chr14_4941171 Chr14_5155273
Chr14_5036624
16,3 Chr14_6504279 Chr14_6588893
Chr14_7303599 Chr14_6159442
17,2 Chr14_8022820 Chr14_7968100
Chr14_7834056
18,9 Chr14_8216083 Chr14_10712007
19,8 Chr14_10066461 Chr14_8264067
Chr14_12208891 Chr14_11211377
20,6 Chr14_12260459 Chr14_12502960
21,5 Chr14_12286310
23,2 Chr14_12702579
24,1 Chr14_12956779
24,9 Chr14_13045875 Chr14_13120432
27,5 Chr14_13396843
28,4 Chr14_13626686
30,1 Chr14_13664802
31,8 Chr14_14200327
Chr14_14487488 Chr14_14928272
32,7 Chr14_14593773 Chr14_14772452
Chr14_15111274 Chr14_15163956
34,4 Chr14_15139913
Chr14_15260975
36,1 Chr14_16108632 Chr14_16065415
Chr14_16470314 Chr14_16269241
37,0 Chr14_16217163
39,6 Chr14_16596914
Chr14_17113467 Chr14_17156923
42,2 Chr14_17701900
43,9 Chr14_18307170
46,5 Chr14_18770856 Chr14_18601892
47,4 Chr14_19011192 Chr14_18959905
48,3 Chr14_19054821
50,9 Chr14_19449363
51,7 Chr14_19812293 Chr14_19726099
53,4 Chr14_19944696
54,3 Chr14_20354365 Chr14_20095233
Chr14_20296172
56,0 Chr14_20846106 Chr14_21017071
Chr14_20988868
57,7 Chr14_21165264
58,6 Chr14_21400949 Chr14_21544936
Chr14_21453005 Chr14_21262855
Chr14_21369373
CP15
0,0 Chr15_634152 Chr15_581721
0,9 Chr15_728915 Chr15_795964
Chr15_675105
1,7 Chr15_881216
2,6 Chr15_1200242
4,3 Chr15_1356686 Chr15_1278660
5,1 Chr15_1559494
6,9 Chr15_1944755
7,7 Chr15_1721959 Chr15_1830363
Chr15_1987195 Chr15_2163274
8,6 Chr15_2187255 Chr15_2239375
Chr15_2012529 Chr15_2076164
Chr15_2262602
9,4 Chr15_2658583 Chr15_2514166
Chr15_2877047 Chr15_2757786
10,3 Chr15_2385285
Chr15_2961471 Chr15_3002966
12,0 Chr15_3132078
12,9 Chr15_3313194
Chr15_3535493 Chr15_3614029
16,4 Chr15_4016385 Chr15_3848838
Chr15_3802568 Chr15_3957050
19,0 Chr15_4050497
19,8 Chr15_4369775
20,7 Chr15_4723524 Chr15_4781318
21,5 Chr15_5215898
Chr15_5597518 Chr15_5532509
22,4 tig00000110_30527 Chr15_5305554
23,3 Chr15_5721671 Chr15_6201133
Chr15_5843325 Chr15_5904799
25,0 Chr15_6417532 Chr15_6367285
Chr15_6460190 Chr15_6675617
29,4 Chr15_6611506 Chr15_6652638
31,1 Chr15_7238920
32,9 Chr15_7305418 Chr15_7515659
33,7 Chr15_7730817 Chr15_8098008
36,3 Chr15_8553951
37,2 Chr15_8721325
Chr15_8813529
38,9 Chr15_8936191 Chr15_10519353
Chr15_9431189 Chr15_8995677
Chr15_10248642 Chr15_9284559
39,2 Chr15_9129716
39,5 Chr15_9252353
39,8 Chr15_9153053
40,6 Chr15_10737091
42,3 Chr15_10985935 Chr15_10944951
Chr15_11807871 Chr15_11389469
44,9 Chr15_11095717 Chr15_11607949
45,8 Chr15_11973620
46,7 Chr15_12510933 Chr15_12414520
48,4 Chr15_12391721
49,2 Chr15_12801012
Chr15_13046305 Chr15_12952701
50,1 Chr15_13907379 Chr15_13522912
50,9 Chr15_13453958 Chr15_13706379
51,8 Chr15_14251651 Chr15_14184461
52,6 Chr15_14403300
55,3 Chr15_14621572
56,1 Chr15_14740435
Chr15_14866100 Chr15_14839736
57,0 Chr15_15011835
57,8 Chr15_15473267 Chr15_15659167
59,5 Chr15_16055331 Chr15_16083716
60,4 Chr15_15959690 Chr15_16206016
62,1 Chr15_16340413
63,8 Chr15_16825437
64,7 Chr15_17259217 Chr15_17000334
65,6 Chr15_17320725
66,4 Chr15_17796451 Chr15_17595487
Chr15_17881343 Chr15_17725547
67,3 Chr15_18136985
Chr15_18329790 Chr15_19550100
Chr15_19195393 Chr15_18485112
Chr15_19791160 Chr15_19590730
Chr15_19035274 Chr15_19926519
69,9 Chr15_20068534
70,7 Chr15_20181838
71,6 Chr15_20665756
72,4 Chr15_21004082 Chr15_21345856
73,3 Chr15_21031832
74,1 Chr15_21532168
75,0 Chr15_22111319 Chr15_21626070
75,9 Chr15_22228657
76,7 Chr15_23128708 Chr15_22314946
Chr15_21812772 Chr15_21972437
79,3 Chr15_23651940
tig00000395_203880 Chr15_24799212
tig00000395_53662
Chr15_25245791 Chr15_28659375
Chr15_25493474 Chr15_28686506
80,2 Chr15_25554632
81,0 Chr15_28796989
81,9 Chr15_28954451
82,7 Chr15_29488939 Chr15_29421034
86,8 Chr15_29882362
88,9 Chr15_31498671
91,5 Chr15_31869088
92,3 Chr15_32222166 Chr15_32423963
93,2 Chr15_32544216
94,1 Chr15_33252988
Chr15_33664145 Chr15_33724162
101,3 Chr15_35029297 Chr15_34512796
Chr15_35412289 Chr15_35550349
Chr15_35225978
102,2 Chr15_35715304 Chr15_35853952
Chr15_35573778
103,0 Chr15_36154374 Chr15_36001322
103,9 Chr15_36613071 Chr15_36546533
104,8 Chr15_36715743
107,4 Chr15_37384953
110,0 Chr15_38132242

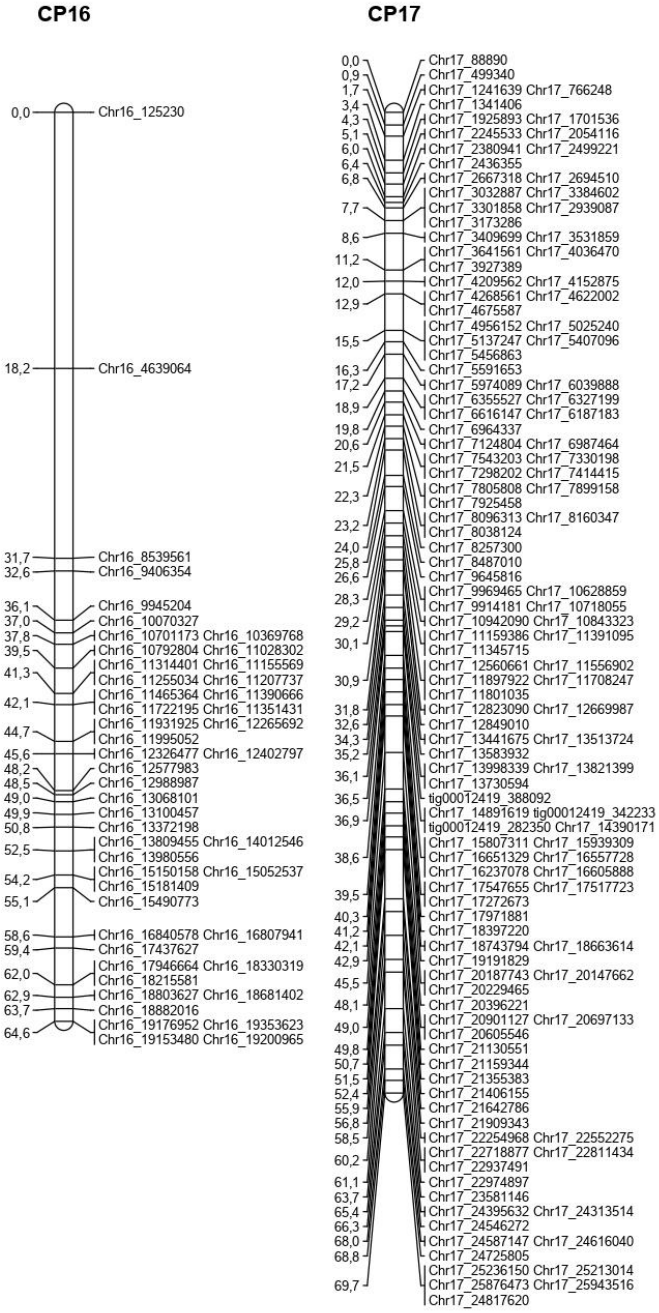
CP16
0,0 Chr16_125230
18,2 Chr16_4639064
31,7 Chr16_8539561
32,6 Chr16_9406354
36,1 Chr16_9945204
37,0 Chr16_10070327
37,8 Chr16_10701173 Chr16_10369768
39,5 Chr16_10792804 Chr16_11028302
41,3 Chr16_11314401 Chr16_11155569
Chr16_11255034 Chr16_11207737
42,1 Chr16_11465364 Chr16_11390666
Chr16_11722195 Chr16_11351431
44,7 Chr16_11931925 Chr16_12265692
Chr16_11995052
45,6 Chr16_12326477 Chr16_12402797
48,2 Chr16_12577983
48,5 Chr16_12988987
49,0 Chr16_13068101
49,9 Chr16_13100457
50,8 Chr16_13372198
52,5 Chr16_13809455 Chr16_14012546
Chr16_13980556
54,2 Chr16_15150158 Chr16_15052537
Chr16_15181409
55,1 Chr16_15490773
58,6 Chr16_16840578 Chr16_16807941
59,4 Chr16_17437627
62,0 Chr16_17946664 Chr16_18330319
Chr16_18215581
62,9 Chr16_18803627 Chr16_18681402
63,7 Chr16_18882016
64,6 Chr16_19176952 Chr16_19353623
Chr16_19153480 Chr16_19200965
CP17
0,0 Chr17_88890
0,9 Chr17_499340
1,7 Chr17_1241639 Chr17_766248
3,4 Chr17_1341406
4,3 Chr17_1925893 Chr17_1701536
5,1 Chr17_2245533 Chr17_2054116
6,0 Chr17_2380941 Chr17_2499221
6,4 Chr17_2436355
6,8 Chr17_2667318 Chr17_2694510
Chr17_3032887 Chr17_3384602
7,7 Chr17_3301858 Chr17_2939087
Chr17_3173286
8,6 Chr17_3409699 Chr17_3531859
11,2 Chr17_3641561 Chr17_4036470
Chr17_3927389
12,0 Chr17_4209562 Chr17_4152875
12,9 Chr17_4268561 Chr17_4622002
Chr17_4675587
Chr17_4956152 Chr17_5025240
15,5 Chr17_5137247 Chr17_5407096
Chr17_5456863
16,3 Chr17_5591653
17,2 Chr17_5974089 Chr17_6039888
18,9 Chr17_6355527 Chr17_6327199
Chr17_6616147 Chr17_6187183
19,8 Chr17_6964337
20,6 Chr17_7124804 Chr17_6987464
21,5 Chr17_7543203 Chr17_7330198
Chr17_7298202 Chr17_7414415
22,3 Chr17_7805808 Chr17_7899158
Chr17_7925458
23,2 Chr17_8096313 Chr17_8160347
Chr17_8038124
24,0 Chr17_8257300
25,8 Chr17_8487010
26,6 Chr17_9645816
28,3 Chr17_9969465 Chr17_10628859
29,2 Chr17_9914181 Chr17_10718055
30,1 Chr17_10942090 Chr17_10843323
Chr17_11159386 Chr17_11391095
Chr17_11345715
30,9 Chr17_12560661 Chr17_11556902
Chr17_11897922 Chr17_11708247
Chr17_11801035
31,8 Chr17_12823090 Chr17_12669987
32,6 Chr17_12849010
34,3 Chr17_13441675 Chr17_13513724
35,2 Chr17_13583932
36,1 Chr17_13998339 Chr17_13821399
Chr17_13730594
36,5 tig00012419_388092
36,9 Chr17_14891619 tig00012419_342233
tig00012419_282350 Chr17_14390171
38,6 Chr17_15807311 Chr17_15939309
Chr17_16651329 Chr17_16557728
Chr17_16237078 Chr17_16605888
39,5 Chr17_17547655 Chr17_17517723
Chr17_17272673
40,3 Chr17_17971881
41,2 Chr17_18397220
42,1 Chr17_18743794 Chr17_18663614
42,9 Chr17_19191829
45,5 Chr17_20187743 Chr17_20147662
Chr17_20229465
48,1 Chr17_20396221
49,0 Chr17_20901127 Chr17_20697133
Chr17_20605546
49,8 Chr17_21130551
50,7 Chr17_21159344
51,5 Chr17_21355383
52,4 Chr17_21406155
55,9 Chr17_21642786
56,8 Chr17_21909343
58,5 Chr17_22254968 Chr17_22552275
60,2 Chr17_22718877 Chr17_22811434
Chr17_22937491
61,1 Chr17_22974897
63,7 Chr17_23581146
65,4 Chr17_24395632 Chr17_24313514
66,3 Chr17_24546272
68,0 Chr17_24587147 Chr17_24616040
68,8 Chr17_24725805
Chr17_25236150 Chr17_25213014
69,7 Chr17_25876473 Chr17_25943516
Chr17_24817620